STRUCTURE AND ELECTRICAL PROPERTIES OF THIOPHENE POLYMERS, AND THE EFFECT OF DILUENTS ON THE GLASS TRANSITION TEMPERATURE OF STYRENE/DIVINYLBENZENE POLYMER NETWORKS

By

MARIO HUMBERTO GUTIERREZ

Bachelor of Science
Universidad de Nuevo Leon
Monterrey N.L. Mexico
1972

Master of Science
C.I.E.A. del I.P.N.
Mexico D.F., Mexico
1977

Submited to the Faculty of the
Graduate College of the
Oklahoma State University
in partial fulfillment of
the requirements for
the Degree of
DOCTOR OF PHILOSOPHY
July, 1985

STRUCTURE AND ELECTRICAL PROPERTIES OF THIOPHENE POLYMERS, AND THE EFFECT OF DILUENTS ON THE GLASS TRANSITION TEMPERATURE OF STYRENE/DIVINYLBENZENE POLYMER NETWORKS

Thesis Approved:

Warren T. Ford
Thesis Adviser

Wayne L. Scott

J. Paul Devlin

Norman N. Durham
Dean of the Graduate College

ACKNOWLEDGMENTS

The author wishes to express his sincere appreciation to his major adviser Dr. Warren T. Ford for his support, instructions, and patience, he has been an example of a hard-working and oustanding scientist.

Appreciation is also extended to the other committee members who made valuable contributions to my plan of study and research projecect

I want to extend my appreciation to my colleagues in Dr. Ford's research group for their helpful suggestions and companionship.

Grateful acknowledgment is given to CONACYT (Consejo Nacional de Ciencia y Tecnologia, Mexico D.F.) for providing the scholarship during my graduate studies.

At the culmination of my formal education I thank my mother, Petrita V. de Gutierrez, for her understanding and moral support during the course of this study. My greatest debt, however, is to my wonderful family, to my wife, Nelly, and to our two daughters, Nellyta and Cecy, for all they have had to sacrifice during my graduate work. This dissertation is dedicated to them because without their patience, understanding, and the continual love, I would never have undertaken the work that the following pages represent.

TABLE OF CONTENTS

PART I

PART II

LIST OF TABLES

PART I

PART II

LIST OF FIGURES

PART I

PART II

Figure Page

PART I

STRUCTURE AND ELECTRICAL PROPERTIES OF THIOPHENE POLYMERS

CHAPTER I

HISTORICAL BACKGROUND

The study of the electronic conductivity of organic solid compounds may be traced back to the beginning of the century. The discovery of the photoconduction of solid anthracene was described by Pochettino in 1906 (1); but it was not until the 1960's when polymers with higher electrical conductivity such as polyacene quinone radicals (PAQR) with conductivities in the range from 10^{-4} to 10^{-10} $ohm^{-1}cm^{-1}$ (2,3), trans-polyacetylene (5×10^{-5} ohm^{-1} cm^{-1}) (4), and polymeric tetracyanoethylene film (5×10^{-4} $ohm^{-1}cm^{-1}$) (5,6) were discovered.

Recent research has shown that polymers exhibit a wide range of electrical conductive properties. Some macromolecular materials have conductivities similar to those of metals. The best known and most highly conducting of them is a polyacetylene film which was doped with AsF_5 at room temperature; its highest conductivity was 5.6×10^{2} $ohm^{-1}cm^{-1}$ (7). Doped poly(1,4-phenylene) (8) is also highly conducting.

An organic semiconductor may be defined as a solid which is capable of supporting electronic conduction.

A major goal of present research programs is to understand the mechanism of electronic conductivity in such materials and relate these mechanisms to the physical-chemical structure of the solid.

It is customary to consider organic semiconductors as materials which exhibit electronic conductivities of 10^{2} to 10^{-7} $ohm^{-1}cm^{-1}$, in between those of metals and those of insulators. (See Figure 1) (9).

Semiconducting organic solids fall into three major categories: molecular crystals (Cu-phthalocyanine 4×10^{-3} $ohm^{-1}cm^{-1}$ (11), violanthrone 2×10^{-3} $ohm^{-1}cm^{-1}$ (11); polymers (highly crystalline trans polyacetylene 1×10^{-5} $ohm^{-1}cm^{-1}$ (4), poly(1,4-phenylene) 10^{-10} $ohm^{-1}cm^{-1}$ (8); and charge transfer complexes (tetrathiafulvalene tetracyanoquinodimethane 5 $ohm^{-1}cm^{-1}$ (11).

Polymers are a versatile class of materials because of the range of chemical structures and physical forms that can be synthesized and the ways in which changes can be made in their structures in a local or general way. They can exist as amorphous, crystalline or as a mixture of crystalline and amorphous materials.

We can divide polymers with carbon atoms in the main chain into two types:

TYPE I: This type consists of macromolecules which contain a main chain linked through bonds; such as polyethylene, poly(vinyl chloride), and polystyrene. These

polymers are electrical insulators because of the localization of the electrons.

TYPE II: This type consists of macromolecules with conjugated double bonds or heterocyclic rings in the main chain, such as polyvinylenes, polyacetylenes polythiophene, and polypyrrole. Since the electrons become delocalized over the entire conjugated system, these appear to be the best candidates to obtain polymers with high conductivity (8).

Polymers of the second type are of considerable interest because their conductivities can be increased several orders of magnitude by the addition of either electron donor or electron acceptor dopants. Materials with conductivities close to those of conventional metals can be produced by controlling the dopant concentration (9). For instance, undoped trans-polyacetylene is a semiconductor with a conductivity of 10^{-5} to 10^{-6} $ohm^{-1}cm^{-1}$. By doping with the electron acceptors AsF_5 or halogens, its conductivity is increased to 1000 $ohm^{-1}cm^{-1}$, comparable with that of mercury (12,13).

We have been interested in assessing the effect of structural units on polymer conductivity, in particular the replacements of the benzene with the thiophene ring in the main chain of some of these aromatic polymers. Thiophene was chosen because it is stable, possesses known aromatic character, has a lower oxidation potential than benzene, and might provide structures with more nearly coplanar aromatic rings.

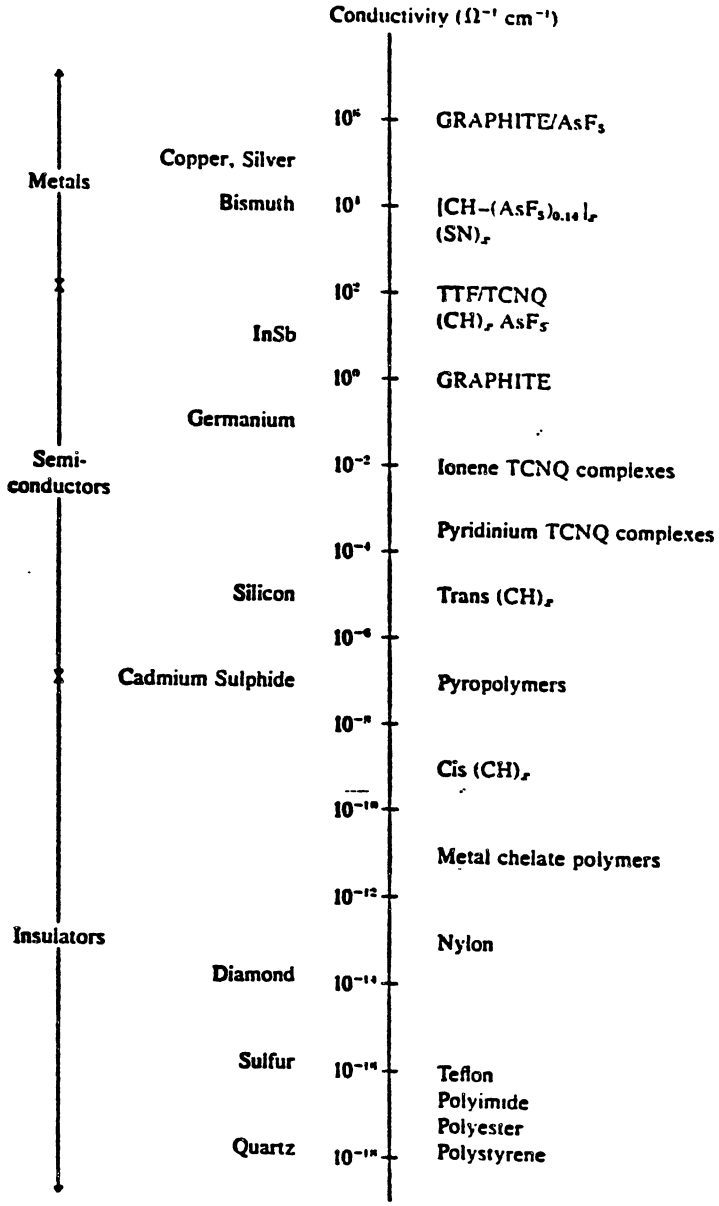
Conductivity (Ω^{-1} cm^{-1})
Metals
Semi-conductors
Insulators
Copper, Silver
Bismuth
InSb
Germanium
Silicon
Cadmium Sulphide
Diamond
Sulfur
Quartz
10^{5}
10^{3}
10^{2}
10^{0}
10^{-2}
10^{-4}
10^{-6}
10^{-8}
10^{-10}
10^{-12}
10^{-14}
10^{-16}
10^{-18}
GRAPHITE/AsF_5
$[CH-(AsF_5)_{0.14}]_x$
$(SN)_x$
TTF/TCNQ
$(CH)_x$ AsF_5
GRAPHITE
Ionene TCNQ complexes
Pyridinium TCNQ complexes
Trans $(CH)_x$
Pyropolymers
Cis $(CH)_x$
Metal chelate polymers
Nylon
Teflon
Polyimide
Polyester
Polystyrene

The literature contains various reports of the synthesis and characterization of thiophene polymers and oligomers. Thiophene has been polymerized with a variety of initiators: sulfuric acid, hydrofluoric acid, trifluoroacetic acid, iron(III) chloride, aluminum chloride, Ziegler catalysts and rays. However, evidence indicates that with acidic promotors, the chains consist of alternating thiophene and tetrahydrothiophene moieties (14-17). (I)

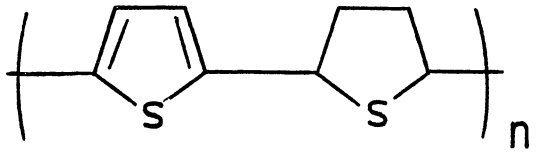

I

Our interest however is to synthesize poly(2,5-thienylene sulfide) PTS (II) by Edmonds and Hill's method (18) used for preparation of poly(1,4-phenylene sulfide) (PPS), and poly(2,5-thienylene-co-1,4-phenylene) (III) by Yamamoto's method (19).

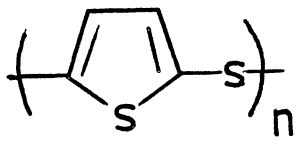

II

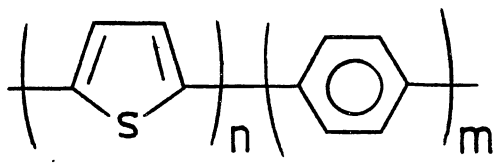

III

Many attempts have been made to prepare poly(2,5-thienylene sulfide). Jones and Moodie (20) reported two methods, condensation of thiophene with sulfur dichloride, and the self-condensation of 2-chloro-5-thiophenethiol promoted by Cu_2O in DMF. The polymers obtained by both methods were linear in structure and probably of low molecular weight. The product of the reaction from 2,5-dibromothiophene and $Na_2S.9H_2O$ in N-methylpyrrolidinone (NMP) was a dark-brown powder, but no properties were reported.

Ramsey and Kovacic (21) studied the polymerization of 2,5-dichlorothiopohene and 2,3,5-trichlorothiophene with aluminum chloride-cupric chloride in CS_2. The polymer from 2,5-dichlorothiophene was a light brown powder which turned to a red-black viscous form at 115-118 °C, and became a red mobile oil at 140-150 °C. The proposed structure for this polymer was:

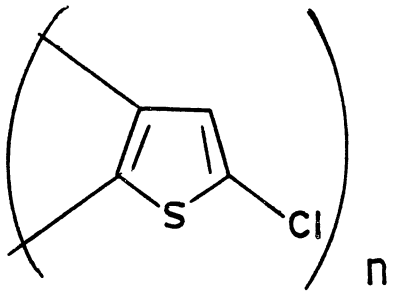

IV

Voronokov et.al. (22) synthesized the poly-(2,5-thienylene sulfide) from 5,5'-dichloro-2,2'-dithienylene sulfide) and $Na_2S.9H_2O$ in N-methylpyrrolidinone. This polymer had a number average molecular weight of 1000, and it was less thermally stable than PPS.

On the other hand, Todres and coworkers (23) tried to produce a condensation product with the structure of poly(2,5-thienylene sulfide) from 2,5-dithiocyanato-thiophene by electrolytic oxidation using $(C_{10}H_{21})_4NClO_4$ as supporting electrolyte, but the product had low molecular weight (V).

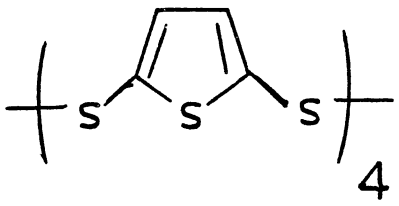

V

Recently Cava and coworkers (24,25) reported the synthesis of poly(2,5-thienylene selenide) (PTSe) by reaction of bis-(4-bromophenyl)diselenide with electrolytic copper in refluxing n-hexanol pyridine, and poly(2,5-thienylene sulfide) (PTS) by treatment of 2,2'-dithienyl disulfide with one equivalent of SO_2Cl_2 at room temperature.

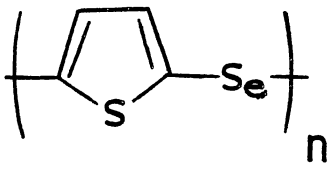

PTSe

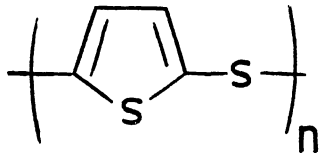

PTS

These pure polymers were oxidized with AsF_5. The conductivities after oxidation were for PTSe 0.12 $ohm^{-1}cm^{-1}$, and for PTS 2.6×10^{-5} $ohm^{-1}cm^{-1}$. They did not report oxidation with I_2.

Several other studies regarding synthesis of polythiophenes and their electrical properties have been reported (26-33). For example, Lin and Dudek (26) synthesized poly(2,5-thienylene) using different catalysts. This polymer was a powder which had a color ranging from dark red to black, depending on the type of catalyst used and reaction conditions. This polymer had an absorption in the visible region, which indicates there is a strong overlap between the neighboring thiophene rings. It was observed that as the number of thiophene

units increases, the optical absorption of poly(2,5-thienylene) shifts toward a longer wavelength, resulting in a change in color from yellow to red and then to black. After compressing this polymer into a black pellet, its conductivity at room temperature was 10^{-10} - 10^{-11} $ohm^{-1}cm^{-1}$, but doping with iodine vapor for a few hours gave a conductivity of 0.1 $ohm^{-1}cm^{-1}$. The conductivity reached 6 $ohm^{-1}cm^{-1}$ when it was heated at 900 °C in He for 5-15 min.

On the other hand, Yamamoto and coworkers (19) found a considerable difference between the properties of poly(2,5-thienylene) and those of the poly(2,4-thienylene). The poly(2,5-thienylene) showed higher affinity toward electron aceptors such as I_2 and SO_3, and its electrical conductivity was enhanced from 5 x 10^{-11} to 4 x 10^{-2} $ohm^{-1}cm^{-1}$ by doping with iodine, whereas poly(2,4-thienylene) interacted only weakly with I_2 with a small enhancement of the electric conductivity. This difference could be ascribed to the difference in degree of double bond conjugation between these two polymers.

Ni(II)-catalyzed coupling of the Grignard reagents from 2,5-dihalothiophenes has been another method to prepare poly(2,5-thienylene) as a powder (19, 27-29).

By electrolytic oxidation of thiophene (30-35) a film of this polymer can be prepared. Its conductivity increases from 10^{-10} to 0.04 (19) or 0.1 $ohm^{-1}cm^{-1}$ (27) upon

oxidation with iodine and to 14 $ohm^{-1}cm^{-1}$ upon oxidation with AsF_5 (29).

Following the procedure of Yamamoto et.al. (19), the polymer which results from the reaction between p-dichlorobenzene and 2,5-dichlorothiophene was prepared. Basically the reaction is a polycondensation utilizing transition metal-catalyzed C-C coupling.

Previously an alternating thienylene/phenylene copolymer was prepared by Bracke (36) using polydiethynylbenzene and hydrogen sulfide in hexamethylphosphoric triamide (HMPA) as solvent. The product, an orange powder, was insoluble in all solvents tried. The IR spectrum of this polymer showed a band at 810 cm^{-1} which is common to 2,5-diphenylthiophene and to the polythiophene. The absorption is indicative of 2,5-disubstitution.

In the present work our goal is to prepare conducting polymers that are stable in air and do not require powerful oxidants and Lewis acids such as AsF_5. For this reason, 2,5-dichlorothiophene, and tetrabromothiophene have been polymerized with anhydrous sodium sulfide in N-methylpyrrolidone (NMP) at 250 C to insoluble products which contain structural fragments derived from both the starting thiophene and the NMP. The copolymers absorb 0.5 to 1.0 times their weight of iodine to give materials with electrical conductivities of about 10^{-5} $(ohm\ cm)^{-1}$ at 16 kbar and 10^{-7} $(ohm\ cm)^{-1}$ at atmospheric pressure (45).

CHAPTER II

EXPERIMENTAL

Analytical Procedures and Apparatus

Elemental analyses were performed by Galbraith Laboratories, Knoxville, Tennessee and by MicAnal Organic Microanalysis, Tucson, Arizona. IR spectra were obtained with KBr discs with a Digilab FTS-20S spectrometer equipped with a diffuse reflectance infrared Fourier-transform (DRIFT) apparatus (Harrick Scientific Corporation model number DRA MIX-1). For ^{13}C-NMR spectra at 25.2 MHz a Varian XL-100 NMR spectrometer with a Nicolet TT-100 PFT unit was used. ^{1}H-NMR spectra at 300 MHz were recorded with a Varian XL-300 NMR spectrometer. Conductivities were measured on pellets pressed at 16 Kbar by the dc-two-probe method (37).

Reagents and Solvents

Reagents were obtained from Aldrich Chemical Co., unless otherwise indicated, except for anhydrous sodium sulfide (Alfa Products). Purity of these compounds was determined by I.R., ^{1}H-NMR, ^{13}C-NMR and gas chromatography; because of their purity these chemicals were used directly.

Tetrahydrofuran was freshly distilled from benzophenone and sodium under nitrogen.

Conductivity Measurements

Determinations of the conductivity in this work were made using the method described by Pohl and Wyhof (37). In our work, the iodine doped polymers were measured on pellets pressed at 16 kbar by the dc two-contact method at room temperature. The typical thickness of a pellet was 5 to 7 x 10^{-3} inches and the diameter was 0.3 to 0.5 cm.

The conductivity values are obtained from the resistance measurements by using the following equation:

$$\rho = \frac{R \times \Pi \times r^2}{l \times 2.54 \text{ cm/inch}}$$

where ρ = resistivity in ohms-cm

R = resistance of the sample in ohms

r = radius of sample in inches

l = thickness of sample in inches

The thickness of the sample was measured with a micrometer caliper and the diameter of the pellet with a scale.

Doping Procedure

Doping of a polymer with iodine was carried out on several 30 mg samples of the polymer in separate glass cups which were placed in a desiccator with 5-10 g of

iodine at room temperature and atmospheric pressure. Periodically the samples were removed, weighed, and returned to the desiccator. The maximum absorption of I_2 was reached in 24 h.

Polymerization of 2,5-Dichlorothiophene in NMP

A mixture of 2,5-dichlorothiophene (2.02 g, 13.2 mmol), anhydrous sodium sulfide (1.00 g, 12.8 mmol), and 4 mL of N-methylpyrrolidinone (NMP) was sealed under vacuum in a heavy-walled glass tube and heated at 250 °C for 3 h. The brown product (sample MG-4362) was washed thoroughly with water, Soxhlet extracted with water, acetone and CH_2Cl_2 for 24 h, and dried under vacuum at 60 °C for 24 h to yield 0.784 g of insoluble product. An additional 0.280 g of solid from the acetone extract and 0.063 g of solid from the dichloromethane extract were recovered. The insoluble fraction did not soften upon heating to 500 °C in air. The ^{13}C-NMR spectrum in chloroform at room temperature also showed a weak peak at 191 ppm. IR of the insoluble fraction: 3080(m), 2930(m), 1700(s), 1425(m), 1375(m), 1020(m), 815(s), 785(sh), 710(s) cm^{-1}.

Anal. of the insoluble fraction. Calcd for $[(C_4H_2S)_3(C_5H_7NO)]_n$: C 59.4, H 3.8, N 4.1, O 4.7, S 28.0. found: C 56.7, H 3.1, N 3.8, O 7.8, S 25.9, Cl 0.66, ash 0.1. Sum 98.1.

From the Cl analysis the insoluble fraction has M_n 2650 assuming 2 g-atom Cl/mol.

Conductivities of the original undoped MG-4362 are shown on Table II.

A sample (30 mg) of MG-4362 was exposed to iodine at 30 °C. After eight hours the sample's weight was 38.6 mg (see Figure 1) and the final weight after 24 h of doping was 53.5 mg.

Conductivities of the doped MG-4362 at room temperature are shown in Table III.

A second sample (30 mg) of MG-4362 was held for 96 h under I_2 at room temperature. The final weight after absorption of iodine was 73.1 mg. It was left to lose its absorbed I_2 at 30 °C. After eight days, the sample lost 49 mg of iodine (67%) (see Figure 2).

A third sample (30 mg) of MG-4362 was doped with iodine for 15 days at room temperature, at the end of this time the sample absorbed 54 mg of iodine. The sample was extracted with benzene for 48 h. Its weight after this time was 63.4 mg (20.6 mg of I_2 was extracted), and 33.4 mg of iodine remained. Its conductivity at room temperature after extraction is reported in Table IV.

Polymerization of 2,5-Dichlorothiophene without NMP

A white product which was soluble in water was obtained after heating a mixture of 2,5-dichlorothiophene (2.02 g, 13.2 mmol) and anhydrous sodium sulfide (1.00 g, 12.8 mmol) for 3 h at 250 °C.

A second sample with the same molar ratio was prepared and heated for 15 h in a heavy-walled glass tube at 350 °C A white product was obtained, and again it dissolved completely after washing with water.

Polymerization of 2,5-Dichlorothiophene in DMF

A mixture of 2,5-dichlorothiophene (2.02 g, 13.2 mmol), and 4 mL of DMF gave a pink solution. When Na_2S (1.00 g, 12.8 mmol) was added, the mixture changed to light yellow color before heating. The mixture was heated in a sealed tube for 3 h at 250 °C.

A dark brown oily liquid with a foul odor was obtained. It was miscible with H_2O and methanol.

Polymerization of 2,5-Dichlorothiophene in DMSO

A mixture of 2,5-dichlorothiophene (2.02 g, 13.2 mmol), anhydrous sodium sulfide (1.00 g, 12.8 mmol) and 4 mL of dimethyl sulfoxide (DMSO) was heated in a heavy-walled glass tube at 250 °C for 45 min. The ampoule broke, but a black solid was obtained (0.94 g) after washing with water, acetone and methylene chloride. The black product after drying under vacuum at 60 °C for 24 h weighed 0.7083 g. This product was not analyzed.

Polymerization of 2,5-Dibromothiophene in NMP

A mixture of 2,5-dibromothiophene (1.59 g, 6.6 mmol), anhydrous sodium sulfide (0.5 g, 6.4 mmol) and 2 mL of N-methylpyrrolidinone (NMP) was heated in a heavy-walled glass at 200 C for 4 h. The black product was washed thoroughly with water, Soxhlet extracted with water, acetone and CH_2Cl_2 for 24 h, and dried under vacuum at 60 °C for 24 h to yield 0.4254 g of insoluble solid. IR of the insoluble fraction: 3425, 3100, 2928, 1730, 1700, 1525, 1425, 1315, 1225, 1050, 810, 715, 705 cm^{-1}.

A second sample with the same molar ratio was heated at 150 °C overnight. After this time a brown oily solution was obtained. After filtration 0.3685 g of black solid was obtained. This product was washed thoroughly with water and Soxhlet extracted with acetone and CH_2Cl_2. IR of the insoluble fraction in KBr: 3425, 3075, 2930, 1730, 1700, 1525, 1425, 1350, 1315, 1220, 1050, 810, 710 cm^{-1}.

Attempted polymerizations of 2,5-dibromothiophene and of 3,4-dibromothiophene in different solvents such as DMSO, NMP, bis-(2-methoxyethyl) ether and with phase transfer catalysis by Aliquat 336 (methyltricaprylammonium chloride) in the presence of toluene resulted in the formation of water-soluble products.

Polymerization of 2,3,4,5-Tetrabromothiophene in NMP

A mixture of tetrabromothiophene (4.00 g, 10.0 mmol), anhydrous sodium sulfide (1.553 g, 20.0 mole) and 8 mL of NMP was sealed under vacuum in a heavy-walled glass tube and heated at 250 °C for 3 h. Before heating, the liquid phase was red. After heating, a black product (MG-4466) was washed thoroughly with water, Soxhlet extracted with water, acetone, and dichloromethane, and dried under vacuum at 50 °C for 5 h to yield 0.4019 g of product. An a additional 0.1090 g of solid from the acetone extract and 0.0101 g of solid from dichloromethane extract were obtained. The insoluble fraction did not melt at 500 °C in air. The ^{1}H and ^{13}C-NMR spectra of the acetone-soluble fraction had broad bands in the aliphatic and aromatic regions with an area ratio of 2:1 in the ^{1}H-spectrum. IR of the insoluble fraction: 3100(m), 2935(m), 2875(m), 1690(s), 1425(m), 1375(m), 1305(w), 1110(w), 1025(w), 815(s), 710(m), 660(m) cm^{-1}.

Anal. of the insoluble fraction. Calcd for $[(C_4S_2)(C_5H_5NO)]_n$: C 52.2, H 2.4, N 6.8, O 7.7, S 30.9. Found: C 49.0, H 2.3, N 4.5, O 9.2, S 30.4, Br 0.59, ash 0.55. Sum = 96.5. From the Br analysis the insoluble fraction has $\bar{M}_n$ 16,000 assuming 1 g-atom Br/mol.

Conductivities of the original undoped MG-4466 are shown in Table V.

A sample (30 mg) of MG-4466 was doped with I_2 vapor at 30 °C for 24 h. The sample increased in weight during this time, as be seen in Figure 3. The weight after doping for 8 h was 34.1 mg and after 24 h its weight was 45.8 mg. This is equivalent to 53 wt% I/polymer.

Conductivities of doped polymer MG-4466 are shown in Table VI.

A second sample (30 mg) of MG-4466 was doped for 96 h at room temperature. After this time the sample's weight was 58.1 mg, equivalent to 94 wt% I/polymer.

This sample was left to lose its absorbed I_2 at 30 °C for eight days. After this time the sample lost 14.6 mg, equivalent to 49% of I_2. These results are shown in Figure 4.

A third sample (30 mg) of MG-4466 absorbed 48.1 mg of iodine at room temperature in 22 days. The sample was extracted with benzene for 66 h. Its weight after extraction was 34 mg. The conductivity results are reported in Table VIII.

Polymerization of 2,3,4,5-Tetrabromothiophene by Phase Transfer Catalysis

A mixture of tetrabromothiophene (2.0 g, 5 mmol) toluene (10 mL, Fisher certified reagent), and 10 drops of Adogen 464 (Ashland Chemical Co.) was mixed with $Na_2S.9H_2O$ (2.39 g, 1 mmol) (Fisher, reagent grade) and 2.47 mL of distilled water. This mixture was placed in a flask and

stirred and heated at reflux for 24 h. A light yellow color appeared after 10 min of heating, and the yellow solution turned brown, and then after 30-45 min only an oily, water-miscible liquid was obtained. This oily liquid was stored at 5 °C for a week, but no solid was observed.

Polymerization of Tetrachlorothiophene without Solvent

A mixture of 2,3,4,5-tetrachlorothiophene (Fairfield Chemical Co. Inc.) (1.10 g, 5 mmol) and anhydrous sodium sulfide (0.776 g, 0.01 mol) without solvent was heated in a sealed heavy-walled tube at 180 °C for 22 h.

A gray solid product was washed thoroughly with water, ethanol and acetone. Only 10 mg of product was recovered.

Copolymerization of 2,5-Dichlorothiophene and p-Dichlorobenzene

A mixture of p-dichlorobenzene (Kodak reagent) (1.418 g, 9.65 mmol), magnesium powder (J. T. Baker, purified reagent) (469 mg, 19.3 mg-atom) and dried THF, 10 mL, was stirred under nitrogen. After 15 min, 2,5-dichlorothiophene (1.476 g, 9.65 mmol) was added. A light yellow solution was observed after the addition of 2,5-dichlorothiophene. After 30 min, 20 mg of $Ni(acac)_2$ dissolved in 3 mL of THF was added. A smooth polymerization gave a dark-brown precipitate.

The solution was heated under reflux for 15 h, cooled, and precipitated into 500 mL of 0.2 M HCl-MeOH solution. The isolated polymer MG-4257 was washed repeatedly with methanol and water until the filtrate was free of halide ions. The final product weighed 1.0037 g. An additional 0.790 g of product from the acetone extract and 0.1797 g from the methylene chloride extract were obtained.

The brown MG-4257 fraction which did not disolve in common solvents at room temperature, was analyzed by IR after drying the sample at 50 °C in vacuum for 2 h: 3590, 3035, 3015, 2835, 1675, 1595, 1495, 1095, 1010, 985, 800, 700 cm^{-1}.

^{13}C-NMR ($CDCl_3$) spectrum from the soluble fraction in methylene chloride showed 10.95, 14.0, 23.0 (doublet), 29.6 (triplet), 38.7, 68.15, 120-130 (multiplet), 167.75 ppm.

Anal. of the insoluble fraction. Calcd for $[C_{14}H_{12}SO]_n$: C 73.68, H 5.26, O 7.01, S 14.03. Found: C 61.93, H 3.95, O 8.23, S 13.92, Cl 8.97, ash 3.10.

Conductivities of the original MG-4257 polymer are reported in Table VIII.

A sample (10.3 mg) of MG-4257 exposed to iodine vapor at room temperature for 24 h increased in weight. After 6 h the sample's weight was 25.3 mg. The results are shown in Figure 5. The final weight after 24 h was 26.8 mg.

Conductivities of the doped MG-4257 polymer are reported in Table IX.

A second sample (30 mg) of MG-4257 was doped with iodine for 5 days at room temperature. The final weight of the sample was 57.9 mg. These results are shown in Figure 6.

A third sample (30 mg) of MG-4257 was doped for 24 h with iodine at 30°C. After 8 h the sample's weight was 35.9 mg (See Figure 7). The final weight after 24 h was 53.1 mg.

A fourth sample (30 mg) of this polymer absorbed 50 mg of iodine at room temperature in 24 h, the sample was extracted with benzene for 100 h, and its weight after this time was 32.3 mg (47.7 mg of I_2 was extracted). The remaining (2.3 mg) is equivalent to 7.6 wt% I. Its conductivity was measured at room temperature after the extraction with benzene. The results are shown in Table X.

CHAPTER III

RESULTS AND DISCUSSION

STRUCTURE ANALYSIS

The elemental analysis and spectra of the polymer MG-4362 rule out the target structure poly(thia-2,5-thiophenediyl) (II). The low sulfur content requires either a lack of sulfur bridges between thiophene rings or extrusion of sulfur from thiophene rings during the synthesis. In our experiments the only source of nitrogen is the solvent, N-methylpyrrolidone (NMP). The NMR and IR spectra showed that the polymer contains aliphatic structural fragments. Comparison of the IR spectrum of our polymer from 2,5-dichlorothiophene and sodium sulfide with the IR spectrum of authentic (II) (36,37) showed that our polymer had none of the five major IR bands present in (II). The ^{13}C-NMR spectrum proves that the aliphatic part of the structure is not simply trapped NMP because peaks did not appear at the chemical shifts of NMP (17.7, 29.4, 30.7, 49.3 and 174.8 ppm). The IR peak at 1700 cm^{-1} could be due to the carbonyl group of a γ-lactam, a thienyl ketone or a thioester. The ^{13}C-NMR peak at 191 ppm could be due to a thienyl ketone or a thioester, but non an amide. The elemental analysis fits approximately a

structure $[(C_4H_2S)_3(C_5H_7NO)]_n$ comprised of three thienyl units per NMP fragment, except for excess oxygen. The hydrogen content is not high enough for the excess of oxygen to come from water (if the analytical sample contained moisture), so most likely the excess oxygen came from oxidation of the polymer during or after the synthesis.

Preparation of (II) from 2,5-dibromo thiophene instead of 2,5-dichlorothiophene gave a polymer with the same IR spectrum, but no elemental analysis was obtained.

Attemps to polymerize 2,5-dichlorothiophene with sodium sulfide in the absence of NMP failed to produce high polymers. These attempts included replacement of the NMP with other polar aprotic solvents such as dimethylformamide, dimethylsulfoxide, and diethylene glycol dimethyl ether, and phase transfer catalysis by tricaprylmethylammonium chloride in a boiling mixture of 2,5-dibromothiophene in toluene and saturated aqueous sodium sulfide.

The polymer from tetrabromothiophene also is not formed by simple substitution of sulfur for bromine on the thiophene ring. The elemental analysis approximately fits the formula $[(C_4S_2)(C_5H_5NO)]_n$, except for excess oxygen, and thus (MG-4466) contains nearly equal numbers of structural fragments derived from tetrabromothiophene and NMP. The IR band at 1690 cm^{-1} suggests an aryl ketone, thioester, or amide functional group in the structure.

Loss of nearly all of the bromine and the ^{1}H-NMR signal at 6.9-7.8 ppm indicate replacement of bromine by hydrogen on the thiophene units.

The experimental procedure is essentially the same as that used for preparation of poly(phenylene sulfide) (18), yet the polymers are deficient in sulfur, and NMP is incorporated into the polymers. The formation of PPS from 1,4-dichlorobenzene and sodium sulfide in NMP is thought to proceed by a chain reaction mechanism rather than a step reaction mechanism (45).

Regarding oxidation of samples with I_2, these thiophene polymers (MG-4362) and (MG-4466) showed a high affinity for iodine at room temperature and atmospheric pressure. The conductivities increased by two to four powers of ten by incorporation of iodine. Less than half of the iodine was lost from each sample upon standing in air at room temperature for nine days. Extraction with benzene removed most, but not all of the iodine, and reduced the conductivities. The iodine remaining after extraction may be covalently bound.

Iodine itself is an electrical conductor with a high dependence of conductivity on applied pressure. In our hands the conductivity of iodine cystals pressed into pellets is (16 kb) = 1×10^{-3} and (1 bar) = 2×10^{-7} ohm^{-1} cm^{-1}, in reasonable agreement with another report (40). Given the high conductivity of iodine itself and the high iodine content of our polymers, we cannot say with

certainty whether the increased conductivities obtained by iodine doping are due to oxidation of the polymers to conductive polymer cations with I^- I_3^-, or I_5^- counter ions, or to the conductivity of elemental iodine condensed into the polymers. This uncertainty exists also in other reports of polymers doped with iodine to a semiconducting state (41-44).

Table XI gives a review of properties of the studied polymers.

Comparison with other Thiophene Polymers and Poly(p-Phenylene Sulfide)

All our polymers are insulators before doping. The electrical conductivity is however increased after doping with iodine to give materials with electrical conductivities of about 10^{-5} $(\text{ohm cm})^{-1}$ at 16 kbar and 10^{-7} $(\text{ohm cm})^{-1}$ at atmospheric pressure.

Similar results were obtained by Montheard and coworkers (46). They synthesized conjugated polymers from a polycondensation between di-Grignard aromatic compounds and dihalogenated heterocycles such as 2,5-dibromothiophene. The copolymer prepared from p-dibromobenzene and 2,5-dibromothiophene had a conductivity before doping of 9.5×10^{-13} $(\text{ohm cm})^{-1}$ and after doping a conductivity of 1×10^{-7} $(\text{ohm cm})^{-1}$ at room temperature and atmospheric pressure.

On the other hand, Kobayashi and coworkers (29) synthesized polythiophene in powder form by Ni(II)-catalyzed coupling of the Grignard reagents from 2,5-diiodothiophene and ether/anisole as solvents. With this method it was possible to obtain good yield of higher molecular weight material. The material, as prepared, had a room temperature (pressed pellet) a conductivity of 10^{-9} $(ohm\ cm)^{-1}$ and after exposure to iodine the conductivity was 10^{-1} - 10^{-2} $(ohm\ cm)^{-1}$.

Previous atempts (19, 26, 47) to prepare polythiophene by nickel catalysis of Grinard reagents had produced material of relatively low molecular weight with elemental analysis indicating at least 3% impurities (19).

The conductivities of the polymers prepared by Lin and coworkers (26) were 10^{-10}-10^{-11} $(ohm\ cm)^{-1}$ at room temperature, and after doping with iodine the conductivity was 0.1 $(ohm\ cm)^{-1}$. Those prepared by Yamamoto and coworkers (19) had a conductivity of 5×10^{-11} $(ohm\ cm)^{-1}$ and after doping with iodine at room temperature, the conductivity was 4×10^{-2} $(ohm\ cm)^{-1}$.

Cava and coworkers (24, 25) reported the synthesis of the poly(2,5-thienylene sulfide) by treatment of 2,2'-dithienyl disulfide with one equivalent of SO_2Cl_2. The conductivity of this product after oxidation with AsF_5 was 2.6×10^{-5} $(ohm\ cm)^{-1}$. They did not report the oxidation with iodine.

Finally Chance and coworkers (48) reported that the conductivity of poly(p-phenylene sulfide) (PPS) was increased from 10^{-16} (ohm cm)$^{-1}$ to 25 (ohm cm)$^{-1}$ after treatment with AsF_5 in AsF_3 as solvent.

TABLE II

Conductivity of Undoped Product from Dichlorothiophene and Na_2S in NMP (Polymer MG-4362)

P, Kbar	R, ohm	ohm^{-1} cm^{-1}
16.0	1.5×10^{6}	6.5×10^{-8}
13.0	2.3×10^{6}	4.4×10^{-8}
10.0	4.4×10^{6}	2.3×10^{-8}
6.0	12.5×10^{6}	8.1×10^{-9}
3.0	70.0×10^{6}	1.4×10^{-9}
1.6	42.0×10^{7}	2.4×10^{-10}
0.0	15.0×10^{9}	7.0×10^{-12}

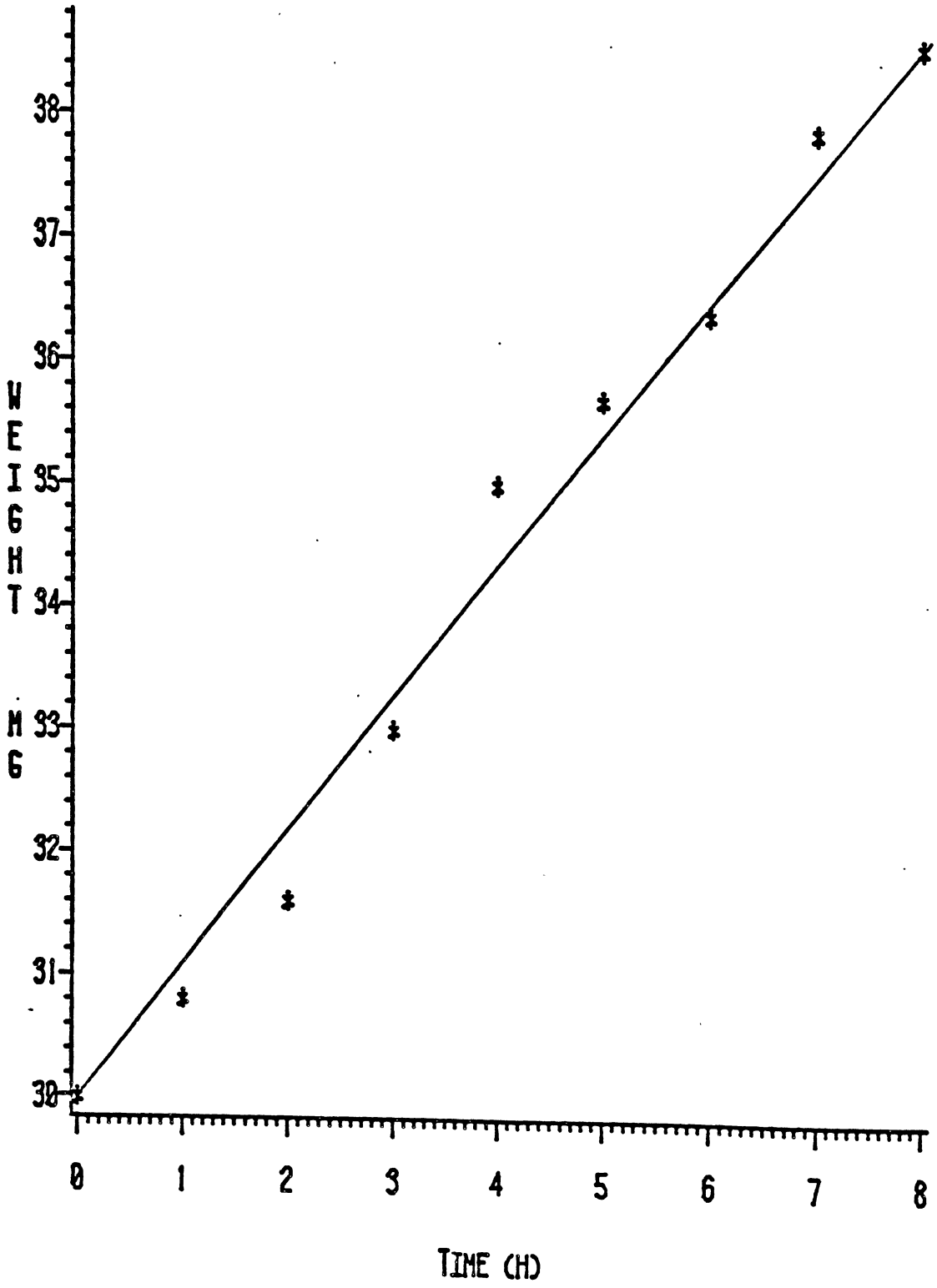

Figure 1. Absorption of I_2 of polymer MG-4362.

TABLE III

Conductivity of Doped Polymer MG-4362*

P, Kbar	R,ohm	ohm^{-1} cm^{-1}
16.0	3.2×10^3	3.0 x 10-5
13.0	4.7×10^3	2.1×10^{-5}
10.0	7.6×10^3	1.3×10^{-5}
6.0	17.5×10^3	5.6×10^{-6}
3.0	64.5×10^3	1.5×10^{-6}
1.6	190.0×10^3	5.1×10^{-7}
0.0	730.0×10^3	1.3×10^{-7}

* This sample was exposed to iodine vapor at 30°C for 24 h.

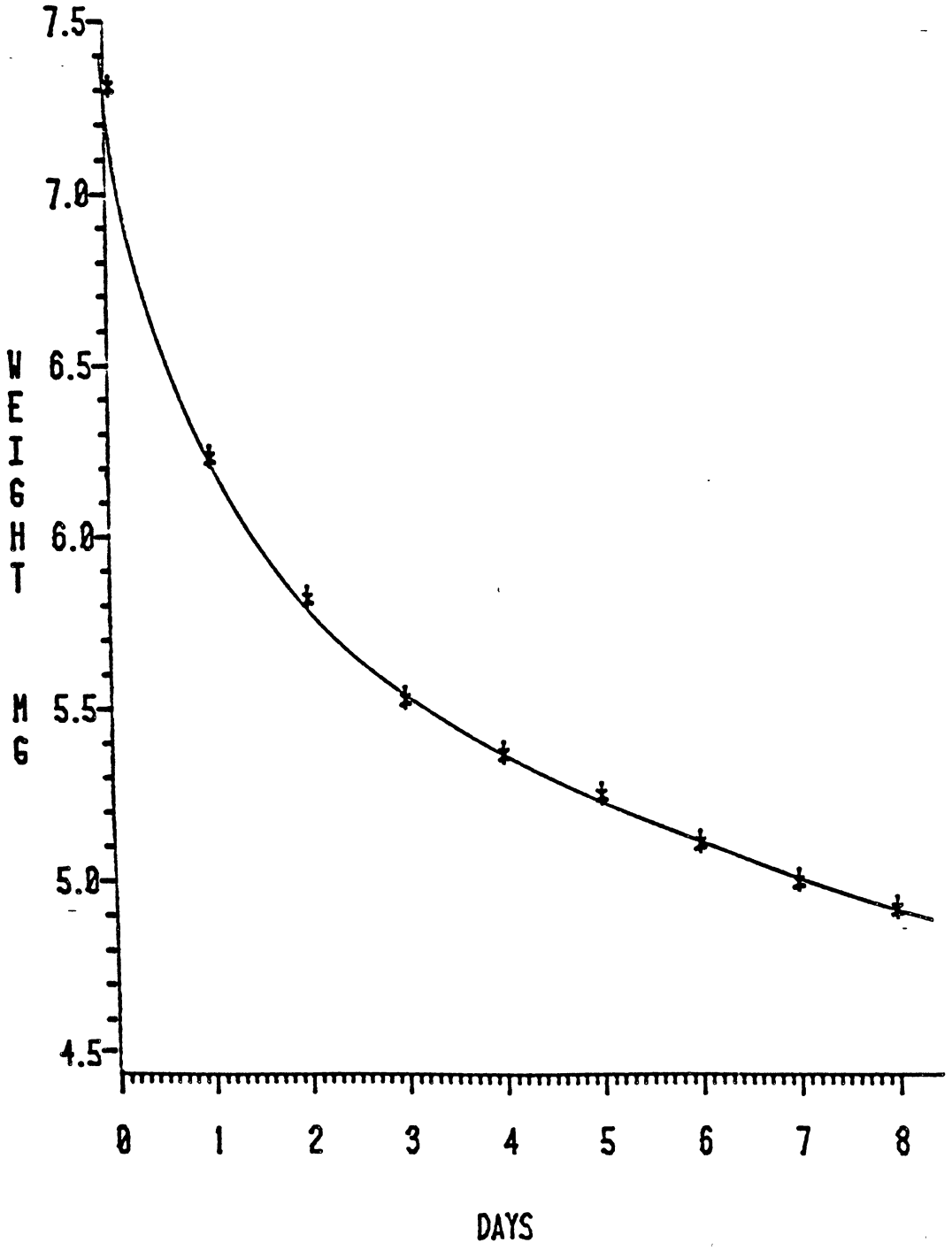

Figure 2. Loss of I_2 at 30 °C from MG-4362.

TABLE IV

Conductivity of MG-4362 after* Extraction of I_2 with Benzene

P, Kbar	R, ohm	$ohm^{-1}\ cm^{-1}$
16.0	1.0×10^5	8.0×10^{-7}
13.0	1.0×10^5	8.0×10^{-7}
10.0	2.0×10^5	4.0×10^{-7}
6.0	4.0×10^5	2.0×10^{-7}
3.0	2.0×10^6	4.0×10^{-8}
1.6	8.5×10^6	9.0×10^{-9}
0.0	2.0×10^7	4.0×10^{-9}

* Sample doped with iodine for fifteen days at room temperature and extracted with benzene for 48 h.

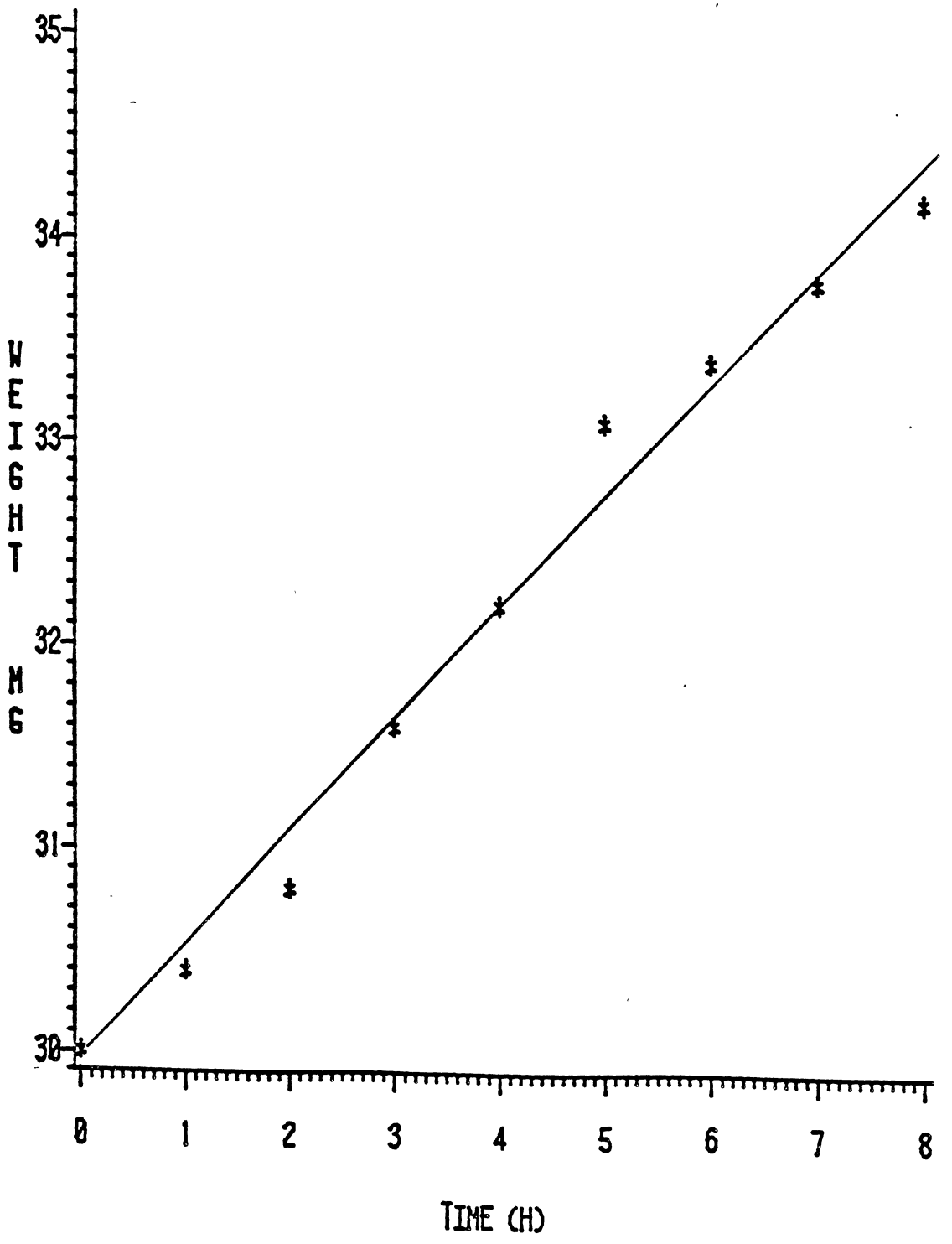

Figure 3. Absorption of I_2 by MG-4466 at 30 °C.

TABLE V

Conductivity of Undoped Product from 1,2,3,4-Tetrabromothiophene and Na_2S in NMP (Polymer MG-4466)

P, Kbar	R, ohm	ohm^{-1} cm^{-1}
16.0	8.0×10^4	6.5×10^{-6}
13.0	1.0×10^5	5.0×10^{-6}
10.0	2.0×10^5	3.0×10^{-6}
6.0	4.0×10^5	1.0×10^{-6}
3.0	2.0×10^6	2.5×10^{-7}
1.6	1.0×10^7	5.0×10^{-8}
0.0	2.0×10^8	3.0×10^{-9}

TABLE VI

Conductivity of Doped Polymer MG-4466*

P, Kbar	R, ohm	ohm^{-1} cm^{-1}
16.0	17.5×10^3	8.0×10^{-6}
13.0	30.0×10^3	5.0×10^{-6}
10.0	48.0×10^3	3.0×10^{-6}
6.0	119.0×10^3	1.0×10^{-6}
3.0	530.0×10^3	3.0×10^{-7}
1.6	1960.0×10^3	7.0×10^{-8}
0.0	2400.0×10^3	6.0×10^{-8}

* Sample doped with iodine vapor at 30°C for 24 h.

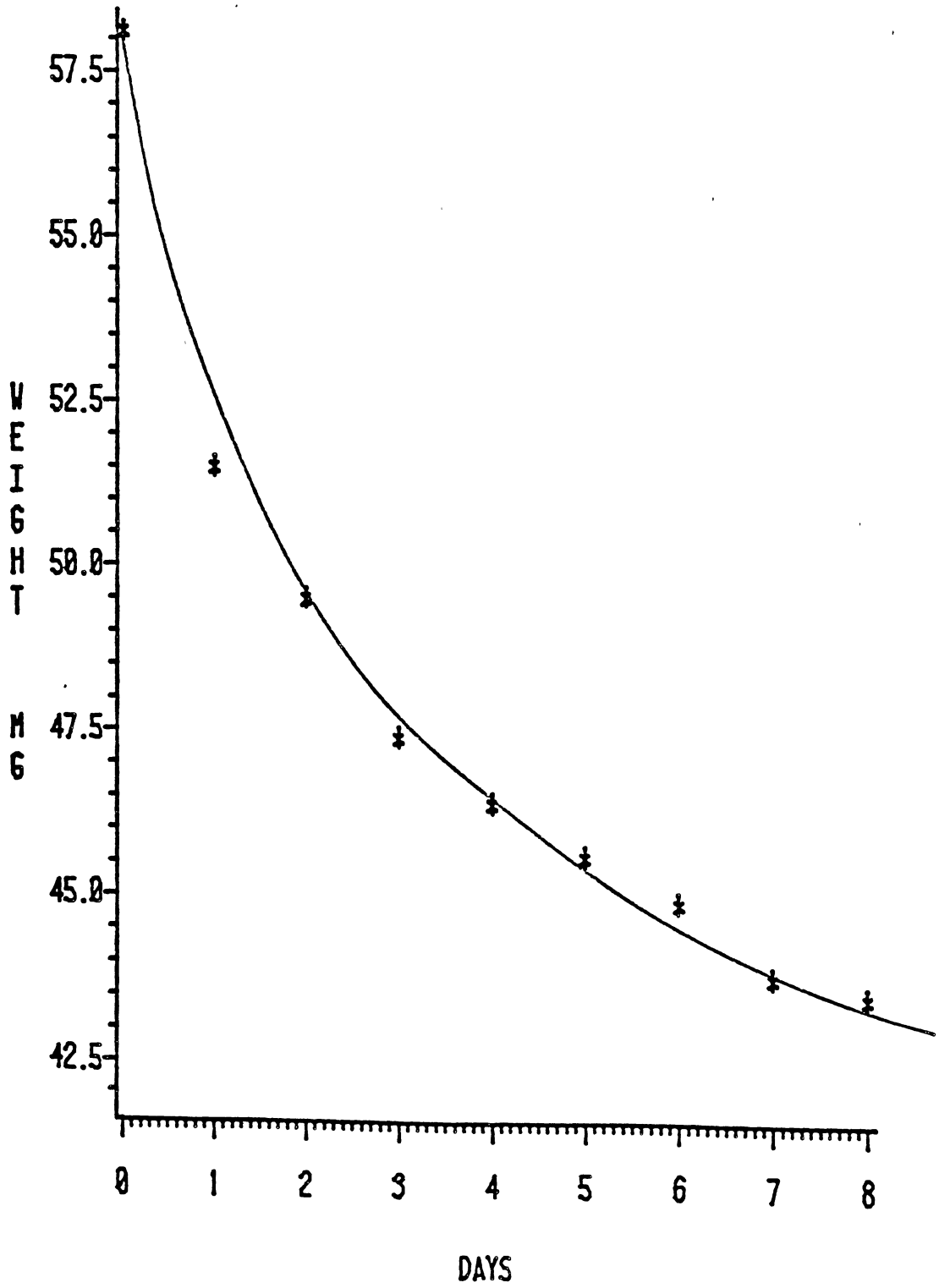

Figure 4. Loss of I_2 at room temperature from MG-4466.

TABLE VII

Conductivity of Polymer MG-4466 after Extraction with Benzene*

P, Kbar	R, ohm	$ohm^{-1}\ cm^{-1}$
16.0	2.0×10^5	3.0×10^{-7}
13.0	3.0×10^5	2.0×10^{-7}
10.0	4.0×10^5	1.5×10^{-7}
6.0	6.0×10^5	1.0×10^{-7}
3.0	26.0×10^5	2.0×10^{-8}
1.6	80.0×10^5	7.5×10^{-9}
0.0	32.0×10^6	1.8×10^{-9}

* Sample doped for 22 days and extracted with benzene for 66 h.

TABLE VIII

Conductivity of Undoped Polymer from 2,5-Dichlorothiophene and p-Dichlorobenzene, Polymer (MG-4257)

P, Kbar	R, ohm	$ohm^{-1}\ cm^{-1}$
16.0	1.0×10^{8}	8.0×10^{-10}
13.0	1.5×10^{8}	5.0×10^{-10}
10.0	2.0×10^{8}	4.0×10^{-10}
6.0	3.0×10^{8}	3.0×10^{-10}
3.0	20.0×10^{8}	4.0×10^{-11}
1.6	75.0×10^{8}	2.0×10^{-11}
0.0	120.0×10^{8}	7.0×10^{-12}

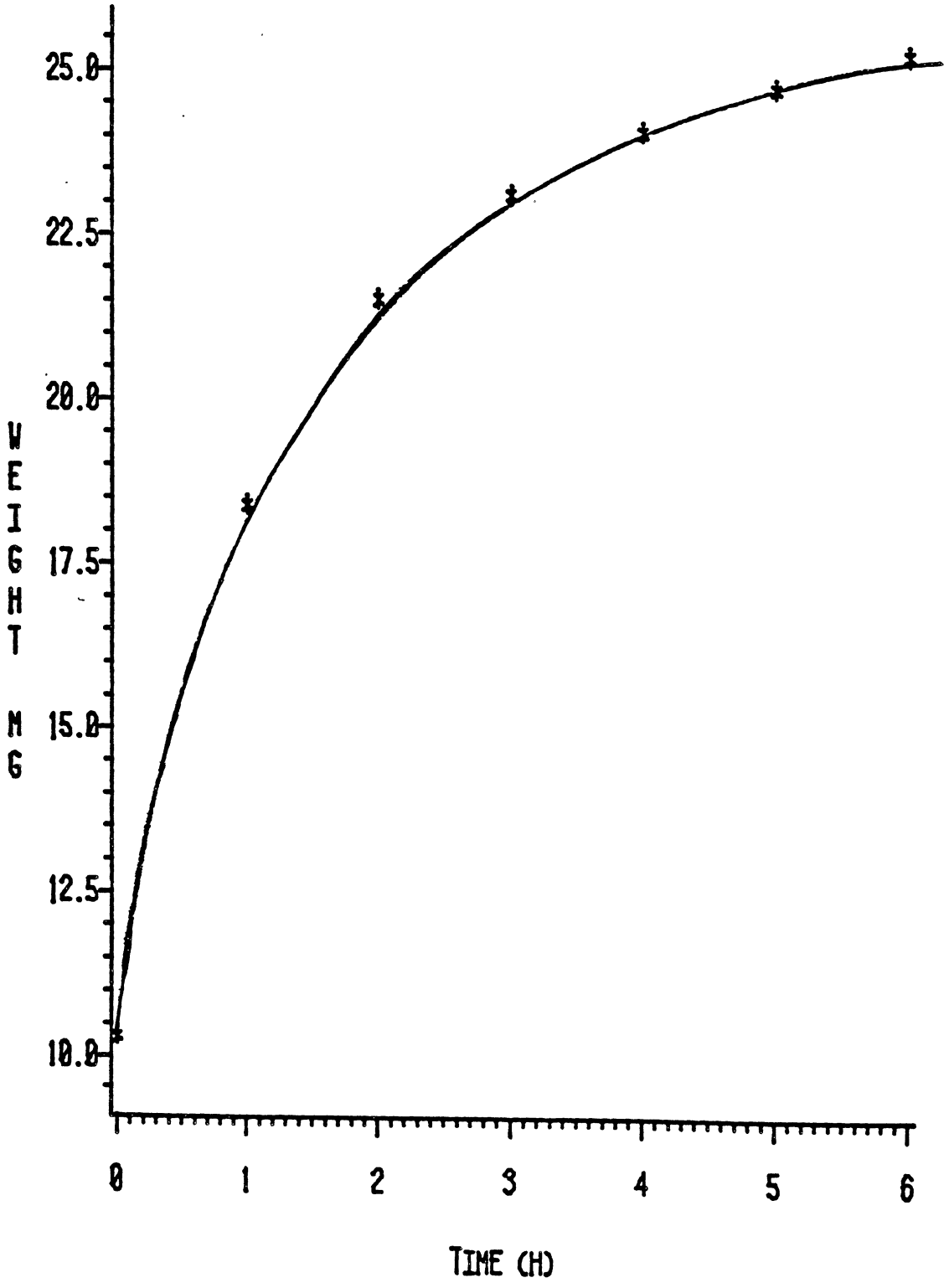

Figure 5. Absorption of I_2 by MG-4257 at room temperature.

TABLE IX

Cunductivity of Doped MG-4257*

P, kbar	R, ohm	ohm^{-1} cm^{-1}
16.0	3.0×10^5	3.0×10^{-5}
13.0	3.0×10^5	3.0×10^{-5}
10.0	2.0×10^3	4.5×10^{-5}
6.0	2.0×10^3	4.5×10^{-5}
3.0	2.0×10^3	4.5×10^{-5}
1.6	4.0×10^3	2.0×10^{-5}
0.0	5.0×10^3	2.0×10^{-5}

* Sample doped with iodine for 24 h at 30°C.

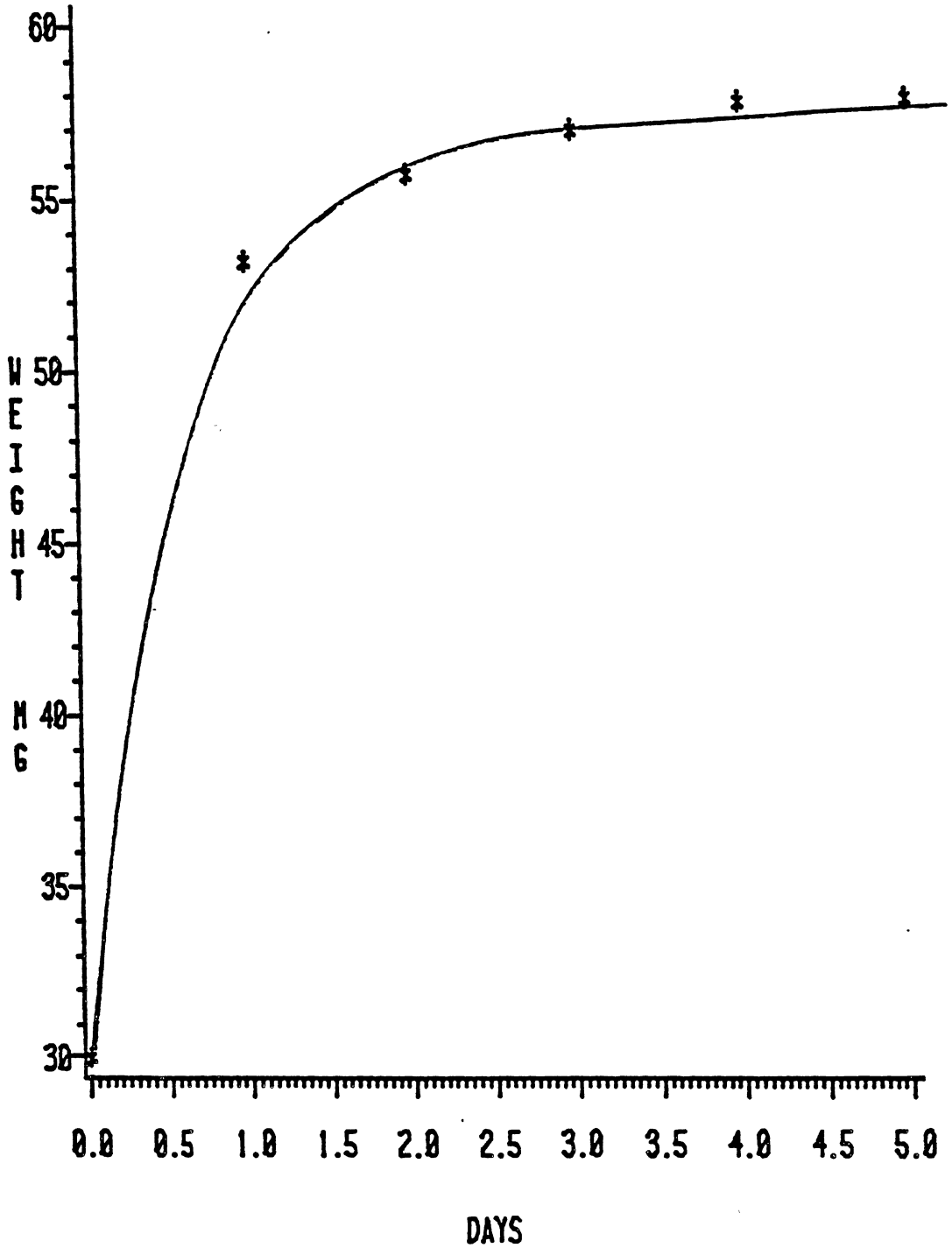

Figure 6. Absorption of I_2 at room temperature by MG-4257 for 5 days.

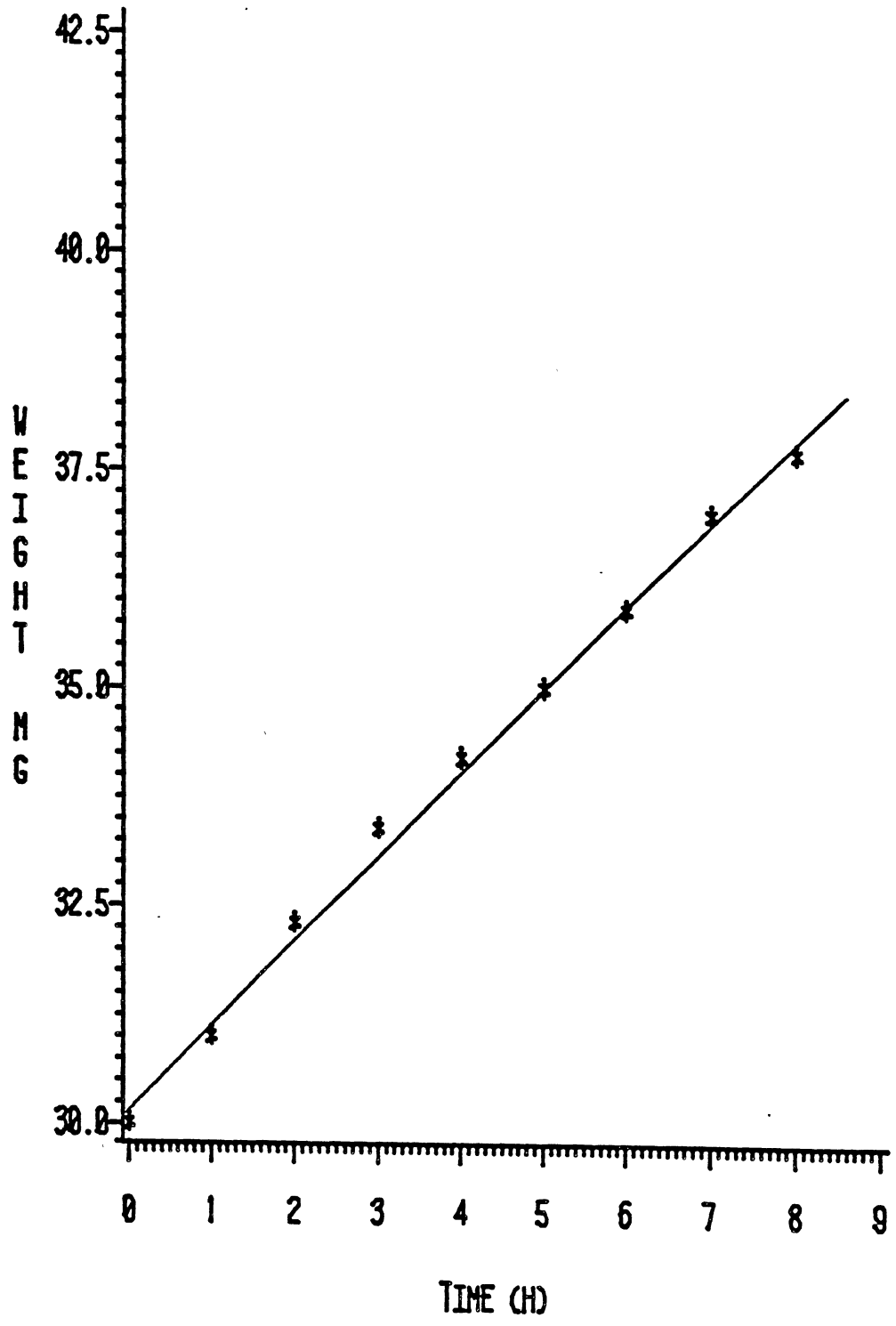

Figure 7. Absorption of I_2 by MG-4257 at 30 °C.

TABLE X

Conductivity of Doped MG-4257* after Extraction with Benzene

P, kbar	R, ohm	$ohm^{-1}\ cm^{-1}$
16.0	1.1×10^{7}	7.0×10^{-9}
13.0	1.3×10^{7}	6.0×10^{-9}
10.0	1.6×10^{7}	5.0×10^{-9}
6.0	1.7×10^{7}	4.5×10^{-9}
3.0	2.4×10^{7}	3.0×10^{-9}
1.6	5.0×10^{7}	1.5×10^{-9}
0.0	7.0×10^{7}	1.0×10^{-9}

* Sample doped with iodine for 24 h and extracted with benzene for 100 h.

TABLE XI

Properties of Thiophene Polymers

Property	Polymer		
	MG-4362	MG-4466	MG-4257
Color	dark brown	black	brown
Conductivity undoped $(ohm\ cm)^{-1}$			
at 16 kbar	6.5×10^{-8}	6.5×10^{-6}	8.0×10^{-10}
at 1 bar	7.0×10^{-12}	3.0×10^{-12}	1.5×10^{-11}
Affinity for I_2 (g I/g polymer)	0.93	0.53	0.77
Conductivity doped $(ohm\ cm)^{-1}$			
at 16 kbar	3.0×10^{-5}	8.0×10^{-6}	2.0×10^{-6}
at 1 bar	1.0×10^{-7}	6.0×10^{-8}	1.0×10^{-8}
Retention of I_2 in air (g I/g polymer)[a]	0.64	0.45	0.53
Retention of I_2 after benzene extraction (g I/g polymer)	1.11[b]	0.45[c]	0.08[d]
Conductivity after extraction $(ohm\ cm)^{-1}$			
at 16 kbar	8.0×10^{-7}	3.0×10^{-7}	7.0×10^{-9}
at 1 bar	3.0×10^{-9}	2.0×10^{-9}	1.5×10^{-9}

a) After standing in air for 9 days at 30 °C.
b) 48 h extraction of sample originally doped for 15 days.
c) 66 h extraction of sample originally doped for 22 days to 1.6 g I/polymer.
d) 24 h of doping with I_2 and 100 h extraction with benzene

BIBLIOGRAPHY

1. A. Pochettino, Acad. Linces Rendic., 15, 355 (1906)

2. H. A. Pohl, J. A. Bornmann, and W. Itoh, Semiconducting Polymers, Princenton University Plastics Lab. Tech. Rpt.60 C, January 1961; "Papers presented at the St. Louis Meeting", March, 1961. Am. Chem. Soc., Div. Polymer Chemistry, Vol. 1, No. 2, p.211

3. H. A. Pohl and D. A. Opp, J. Chem. Soc., 66, 2121 (1962).

4. M. Hatano, S. Kambara, S. Andokamoto, J. Polym. Sci., 51, S26 (1961)

5. A. A. Berlin, L. J. Boguslavskii, R. Kh. Burstein, N. G. Matveeva, A. I. Sherle, and N. A. Shurmovskaia, Dokl. Akad. Nauk SSSR, 136, 1127 (1961).

6. L. J. Boguslavskii, and L. S. Stilbans, Dokl. Akad. Nauk SSSR, 147, 1114 (1962).

7. C. K. Chiang, M. A. Druy, S. C. Gau, A. J. Heeger, E. J. Louis, A. G. MacDiarmid, Y. W. Park, H. Shirakawa, J. Am. Chem. Soc., 100, 1013 (1978).

8. R. H. Baughman, J. L. Bredas, R. R. Chance, R. L. Elsenbaumer and L. W. Shacklette, Chem. Rev., 82, 209 (1982).

9. "Electrical Properties of Polymers", Donald E. Seanor, Ed., Academic Press, New York 1982.

10. Y. Okamoto and W. Brenner, "Organic Semiconductors", Reinhold Publishing Corp., New York 1964.

11. R. C. Wheland and J. L. Gillson, J. Am. Chem. Soc., 98, 3916 (1976).

12. J. Mort, A. Troup, S. Grammatica, D. J. Sandman, J. Electron. Matter, 9, 411 (1980).

13. D. J. Berets and D. S. Smith, Trans. Far. Soc., 64, 823 (1968).

14. C. K. Chiang, Y. W. Park, A. J. Heeger, H. Shirakawa, E. J. Louis, A. G. MacDiarmid, J. Chem. Phys., 69, 5098 (1978).

15. D. Margosian and P. Kovacic, J. Polym. Sci. Polym. Chem. Ed. 17, 3695 (1979).

16. P. Kovacic and K. N. McFarland, J. Polym. Sci. Polym. Chem. Ed. 17, 1963 (1979).

17. S. L. Maisel, G. C. Johnson and H. D. Hartough., J. Am. Chem. Soc. 72, 1910 (1950).

18. J. Edmonds and H. W. Hill, Jr., U.S. Patent 3,354,129 to Phillips Petroleum Co. (1967). Chem. Abst. 68, 13598e (1968).

19. T. Yamamoto, K. Sanechika, and A. Yamamoto, J. Polym. Sci.: Polym. Lett. Ed., 18, 9 (1980).

20. E. Jones and I. M. Moodie, J. Polym. Sci. C, 2881 (1967).

21. J. S. Ramsey and P. Kovacic, J. Polym. Sci. A-1, 7, 127 (1969).

22. M. G. Voronokov, A. K. Khaliullin, V. Z. Annenkova, L. M. Antonik, L. M. Kamkina, E. N. Deryagina, and T. I. Vakui'skaya, Dokl. Akad. Nauk. SSSR, 228, 1341 (1976).

23. Z. V. Todres, S. P. Avagyn, and D. N. Kursanov, Zh. Org. Khim., 11, 2457 (1975).

24. M. P. Cava, M. V. Lakshmikantham, K.-Y. Jen, N. Benfaremo, W. S. Huang and A. G. MacDiarmid, Polymer Preprints, 24(1), 251 (1983).

25. K.-Y. Jen, N. Benfaremo, M. P. Cava, W.-S. Huang, and A. G. MacDiarmid, J. Chem. Soc., Chem. Commun., 633 (1983).

26. J. W.-P. Lin and L. P. Dudek, J. Polym. Sci.: Polym. Chem. Ed. 18, 2869 (1980).

27. G. Kossmehl and G. Chatzitheodorou, Mol. Cryst. Liq. Cryst., 83, 291 (1982).

28. C. Z. Hotz, P. Kovacic, and I. A. Khoury, J. Polym. Sci., Polym. Chem. Ed. 21, 2617 (1983).

29. M. Kobayashi, J. Chen, T.-C. Chung, F. Moraes, A. J. Heeger, and F. Wudl, Synthetic Metals, 9, 77 (1984).

30. A. Diaz, Chem. Scripta, 17, 145 (1981).

31. G. Tourillon and F. Garnier, J. Electroanal. Chem. 135, 173 (1982).

32. R. J. Waltman, J. Bargon, and A. F. Diaz, J. Phys. Chem., 87, 1459 (1983).

33. K. Kaneto, Y. Kohno, K. Yoshino, and Y. Invishi, J. Chem. Soc., Chem. Commun., 382 (1983).

34. G. Tourillon and F. Garnier, J Phys. Chem., 87, 2289 (1983).

35. T. Yamamoto, J. Chem. Soc. Chem. Commun., 187 (1981).

36. W. Bracke, J. Polym. Sci. Part A-1, 10, 975 (1972).

37. H. A. Pohl and J. R. Wyhof, J. Polym. Sci. Part A-1, 10, 387 (1972).

38. M. P. Cava, M. V. Lakshmikantham, K.-Y. Jen, N. Benfaremo , W. S. Huang, and A. G. MacDiarmid, Polym. Preprints, 24(1), 251 (1983).

39. K.-Y. Jen, N. Benfaremo, M. P. Cava, W.-S. Huang, and A. G. MacDiarmid, J. Chem. Soc., Chem. Commun., 633 (1983).

40. V. A. Zhorin and Yu. A. Berlin, J. Polym. Sci., Polym. Phys. Ed., 21, 929 (1983).

41. T. Yamamoto, K. Sanechika, and A. Yamamoto, Chem. Lett., 1079 (1981).

42. K. Sanechika, T. Yamamoto, and A. Yamamoto, J. Polym. Sci., Polym. Chem. Ed., 20, 365 (1982).

43. S. Tanaka, M. Sato, K. Kaeriyama, H. Kanetsuna, M. Kato, and Y. Suda, Makromol. Chem., Rapid Commun., 4, 231 (1983).

44. G. Kossmehl and M. Samandari, Makromol. Chem., 184, 2437 (1983).

45. M. H. Gutierrez, W. T. Ford, H. A. Pohl, J. Polym. Sci., Polym. Chem. Ed., 22, 3789 (1984)

46. J. P. Montheard and T. Pascal, Synthetic Metals, 9, 389 (1984).

47. C. Kossmehl and G. Chatzithedorou, Makromol. Chem. Rapid Commun., 2, 551 (1981).

48. J. E. Frommer, R. L. Elsenbaumer, and R. R. Chance, Organic Coatings and Applied Polymer Science Proceedings, 48, 552 (1983).

PART II

THE EFFECT OF DILUENTS ON THE GLASS TRANSITION TEMPERATURE OF STYRENE/DIVINYLBENZENE POLYMER NETWORKS

CHAPTER I

HISTORICAL BACKGROUND

Introduction

The depression of the glass transition temperature (T_g) by diluents (plasticizers) and composition dependence of T_g in polymer-polymer and polymer-diluent mixtures have been known for some time (1,2). Several empirical approaches (3,4), theoretical essays based on configurational entropy theories (5), and a classical thermodynamic interpretation (6) of the glass transition in polymer-diluent systems have been applied to interpret experimental results.

Recently Karasz and coworkers (7) studied the depression of glass transition temperature in polystyrene and styrene/divinylbenzene networks by addition of some diluents, such as ethylbenzene, ethyl acetate and m-diethylbenzene. They found that for the case of ethylbenzene, the experimental results had good quantitative agreement with the theory which predicts that, for a given diluent, the depression of T_g depends upon the change in heat capacity of the pure polymer or network.

The purpose of this study is to examine the T_g behavior of crosslinked polystyrene-divinylbenzene gels using as diluents toluene, chloroform, tetrahydrofuran (THF), and N,N-dimethylformamide (DMF), varying the degree of crosslinking of the networks, composition of network and structure of the plasticizing molecule.

The copolymer system

The copolymerization of divinylbenzene with styrene was first carried out by Staudinger (8) in order to demonstrate that crosslinking caused by the divinyl monomer would make the polystyrene insoluble in all solvents. The insoluble networks obtained from copolymerization of these two monomers have become important as backbone for synthetic ion exchange resins (9-11), in polymer-supported organic synthesis and in polymer-supported catalysts. Often the copolymers have attached chloromethyl groups that can be converted easily to polymer-bound esters and thioesters and to quaternary ammonium and phosphonium ions (12-14).

Polystyrene normally is a highly rigid and brittle resin. The use of a low concentration of divinylbenzene (DVB) to crosslink polystyrene results in a toughened product; higher concentration results in copolymers having lower tensile and impact strengths (15).

One method used to measure the degree of crosslinking of this copolymer was that used by Pepper (16) which involves the measurements of toluene absorbed by beads of

different degrees of crosslinking. This method applies Flory's equation (16) for a network polymer swollen by a solvent in order to calculate the molecular weight between crosslinks (M_c).

Plasticizers

Plasticizers are low molecular weight liquids or solids added to plastics and polymers to soften them. Plasticizers bring about this softening action by dissolving in the high polymer and lowering its glass transition temperature. Plasticizers may also serve another purpose. They lower the melt viscocity, thus making the material process or fabricate more easily and at a lower temperature. For practical reasons plasticizers must be relatively non-volatile, so they are usually limited to liquids with molecular weights of at least several hundred.

Most plasticizers have glass transition temperatures in the range from -50 to -150°C (17). The lower the glass transition temperature of the plasticizer, the more efficient it is in lowering T_g of the polymer-plasticizer mixture. Efficient plasticizers generally have low viscocities and low temperature coefficients of viscosity.

In some systems the plasticizer has a solubility limit, so at higher concentrations the plasticizer separates out as a second dispersed phase. Above the solubility limit,

additional plasticizer is ineffective in further reduction of T_g (18).

The glass transition and its depression due to plasticization can be correlated with physical and mechanical properties of polymers. For example Lep'chuk and Sedlis (19) related T_g with tensile strength, elasticity modulus, frost resistance, electrical volume resistivity, and moisture permeability of poly(vinyl chloride) plasticized by various materials.

Kanig (20) in his investigations of the glass temperature of polymer homologs, copolymers and plasticized polymers reached the following conclusions:

a) The smaller the plasticizer molecule, the more effective the plasticizer is in lowering T_g.

b) The efficiency of a plasticizer is greater when the polymer has a high T_g.

c) The first small amounts of plasticizer are the most effective, and increasing amounts become progressively less so.

d) The weaker the plasticizer-plasticizer affinity, in comparison to polymer-polymer affinity, the more efficient the plasticizer becomes.

The glass transition

Glasses constitute a class of amorphous solids prepared by melt-quenching and are distinguished by the unique transition, the so-called glass transition, that they exhibit. In a glass there is a frozen-in disorder in a state of quasi-equilibrium. Theoretical treatments of the glass transition have been either purely equilibrium (21,22) or purely kinetic (23) in nature. Many models (24) have been proposed to explain the glass transition but a clear picture of the nature of the transition has not yet emerged. For reviews of the phenomenon of the glass transition, see Kauzman (25), Boyer (26), and Rao (24).

Several methods have been applied to study the glass transition of organic and inorganic compounds: relaxation spectroscopy (27), mechanical relaxation (28), ultrasonic relaxation (29), Raman spectroscopy (30), NMR spectroscopy (31), spin-probe E.S.R. spectroscopy (32), Mossbauer spectroscopy (33), extended X-ray absorption fine structure (EXAFS) (34), specific volume, differential scanning calorimetry (35-37) and empirical softening point methods.

The glass transition temperature, (T_g) of a polymer is an important parameter, as its physical and mechanical properties change greatly at this temperature. In particular, it is well known that the glass transition temperature is an increasing function of the molecular weight for a linear polymer and of crosslinking density for crosslinked polymers. Theoretical equations of some

complexity which relate the glass transition with the molecular weight have been proposed (38). An empirical correlation based on isofree volume and viscous flow concepts (39) can be obtained in the form:

$$T_g = T_{g\infty} - K/\bar{M}_n \qquad [1]$$

T_g = glass transition for a polymer of finite molecular weight.

$T_{g\infty}$ = glass transition for an infinitely long polymer.

$\bar{M}_n$ = number average molecular weight.

K = empirical constant.

T_g has a significance to the theoretical polymer scientist, since it is the temperature below which, under the conditions of the experiment, there is no long range rotational movement about the bonds which make up the backbone of the polymer molecule, and hence below T_g the polymer is no longer capable of rubber-like behavior. In the glassy state a polymer cannot be deformed to the extent which is possible above its T_g.

Ueberreiter and Kanig (40) reported that the glass transition temperature of a polymer, (T_g), is elevated by crosslinking.

There are several different approaches for the correlation of the T_g of mixed amorphous systems. The simplest experimental equation for the change in T_g of a polymeric system with the addition of a plasticizer is (4):

$$T_g = T_{g1} - \beta\, w_2 \qquad [2]$$

T_{g1} = the polymer glass transition.

w_2 = weight fraction of plasticizer.

β = constant which varies from 200 to 500 K for different diluents in polystyrene.

This form of T_g equation has been obtained by a number of authors and by a variety of methods.

Kelly and Bueche (41) derived an equation considering polymer and solvent coefficients of thermal expansion and the effect of free volume on T_g:

$$T_g = \frac{\alpha_2 V_2 T_g + \alpha_1 (1-V_2) T_{g1}}{\alpha_2 V_2 + \alpha_1 (1-V_2)} \qquad [3]$$

where V_2 is the volume fraction of the solvent and α_2 and α_1 are the thermal coefficients of expansion of the solvent and polymer, respectively. This equation is considered valid only if dipolar interactions between the plasticizer and polymer are negligible.

On the other hand, Jenkel and Heusch (42) allowed for interactions between components, and they added an interaction term to the weighted T_g values of the pure components.

$$T_g = w_2 T_{g2} + w_1 T_{g1} + X w_2 w_1 \qquad [4]$$

where X is the interaction constant, and w_2 and w_1 are weight fractions of solvent and polymer respectively.

Pochan and coworkers (44) developed an empirical equation which relates the glass transition of mixed systems to their pure component T_g's:

$$\ln T_g = w_1 \ln T_{g1} + w_2 \ln T_{g2} \qquad [5]$$

where w_i is either volume or weight fraction of each component.

Other equations of the form of equation [1] are as follows:

Jenckel and Heusch (42) proposed an isofree volume relation (which means that the "free volume" or volume of the "holes" between segments in a sample such as polystyrene is a constant below its T_g, independent of both molecular weight and temperature):

$$T_g = T_{g1} - (\beta/\alpha) w_2 \qquad [6]$$

here w_2 = weight fraction of the diluent.

β = contribution of diluent to the increase of free volume.

α = difference between the thermal expansion coefficients above and below the glass transition temperature.

A viscous flow approach was followed by Kauzmann and Eyring (43) and the equation developed by them is given as:

$$T_g = a - bw_2 \qquad [7]$$

where a and b are constants.

Fox and Loshaek (44) on the other hand, have shown that the glass transition temperature (T_g) of a network can be related to the concentration of crosslinks by the equation

$$T_g = T_{g\infty} + K_\infty \rho - K \times 10^3/M \qquad [8]$$

Here, $T_{g\infty}$ = glass transition temperature of the corresponding uncrosslinked, infinite molecular weight polymer.

ρ = concentration of crosslink (in mole/g).

M = molecular weight of the primary polymer chains in (g/mole).

K_∞ and K = constants.

Different equations have been derived for the case of a polymer-polymer mixture. For example, Wood (45) gives the glass transition temperature as a weighted average of the glass transition temperatures of the components:

$$\alpha_1 M_1 M_{w1}(T_g - T_{g1}) + \alpha_2 M_2 M_{w2}(T_g - T_{g2}) = 0 \qquad [9]$$

M_1 and M_2 = mole fractions of the components of the mixture.

M_{wi} = the 'mer' (repeat unit) molecular weights of the polymers

T_{gi} = pure component glass transitions

α_i = thermal expansion coefficients of the pure components.

If the α_i are the differences in thermal expansion coefficients above and below T_g, equation [9] reduces to the Gordon-Taylor equation (46).

$$(1-w_2)(T_g-T_{g1}) + w_2K(T_g-T_{g2}) = 0 \qquad [10]$$

where the w_i are the component weight fractions and K is a constant, usually positive, which takes the place of the thermal expansion coefficients given in equation [9].

Fox (47) derived a simpler version of the Wood equation assuming that the quantity $\alpha_1 M_{w1} T_{g1} / \alpha_2 M_{w2} T_{g2} = 1$ producing:

$$1/T_g = M_1/T_{g1} + M_2/T_{g2} \qquad [11]$$

Finally Karasz and coworkers (48) used a quasi-thermodynamic theory to derive an expression for the depression of the glass transition temperature T_g of a polymer network by a diluent. This equation is given as:

$$T_g = \frac{X_1 \, \Delta C_p^{act}(X) T_{g1}(X) + X_2 \, \Delta C_{p2} T_{g2}}{X_1 \, \Delta C_p^{act}(X) + X_2 \, \Delta C_{p2}} \qquad [12]$$

where $$\Delta C_p^{act}(X) = \frac{\Delta C_{p1}(X=0) T_{g1}(X=0)}{T_{g1}(X)}$$

and X_1 and X_2 = mol fraction or weight fraction of polymer and diluent respectively

$T_{g1}(X)$ = glass transition temperature of network with (X) composition.

ΔC_{p1} = change of heat capacity of the polymer network.

ΔC_{p2} = change of heat capacity of the diluent at T_{g2}.

A limitation of this equation is that ΔC_{p2} values of diluents are not available in the literature.

CHAPTER II

EXPERIMENTAL

Reagents and Solvents

Styrene (Aldrich), and 55% active divinylbenzene (Polysciences) were used as received without removal of inhibitors. They did not contain any material that precipitated on addition to methanol. Azobisisobutyronitrile (AIBN, Aldrich), Gelatin (Knox Gelatin Co., pharmaceutical grade, lime hydrolyzed), poly(diallyldimethylammonium chloride) (Calgon Corp., Cat Floc T), and sodium dodecylbenzensulfonate (Polysciences) were used without purification.

The copolymers used in this work were polystyrenes crosslinked with divinylbenzene. The 2, 6, and 10% crosslinked were prepared using the procedure described by Ford and Balakrishnan (14). The 1% crosslinked sample was from Lab. Systems. Inc., and vinylbenzyl chloride (VBC) from Dow Chemical Co.

Analytical Procedure and Apparatus

The glass transition temperatures of the polymers were determined with a Perkin-Elmer differential scanning

calorimeter (DSC-2C) by the midpoint method. Values of C_p were determined using alpha aluminum oxide (corundum) of known specific heat (49) as reference. The differential scanning calorimeter was equiped with a thermal analysis data station (TADS) system (Model 3600 Perkin-Elmer) which was used to analyze the T_g and ΔC_p of the thermograms using the software programs provided with the equipment. Aluminum pans were used for copolymers without diluent systems, and sealed stainless steel pans were used for the gels with solvent.

For the sample preparation the crosslinked polymer beads, particle-diameter 45-75 m (200-325 mesh size), were swelled in toluene, chloroform, DMF, or THF. The samples were allowed to reach equilibrium at room temperature for 5 days, according to Pepper's method (9).

A Perkin-Elmer TGS-2 microbalance was used for weighing of samples. Different weight fractions of solvent were obtained by partial evaporation of solvent from saturated swelled gels. After the T_g measurement the lids of stainless steel pans containing the samples were perforated, and the samples were heated at 130 °C for 24 h to evaporate the solvent. The weight of solvent (4-20 mg) is determined by difference before and after evaporation.

Two other procedures were attempted for preparation of the polymer-diluent samples. One of them involved the absorption of solvent by the copolymer in a saturated atmosphere of solvent in a closed container. The other

method involved the use of a syringe to add a known amount of solvent to a weighed sample of copolymer. Unfortunately, these two methods did not give good results. This is probably due to the non-homogeneous distribution of the solvent in the copolymer by the second method and to incomplete equilibration by the first method.

The glass transition temperature, deduced by calorimetric analysis, depends on the thermal history of the polymer and on the speed of heating and cooling. To make the measurements among the different samples comparable, each swollen sample was heated and cooled three times at 40 K/min.

With the intention of increasing the reproducibility of the measurements, the T_g's of dried copolymers were measured for different values of heating rate and extrapolated to zero heating rate. The correction factor obtained here was used for the swollen samples when the instrument was calibrated with a standard only at one heating rate. When the instrument was calibrated with standards at different heating rates there was no reason to use these correction factors.

Experiments at subambient temperatures involved the use of liquid nitrogen as a coolant, and from 100 K to 350 K, helium was used as a purge gas. Nitrogen was used as purge gas at temperatures higher than 350 K. The level of liquid nitrogen coolant, used during sub-ambient runs, was always maintained at a constant level in the cooling pan.

The melting transitions of pure samples of mercury, dodecane, benzoic acid, indium and lead were used for temperature calibration, which was monitored at frequent intervals throughout the series of measurements.

The heat capacity measurements were carried out in quadruplicate at a 20 K/min heating rate under nitrogen. The cooling rate for all the samples in each run was 40 K/min from 20 degrees above of the glass transition. The weight of each sample was 5 to 10 mg in aluminum pans. The base line was obtained with two empty aluminum pans, and the weight of the standard alpha aluminum oxide was 20 mg.

In our measurements, T_g is taken as the mid-point in the thermogram as measured from the extensions of the pre- and post-transition base lines; that is, when the heat capacity changes assumes half the value of this change upon going through the transition. While the choice is somewhat arbitrary and other authors have suggested alternate techniques such as taking T_g as the first evidence of the displacement of the thermogram from the pre-transition baseline, we have found that the above method is the most reliable and reproducible.

Basically the criterion used to get the best value of T_g was that in which two approximately parallel lines extending from pre- and post-transitions were obtained. Following this procedure our T_g values of duplicate runs agreed within 5 K.

RECOMMENDATIONS

The following are recommendations for working with the Perkin-Elmer DSC-2C instrument at subambient temperatures and some suggestions that will make work with this instrument easier.

At subambient temperature, moisture condensed on the sample holder enclosure cover and block. This moisture affected the base line of the thermograms. To avoid this moisture we followed the recomendations given by the D.S.C. manual at subambient temperature but it was necessary to use poly(dimethylsiloxane) high vacuum grease inside of the sample holder enclosure block where the six long binding head screws are located, and in the base were the cold finger is attached. (See Figure 7.3 in the DSC-2C manual). Another recomendation is the use of a desiccant such as anhydrous $CaSO_4$ (drierite) inside the dry box.

The use of liquid nitrogen can reduce the temperature of the sample block to 90 K, but the minimum starting temperature in the software for a thermogram is 100.1 K.

If the scanning autozero function (SAZ) is used to eliminate an element of curvature in the base line, the temperature program must start at a temperature lower than the desired minimum temperature of the thermogram. For example, if a heating rate of 40 K/min is used, 1) start TADS, 2) ask for SAZ program, 3) start heating with control on DSC, and 4) immediately start TADS. After about 30 s

the thermogram begins on the monitor at a temperature 20 K higher than the starting temperature set on the DSC.

During our work at subambient temperature 12-15 liters of liquid nitrogen were consumed per day. It would be convenient to have a liquid nitrogen cylinder near the D.S.C.

At subambient temperature helium was used as a purge gas, but above 350 K the base line was affected. We recommend helium from 100 K to 340 K and nitrogen above 340 K. It is recommended that the holder enclosure be purged with about 20 cc/min of dry He or N_2 per cavity. With the internal restrictor system of the DSC-2C, this flow rate will be realized with an inlet pressure of 20 psi.

One of the more difficult problems during this work was the calibration of the instrument. The slope of the thermogram is sensitive to slope control and ΔT balance control. Slope should be adjusted every time the ΔT balance control is changed. The conditions for calibrating the instrument with aluminum pans were different from those used for stainless steel pans. It was necessary to reduce the slope of the base line with the use of the stainless steel pans. The instrument should be calibrated every time the carrier gas is changed. The slope of the base line is sensitive to the position of the sample holder lids and impurities present in the sampler holder. If residues of organic compounds are present in the sample holder, they can be eliminated by heating the instrument to 1000 K for

10-15 minutes in air. (Be sure that no alumnium pans are present on the sample holder because they can melt and ruin the heating unit).

Do not attempt to force sample holder lids into the cups (they fit easily) because the platinum-iridium post which supports the holders may bend or break-off. When the lids do not fit easily (without using excessive force), it is necesary to reshape them with the reforming tool provided.

During our work it was necessary to use the microbalance of the thermogravimetric analyzer TGS-2 for weighing our samples; vibration of the balance hangdown ribbon and sample pan was observed sometimes during the weighing of stainless steel pans and the pans fell down. To avoid this problem the sample pan of the balance was covered with a piece of aluminum foil to have a smooth surface.

During our experiments we used solder O-rings (40% Pb, 60% Sn) to avoid the glass transition temperature of Viton at 240-250 K. They were prepared from solder wire which was cut in small pieces to fit on the stainless steel sample container. Do not heat the instrument above 670 K when using solder O-rings because they melt and can damage the heater unit.

The Viton O-rings (copolymer of vinylidene fluoride and hexafluoro propylene) are provided with the stainless steel sample containers by Perkin-Elmer. These Viton O-rings

have a temperature range limitation from 245 K (glass transition) to 573 K. At this temperature the Viton O-ring will not survive.

The rate of solvent evaporation from stainless steel/Viton (3 % of chloroform in 12 h) is smaller than that of the stainless steel/solder (1% in 20 min) at room temperature.

CHAPTER III

RESULTS AND DISCUSSION

In many applications of differential scanning calorimetry, notably the determination of purity, the instantaneous rate of melting or crystallization, and the glass transition temperature, the calibration of the instrument is of great importance. All of these determinations are very sensitive to the instrumental conditions. For this reason a series of experiments was carried out to compare our results with those from literature.

Effect of Scanning Rate on Melting Point of Indium

Because the thermal lag between the sample and the temperature sensor of the DSC-2C depends on scan speed, the temperature in the DSC compartment was calibrated for heating rate with melting point standards such as indium, lead, benzoic acid and mercury by using a procedure described by Flynn (50).

We observed that when the DSC-2C is calibrated at low scan rate, the indicated temperature is too high at

faster scan speed. We calibrated the instrument at 5 K/min using indium as standard in aluminum sample pans, we also scanned this standard at 10, 20, 40, and 80 K/min to determine the corrections to apply to the indicated temperature at these scan speeds. These data can be seen in Tables I and II. Correction factors for scanning rate reported on Table II are the factors by which temperature in K indicated on the DSC-2C should be multiplied in order to obtain correct temperatures at the chosen scanning rate.

TABLE I

Effect of Scanning Rate on Melting Point of Indium (10.3 mg)

Scanning Rate	Melting Point, K
5 K/min	429.08
10 K/min	430.04
20 K/min	431.67
40 K/min	434.68
80 K/min	439.67

TABLE II

Correction Factors for Scanning Rate

Scanning Rate	Factor
10 K/min	0.9977
20 K/min	0.9940
40 K/min	0.9871
80 K/min	0.9759

Glass Transition Temperature of PS-CO-DVB-1% + 25% VBC as a Function of Sample Weight

In order to see the effect of sample weight on the glass transition temperature, different sample weights of PS-CO-DVB-1% + 25% VBC (1% crosslinked polystyrene with divinylbenzene and 25% vinylbenzyl chloride) were run at constant scanning rate of 40 K/min and a cooling rate of 320 K/min under nitrogen. The results can be seen in Table III.

TABLE III

Glass Transition Temperature of PS-CO-DVB-1% + 25% VBC as a Function of Sample Weight

	RUNS		
Sample (mg)	2nd	3rd	$\bar{X}$
1.2	377.8	379.2	378.5
5.0	379.1	379.2	379.1
10.0	380.5	380.1	380.3
15.0	380.5	381.4	381.0
20.0	380.9	381.5	381.2

As we can see from this table, larger samples undergo their glass transition at a higher temperature. This is expected because thermal lag should increase with sample size.

Glass Transition Temperature of PS-CO-DVB-2% as a Function of Mesh Size

Five different samples (10 mg) of PS-CO-DVB-2% with different mesh size were run at constant scanning rate (20 K/min) under nitrogen. The purpose of this experiment was to see the influence of mesh size on the glass transition temperature. As we can see from the data on Table IV, the glass transition temperature (average of three runs) apparently does not depend on particle size. The little differences in T_g can be due to differences in pan weights, change in the position of platinum leads on the sample holder, or polymer sample inhomogeneities.

TABLE IV

Effect of Mesh Size on T_g for PS-CO-DVB-2% at 20 K/min

Mesh Size	T_g, K
40-60	386.5
60-100	386.4
100-200	386.2
200-325	385.9
325-400	387.0

Glass Transition as a Function of Cooling Rate for PS-CO-DVB-2% at Constant Heating Rate

The T_g of the PS-CO-DVB-2% (10 mg) was determined at 20 K/min heating rate immediately after it was cooled at different rates. The sample was kept at 400 K for 3 minutes before cooling to allow for relaxation. The data are shown in Table V. The T_g is an average of three runs. No change in T_g outside of experimental error was observed when the samples were cooled at different cooling rates. However, there is a trend in which the T_g value increases for faster cooling rates, which is in good agreement with the experimental results of other authors (51-53).

TABLE V

Effect of Cooling Rate on the Glass Transition for PS-CO-DVB-2% at Constant Heating Rate

Cooling Rate, K/min	T_g, K
20	387.5
40	387.5
80	387.6
160	387.9
320	388.2

Glass Transition after Quenching with Liquid Nitrogen

The T_g of polystyrene and of different networks (10 mg) was determined at 40 K/min heating rate immediately after they were quenched in liquid nitrogen. The T_g values are higher than those reported in Table IX, and this is again in good agreement whith the experimental results of other authors (51-53) that after faster cooling, the subsequent T_g is higher.

This behavior is a result of changes in the structure or configuration of the glass. The time scale on which this structural response occurs is highly temperature dependent and at sufficiently low temperatures becomes so long that a rapid temperature change can "freeze in" the liquid structure. The T_g values of the PS and networks are reported in Table VI.

TABLE VI

Glass Transition Temperature after Quenching with Liquid Nitrogen

Sample	Glass Transition, K
Polystyrene	376.5
PS-CO-DVB-1%	383.2
PS-CO-DVB-2%	388.5
PS-CO-DVB-6%	392.5
PS-CO-DVB-10%	405.7

Glass Transition as a Function of Heating Rate

Different samples of polystyrene and crosslinked networks were heated at different scanning rates. The glass transition temperature increased as the heating rate increased. These data are shown in Table VII. The cooling rate was the same as the heating rate. For each sample at each heating rate an appropriate standard was used for calibration.

It is known (54) that the glass transition is a time-dependent as well as temperature-dependent phenomenon, so it is expected that the glass transition temperature will change with scan speed. To compare results from different equipment using different heating rates, it is necesarry to obtain glass transition temperatures at several scan speeds and extrapolate either to zero speed or to a standard speed.

Glass Transition as a Function of Crosslinking

Thermograms of polystyrene and different networks are shown in Figure 1. The thermograms were run at a scanning rate of 40 K/min under nitrogen. All samples (5-10 mg) had the same thermal history. As we can see from this figure, T_g increases by increasing the content of DVB. The thermogram is the third run for each of these samples.

The increase of T_g by crosslinking was first observed by Ueberreiter and Kanig (40) from plots of volume versus temperature with copolymers of styrene and DVB. In their

TABLE VII

Glass Transition as a Function of Heating Rate

Sample	Scanning Rate				
	0 K/min	10 K/min	20 K/min	40 K/min	80 K/min
Pressed Polystyrene	361.1	363.4	365.9	369.2	377.9
Polystyrene	362.8	365.0	367.6	371.7	380.8
PS-CO-DVB-1% 25% VBC	376.0	377.0	378.6	379.8	390.2
PS-CO-DVB-2%	382.0	384.4	386.6	388.9	394.0
PS-CO-DVB-6% 25% VBC	385.0	387.4	389.2	392.2	400.9
PS-CO-DVB-10%	388.5	390.3	393.4	397.8	407.4

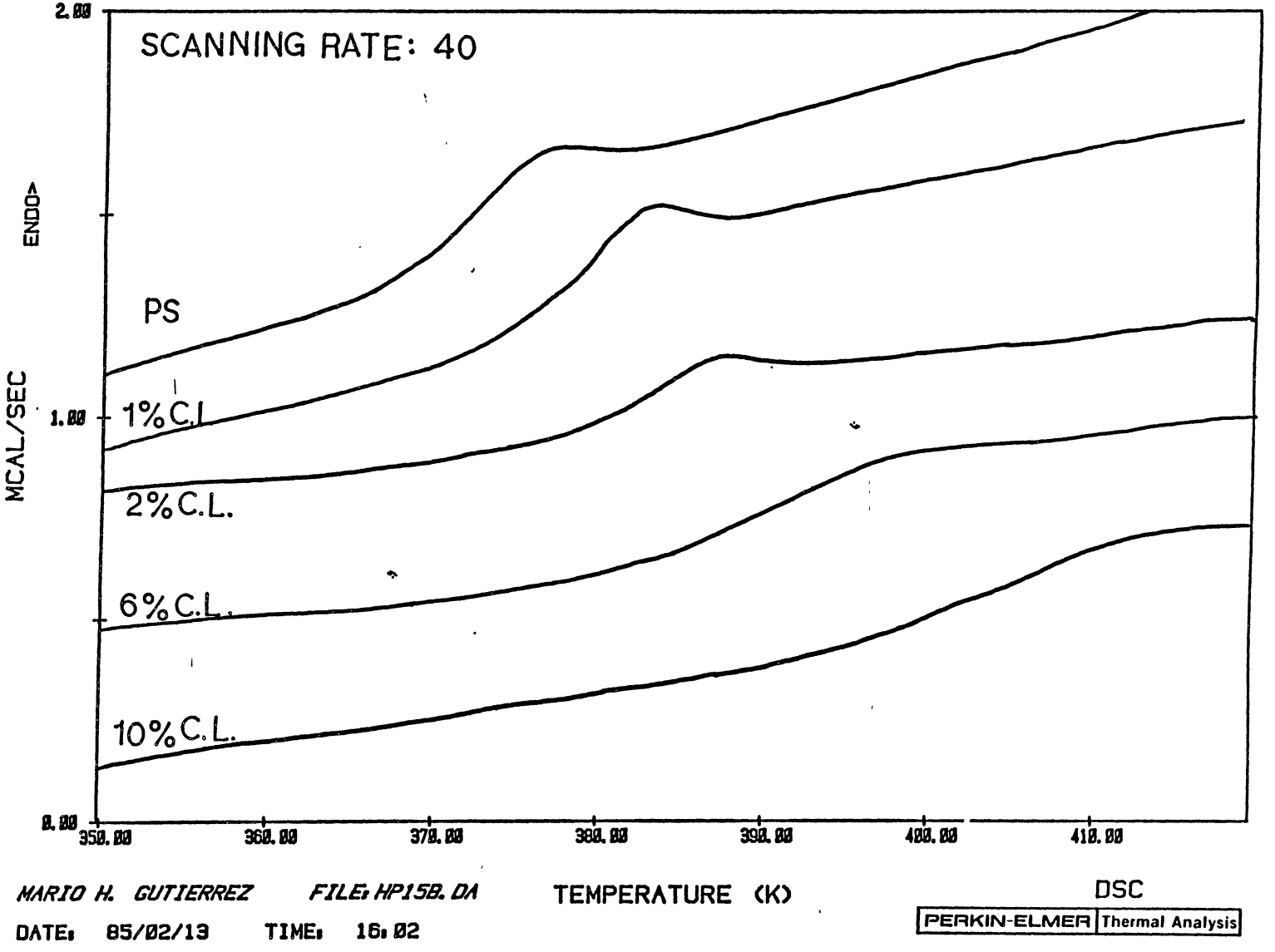

Figure 1. Glass transition as a function of crosslinking.

experiments the T_g was taken at the point of intersection of two straight lines which represent the volume-temperature coefficients in the liquid and in the glassy state. They found that the elevation of the glass transition temperature T, is given by the equation:

$$\Delta T = T_g(n) - T_g(n=0) = 586n \qquad [13]$$

where n = mol fraction divinylbenzene.

On the other hand Glans and Turner (55) reinvestigated the effect of crosslinking on T_g by differential scanning calorimetry of networks prepared by copolymerization of styrene and p-divinylbenzene.

During their work, an endothermic peak near T_g appeared on the first run of a lightly crosslinked network. No such peak appeared in subsequent runs with quench-cooled samples. This phenomenon was observed in our case with the polystyrene and copolymers with 1 and 2% of DVB (See Figure 2). This endotherm is attributed to a thermal relaxation process. It is a function of the heating rate, and it can be explained by purely kinetic considerations (56). During the vitrification, the system is, in effect, inmobilized in a metastable state at a temperature and an energy level which depend appreciably on the cooling rate. The heat capacity of the vitrified system depends only on small amplitude molecular motions, such as the vibrations and partial rotations of the elementary groups. The endotherm observed during subsequent heating corresponds to the onset

of large amplitude motions which are characteristic of the rubbery state. When the vitrified sample is kept at room temperature for a long time (days, weeks, or months), it slowly relaxes to a more stable conformational state at room temperature. The first thermogram of such a sample then shows an endotherm upon heating as soon as long range motion is possible. That endotherm is due to transformation of the polymer chains from their stable conformation at room temperature to their stable conformation at T_g. This peak can complicate the interpretation of the T_g from the thermogram. Sometimes this endothermic peak was superimposed with a glass transition. In order to eliminate it, it is convenient to stop the heating run, cool the sample, and rerun.

Determination of Change in Heat Capacity at T_g by Differential Scanning Calorimetry

From Figure 1, we can see that the change in heat capacity ΔC_p at the glass transition temperature decreases as the crosslinking increases. This phenomenon was observed by Glans and Turner and recently by Karasz and coworkers (7). Similar decreases in ΔC_p at T_g with increased crosslinking were obtained by Moy (57). There is little difference in the ΔC_p values at 10 to 12 percent crosslinking. Moy's values of ΔC_p for 12% crosslinking is little lower than ours for 10% crosslinking (See Table XI). This could be due to the presence of

monomers and/or oligomers of low molecular weight in the commercial samples that Moy used.

The change in heat capacity at T_g was determined by O'Neill's method (37). The sample is subjected to a linear temperature program, and the heat flow rate into the sample is measured continuously. The heat flow rate is proportional to the instantaneous specific heat of the sample. In our experiments α-aluminum oxide (corundum) (Aldrich reagent 60-200 mesh) was used as standard, for which specific heat has been determined to five significant figures in the temperature range 0 to 1200 K (48).

Results from samples of styrene copolymerized with different amounts of DVB are shown in Table VIII. Increased degree of crosslinking lowers the incremental specific heat at T_g.

The incremental specific heat at T_g is associated with the number of the degrees of freedom or structural features that are frozen in the glassy state and set free in the rubbery liquid. Roe and Tonelli (58-59) concluded that the sum of the contributions of the conformational and torsional specific heat of polymer main chains and side groups is related to the specific heat difference between the liquid and glassy state, but these contributions account for much less than the experimental values of ΔC_p. In the limit of high crosslinking, the polymer network may be approximated by a rigid lattice. At this stage we can expect the configurational effects to be minimal and the

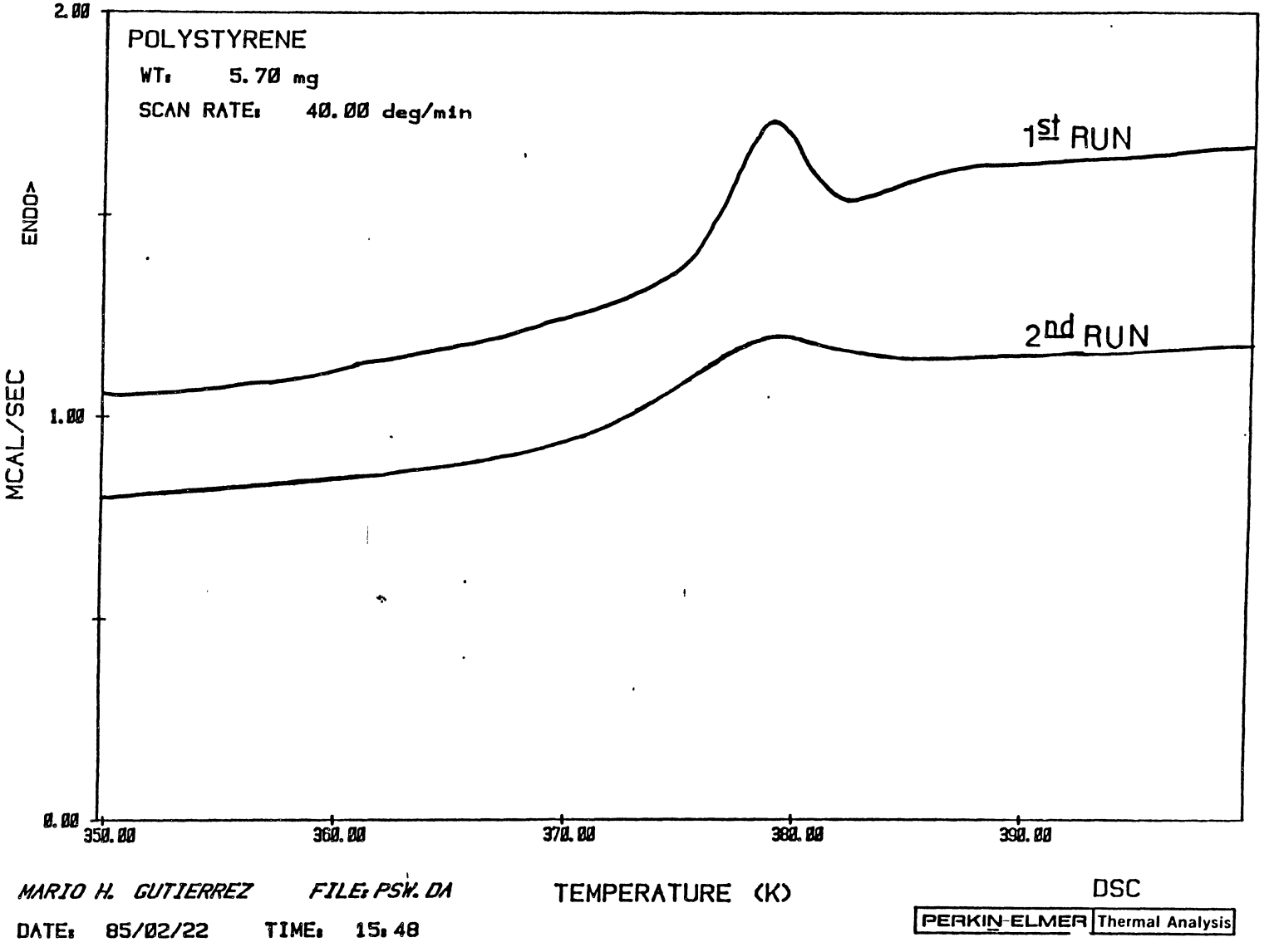

Figure 2. DSC thermograms of polystyrene.

vibrational modes to become an important part of the isobaric heat capacity (59).

Goldstein (60), on the other hand, proposed that the specific heat increment also contains significant contributions from non-configurational sources such as 1) changes in the lattice vibrational frequencies at T_g, 2) changes in the anharmonicity of vibrations at T_g, and 3) the number of molecular groups participating in secondary relaxations.

TABLE VIII

Heat Capacity* at the Glass Transition of PS/DVB Networks

Sample	Run			
	2	3	4	$\bar{X}$
POLYSTYRENE	0.25	0.28	0.26	0.26
PS-CO-DVB-1%	0.25	0.23	0.27	0.25
PS-CO-DVB-2%	0.22	0.21	0.23	0.22
PS-CO-DVB-6%	0.21	0.20	0.20	0.20
PS-CO-DVB-10%	0.12	0.14	0.14	0.14

* abs J/g-deg

Calculation of ΔC_p^{act} and f^{act} for Crosslinked Polystyrenes

DSC measurements of crosslinked samples (Figure 1) show a pronounced widening of the T_g transition range as crosslinking increases due to the fact that the chains between crosslinks are of different lengths. Since the cross-linking is equivalent to the introduction of strong attractive interaction between different chains, this leads to a higher glass transition temperature. With the increasing temperature the longest chains in the network are the first to be activated. Moreover, the crosslinking of polymers chains by covalent bonds reduces the number of units capable of being thermally activated.

Measurements of Uberreiter and Kanig (40) on styrene/divinylbenzene networks show that, for less than four carbon atoms between crosslinks, thermal activation of that part of the network is impossible. ΔC_p becomes vanishingly small at high degrees of crosslinking. The measured incremental change in specific heat represents only the activation of those units that are capable of rotating around the valency bonds of the chain.

Karasz and coworkers (7) define $f^{act}(X)$ as the fraction of chain units capable of being activated at T_g for a degree of crosslinking (X). The incremental change in specific heat per mole of units capable of being activated $\Delta C_p^{act}(X)$ is then given by

$$\Delta C_p^{act}(X) = \Delta C_{p1}(X)/f^{act}(X) \qquad [14]$$

where $\Delta C_{p1}(X)$ is the experimental value of the incremental change in specific heat per mole of chain units.

The fraction of units participating in the glass transition is given by

$$f^{act}(X) = \Delta C_{p1}(X)/\ \Delta C_{p1}(X=0) \qquad [15]$$

However, Simha and Boyer (61) presented arguments that for non-crosslinked polymers the product $\Delta C_{p1}Tg_1$ is approximately constant. For cross-linked polymers this remains equally valid, according to Karasz (7), provided ΔC_{p1} is taken to be the incremental change in specific heat per mole of units capable of being activated (ΔC_p^{act}). Then, instead of assuming that $\Delta C_p^{act}(X)$ is independent of X, it is more reasonable to assume the following:

$$\Delta C_p^{act}(X)T_{g1}(X) = \Delta C_{p1}(X=0)T_{g1}(X=0) \qquad [16]$$

$$\text{or } \Delta C_p^{act}(X) = \Delta C_{p1}(X=0)T_{g1}(X=0)/T_{g1}(X) \qquad [17]$$

Table IX gives different values for ΔC_p^{act} and f^{act} for the different PS/DVB networks. As we can see from these data, the f^{act} and ΔC_p^{act} decrease as the % crosslinking is increased, which is in good agreement with the theory. The T_g values reported in this Table (obtained from samples run under nitrogen) differ somewhat from those reported in Table VI and VII because in Table VI the samples were

TABLE IX

Thermal Property Relationships of PS/DVB Networks

Sample	Tg	ΔCp	ΔCpTg	11.5/ΔCp	f^{act}	ΔCp^{act}
Polystyrene	371	0.26	97.5	27.0	1.00	0.26
PS-CO-DVB-1%	377	0.25	95.3	26.0	0.96	0.26
PS-CO-DVB-2%	382	0.22	85.1	23.0	0.88	0.25
PS-CO-DVB-6%	389	0.20	79.3	21.2	0.80	0.25
PS-CO-DVB-10%	404	0.14	55.3	14.0	0.58	0.24

ΔCp = abs J/g-deg , ΔCpTg = abs J/g , 11.5/ΔCp = (gm/mol-bead)

ΔCp^{act}= abs J/g-deg

quenched with liquid nitrogen and in Table VII the samples were run under variable laboratory air instead of a constant flow of nitrogen.

Another observation from Table IX is that the product $\Delta C_p T_g$, which is considered to be a measure of the fraction of the volume available for the thermal motion of the polymer in the glassy state (61), is not a constant, which means that as the crosslinking increases the increase in free volume at T_g decreases.

Finally, the column 11.5/ ΔC_p is reported because of an empirical observation of Wunderlich (62) that the incremental specific heat at the glass temperature per unit "bead" is constant. ΔC_p = 11.5 J/mole-bead-K, in which a bead is the smallest movable structural unit that contributes to the heat capacity. From our data, as the crosslinking increases, the system becomes more tightly bound, the size of the "equivalent bead" increases, and hence the ΔC_p per unit mass decreases.

Correlation between the Loss of ΔC_p at T_g and the Average Molecular Weight between Crosslinks

The correlation between ΔC_p at T_g and the average molecular weight between crosslinks can be made through swelling measurements. Flory (16) has derived the following equation:

$$-[\ln(1-V_{2m}) + V_{2m} + X_1 V_{2m}^2] = (V_1/\bar{V}M_c)(1-2M_c/M)(V_{2m}^{1/3}-V_{2m}/2) \quad [18]$$

for a network polymer swollen by a solvent. In this equation V_{2m} is the volume fraction of the solute at swelling equilibrium, X_1 is the interaction parameter, V_1 is the molar volume of solvent, M is the primary molecular weight of a polymer chain (assumed to be infinity), M_c is the molecular weight between crosslink points, and $\bar{V}$ is the specific volume of the polymer.

The relationship between volume ratio of swelling q_v and the weight ratio of swelling q_w is given by:

$$q_v = 1/V_{2m} = 1 + (d_2/d_1)q_w - d_2/d_1 \quad [19]$$

where d_1 is the density of the solvent and d_2 is the density of the swollen polymer.

For toluene and polystyrene it is known (63) that $\bar{V}$ = 0.952 mL, V_1 = 105.6 mL, X_1 = 0.38 , d_1 = 0.872 g/mL, and d_2 = 0.978 g/mL. From the last two equations and these data we are able to calculate the average molecular weights between crosslinks, M_c, and the average number of monomer units between crosslinks for PS/DVB networks.

Table X gives the weight swelling ratios (q_w) of the different PS/DVB networks and four different solvents obtained in our laboratory by using Pepper's method (9) and Table XI gives the average molecular weight between crosslinks in PS/DVB networks and those obtained by Moy (57).

TABLE X

Swelling Ratio of the PS/DVB Networks

Sample	q_w			
	Toluene	Chloroform	DMF	THF
PS/DVB 1%	4.2	7.0	2.4	4.1
PS/DVB 2%	3.1	5.5	2.3	2.8
PS/DVB 6%	2.2	4.4	2.2	2.0
PS/DVB 10%	1.8	2.6	1.7	1.4

TABLE XI

Average Molecular Weight between Crosslinks in Toluene-Swollen PS/DVB Networks

Sample	q_w	q_v	V_{2m}	M_c	n	ΔC_p
PS/DVB 1%	4.2	4.5	0.22	5479	52.6	0.25
PS/DVB 2%	3.1	3.3	0.30	2573	24.7	0.22
PS/DVB 2%*				2884	27.7	0.24
PS/DVB 4%*				1505	14.5	0.20
PS/DVB 6%	2.2	2.4	0.41	1116	10.7	0.20
PS/DVB 8%*				450	4.3	0.12
PS/DVB 10%	1.8	1.9	0.51	577	5.5	0.14
PS/DVB 12%*				219	2.1	0.10

* Values reported by Moy (57).

In this table n = mean number of styrene units per crosslinked unit defined as $n = M_c/104$.

From Tables IX and XI we can conclude that ΔC_p at T_g becomes vanishingly small when the number of monomer units between crosslinks is reduced.

Heat Capacity at the Glass Transition Temperature for Toluene

From the thermogram of toluene given in Figure 3 we can appreciate the glass transition at 113 K, the crystallization peak at 135 K and the melting point of toluene at 176 K.

The amount of toluene in the amorphous state responsible for the T_g was calculated by the following procedure: The heat of fusion corresponding to the endothermic peak at 176 K is assumed to be due to the entire sample. Then the heat of crystallization corresponding to the exothermic peak at 136 K is due to the fraction of the sample that was amorphous at the 113 K glass transition. Now from here the toluene was 34% crystalline and 66% amorphous at 113 K when Tg was determined, and only 3.93 mg of the 5.97 mg corresponds to the amorphous state. The ΔH_m of toluene obtained in our laboratory was 17.8 cal/g after the calibration of the instrument with mercury, this value is in good agreement with that reported in the literature 17.17 cal/g (68).

To determine the heat capacity at the glass transition (see Figure 4), we used O'Neill's method (37) with α-Al_2O_3 as standard. The ΔC_p of toluene at the glass transition was 0.56 abs J/deg-g.

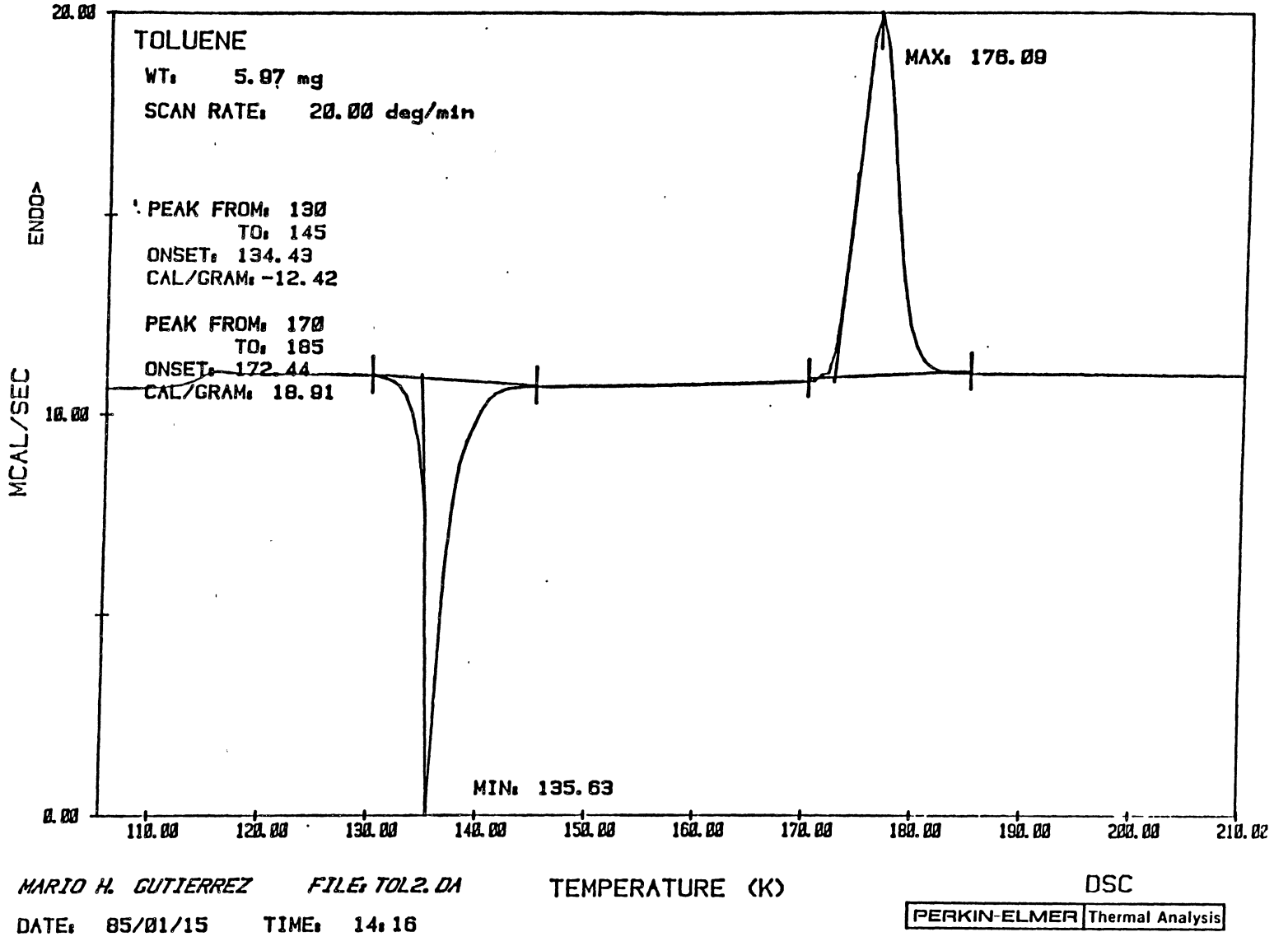

Figure 3. DSC thermogram of toluene.

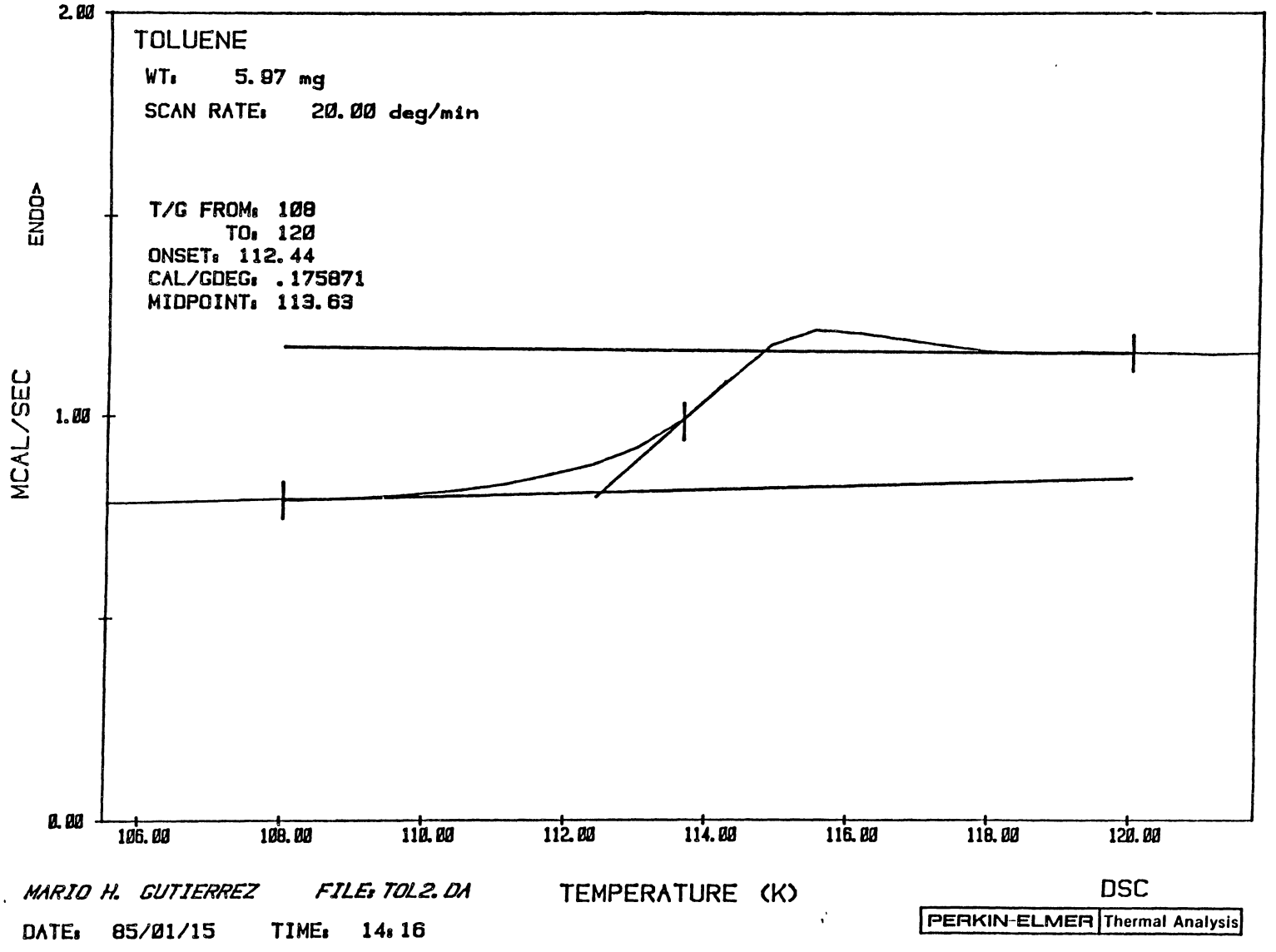

Figure 4. DSC thermogram of toluene showing the glass transition temperature.

Depression of Glass Transition Temperature by Diluents and Comparison with Theoretical Values (Karasz and Pochan Equations)

The mechanical and physical properties of polymers and the diffusivities of small molecules through polymers change at the glass transition temperature, and diluents affect these properties. The depression of glass transition temperature in styrene/divinylbenzene networks by the addition of toluene, chloroform, N,N-dimethyl-formamide (DMF), and tetrahydrofuran (THF), has been investigated by differential scanning calorimetry. The solvents are among those most commonly used for reactions of polymer supported reagents and catalysts, for NMR spectroscopy, and for size exclusion chromatography in polystyrene networks. The experimental results were compared with the equations of Karasz (7) and Pochan (4), but due to the lack of ΔC_p values at T_g of solvents in this investigation and the literature, the Karasz equation could be applied only for the case of toluene, for which the ΔC_p value at T_g was determined by D.S.C. in our laboratory.

Thermograms showing the depression of T_g by different solvents (with solvent concentrations much higher than those used by Karasz and coworkers (7) in their systems)

in different crosslinked samples are in Figures (5-14) for toluene, Figures (19-26) for chloroform, Figures (31-37) for DMF, and Figures (42-46) for THF.

As we can see from this series of thermograms, there are two changes in the slope of the curves, one in the region of 240-260 K that corresponds to the glass transition temperature of Viton O-ring in the stainless steel pan, and a second that corresponds to the glass transition temperature of the gel, which changes as a function of solvent composition.

The T_g of the Viton interfered with determination of T_g of some samples. For this reason replaced Viton with Teflon and with solder (an alloy of 60% Sn - 40% Pb) to eliminate this problem. We also tried Teflon O-rings but discarded them due to the presence of different peaks in the Teflon thermogram in the region of 250-290 K. With solder no signals in the region of 100-300 K were observed. The thermograms of Figures 6-8, 10, 11 and 13 represent those samples with toluene in which solder alloy was present in the stainless steel pan. As we can see from these thermograms the Tg at 240-260 K of Viton is absent and only the melting peak at 180 K of toluene and Tg of the gels can be observed. Another observation in figure 7 and 8 is that at 140-150 K there exists a little exothermic peak, this peak is due to the crystallization of toluene which increases with the increase of the number of the runs. For the case of chloroform, the thermograms of

Figures 20, 22, 24 and 26 represent those samples were the solder alloy was present and only the glass transition of the gel at different solvent compositions are observed. Finally, Figures 33, 35, and 37 for DMF and Figure 43 for THF represent those thermograms in which solder alloy was present.

The one difficulty with solder was that it did not give tightly sealed stainless steel pans, and solvent evaporated slowly from our samples. The amount of chloroform lost at room temperature was of the order of 1% in 20 minutes. The loss of solvent from our samples during T_g determinations was much less because we worked at subambient temperature for no more than 15 minutes with each sample.

Comparisons between experimental values of T_g and those calculated from the Karasz and the Pochan equations for toluene in four polystyrene networks are shown in Figures (15-18).

According to Karasz (48) the glass transition temperature in network polymer/diluent systems (for low diluent concentration) is given by the equation

$$T_{g12} = \frac{X_1 \Delta C_p^{act}(X) T_{g1}(X) + X_2 \Delta C_{p2} T_{g2}}{X_1 \Delta C_p^{act}(X) + X_2 \Delta C_{p2}} \quad [20]$$

which represents an extension of the theoretical treatment given by Couchman (64). The above equations are for two-component systems, where T_{g12} is the glass transition

temperature of the mixture, T_{g1} and T_{g2} are the glass transition temperatures of the pure components, ΔC_{p1} and ΔC_{p2} are the incremental changes in heat capacity at $T_{g1}(X)$ and T_{g2} respectively of the pure components, X refers to the degree of crosslinking, such that X=0 represents polystyrene, X_1 and X_2 are the mole or mass fractions of the pure components and ΔC_p^{act} has been explained in the last section.

The depression of the glass transition temperature as a function of concentration of diluent is given by:

$$\frac{dT_{g12}}{dX_2} = - \frac{\Delta C_{p2}\ Tg_1(X) \quad [T_{g1}(X)-T_{g2}]}{\Delta C_{p1}(X=0)\ T_{g1}(X=0)} \qquad [21]$$

which again is an extended version of the original Couchman equation given by:

$$\frac{dt_{g12}}{dX_2} = \frac{\Delta C_{p2} \quad (T_{g1}-T_{g2})}{\Delta C_{p1}} \qquad [22]$$

Our T_g values for toluene-swollen polystyrene networks deviate from the Karasz equation [20] at high concentrations of solvent, but follow the predicted trend of depression of T_g by solvent.

According to equation [22] the larger the value of ΔC_{p2}, the greater the expected depression of T_g at low diluent concentration. Another observation from this

equation is that as the crosslinking density of a network increases, ΔC_{p1} decreases and then the effectiveness of plasticization by a given amount of diluent increases correspondingly; the T_g depression becomes more sensitive to small quantities of diluent.

In general terms, the effect of solvent on T_g of the networks agrees with both the Karasz and the Pochan equations. For toluene an appreciable deviation of the Karasz equation from the experimental values is observed. Perhaps this equation should be applied only at low solvent concentration.

The T_g values obtained from the empirical Pochan equation given by:

$$\ln T_g = w_1 \ln T_{g1} + w_2 \ln T_{g2} \qquad [23]$$

(where w_i is either volume or weight percent of each component) fit with the experimental data in Figures (15-18) for toluene, and Figures (27-30) for chloroform.

In principle this equation is similar to another Couchman and Karasz equation (64) given by:

$$\ln T_{g12} = Q_1 \ln T_{g2} + (1-Q_1) \ln T_{g1} \qquad [24]$$

where

$$Q_i = \frac{X_2 \ \Delta C_{p2}}{X_2 \ \Delta C_{p2} + X_1 \ \Delta C_{p1}} \qquad [25]$$

here X_1 and X_2 are the mole or mass fractions of the pure components and ΔC_{p1} and ΔC_{p2} are the incremental changes in heat capacity at T_{g1} and T_{g2} respectively.

The used T_g values of the solvents to calculate the Pochan equation were those reported by Lesikar (65) for the THF and chloroform, and Angell (66) for the DMF. These are: toluene 115 K, $CHCl_3$ 105.9 K, DMF 129 K and THF 80 K. For the case of chloroform there exists an uncertainty of the T_g value, Angell (66) reports 105.9 K and 99 K and Suga and coworkers (67) reported a T_g value of 79 K. Our experimental values fit better with the Pochan equation when the value of 105.9 K is chosen as the T_g of chloroform.

Figures (27-30) show the depression of the glass transition temperature of the polymer network as a function of weight fraction of chloroform. If a plot of T_g vs. volume fraction is drawn, the Pochan curve lies above the experimental points. T_g values at concentrations higher than 51 wt% were not possible to obtain due to the interference of the melting point of chloroform at 209 K. At high concentrations of chloroform, the melting point shows a broad peak which make difficult the interpretation of T_g values in this region.

In the cases of DMF and THF there are appreciable deviations from the Pochan equation. The presence of a plateau in the trend of the data see Figures (38-41) for DMF and Figures (47-50) for THF, can be explained as a

phase separation between solvent and polymer network. The polymer networks with DMF were cooled at 160 K and those with THF were cooled at 200 K. If the solvent is frozen it will take longer than the time of the DSC experiment to reequilibrate with the polymer. T_g values at concentrations higher than 45 wt% of DMF and 65 wt% of THF were not obtained due to the interference of the melting point peak at 212 K and 165 K for DMF and THF respectively.

Another possible explanation (for the case of DMF) could be given in terms of compatibility of the solvent with the network. As we can see in Table X, the DMF shows the lowest swelling ratios. Since DMF has a lower compatibility with the network, it causes smaller depressions of glass transition temperature. For the case of THF, the deviation from the Pochan equation could arise from the uncertainty of the value of T_g of THF. The T_g value was obtained by extrapolation of T_g measurements of binary solutions with chloroform using a DTA instrument for the analysis (65). The T_g value of THF alone is so close to liquid nitrogen temperature that the signature of the transition is lost in the starting transient of the DTA measurement.

Before the experiments of DMF and THF were carried out, an experiment with a 1% crosslinked network swollen with toluene was carried out in order to see the "collapse transition". The sample (less than 1 mg) was cooled with liquid nitrogen, and the temperature was monitored with a

Dupont FS 1000 temperature controller. The sample was observed through a microscope mounted on a Dupont Sorvall Microtome MT 6000. During the time of the experiment (2 h), in which the sample was cooled to -120 °C, no appreciable shrinkage of the gel was observed. Only the formation of crystals of water around the beads was observed. Probably the absence of shrinking of this sample indicates little change in the swelling ratio with temperature, or maybe more time was necessary to observe this change.

In conclusion, our experimental data fit in good approximation with both the empirical Pochan equation and the quasi-thermodynamic Karasz equation for toluene and chloroform. Deviations of experimental data from the Karasz equation at high concentrations are expected because the equation was derived at low solvent concentration.

For the cases of DMF and THF, deviations of the experiemntal data from Karasz and Pochan equations can be explained in terms of phase separation between solvent and polymer network or due to uncertainty of the T_g value for the THF solvent.

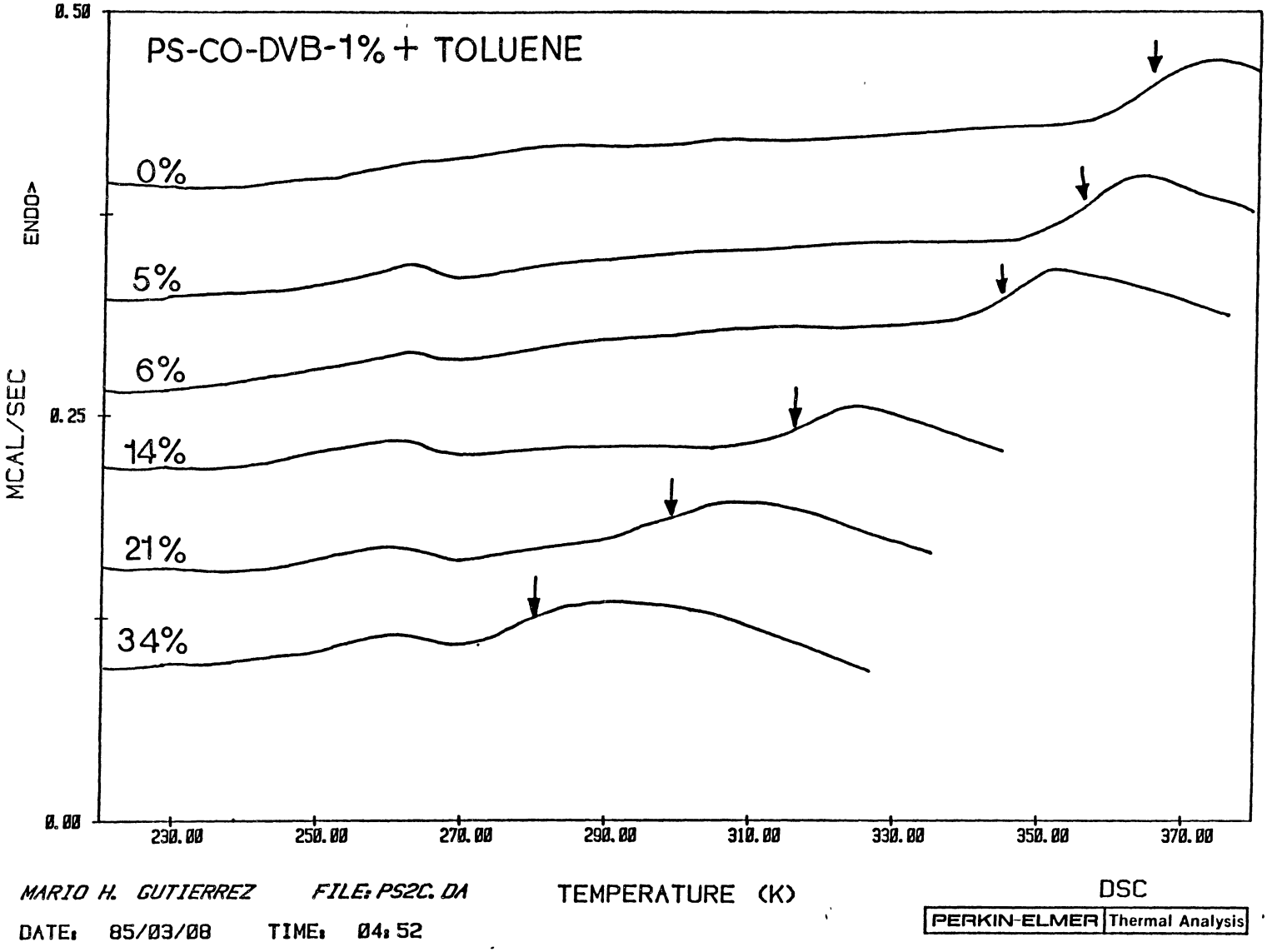

Figure 5. DSC thermograms of 1% DVB crosslinked polystyrene containing different weight percents of toluene

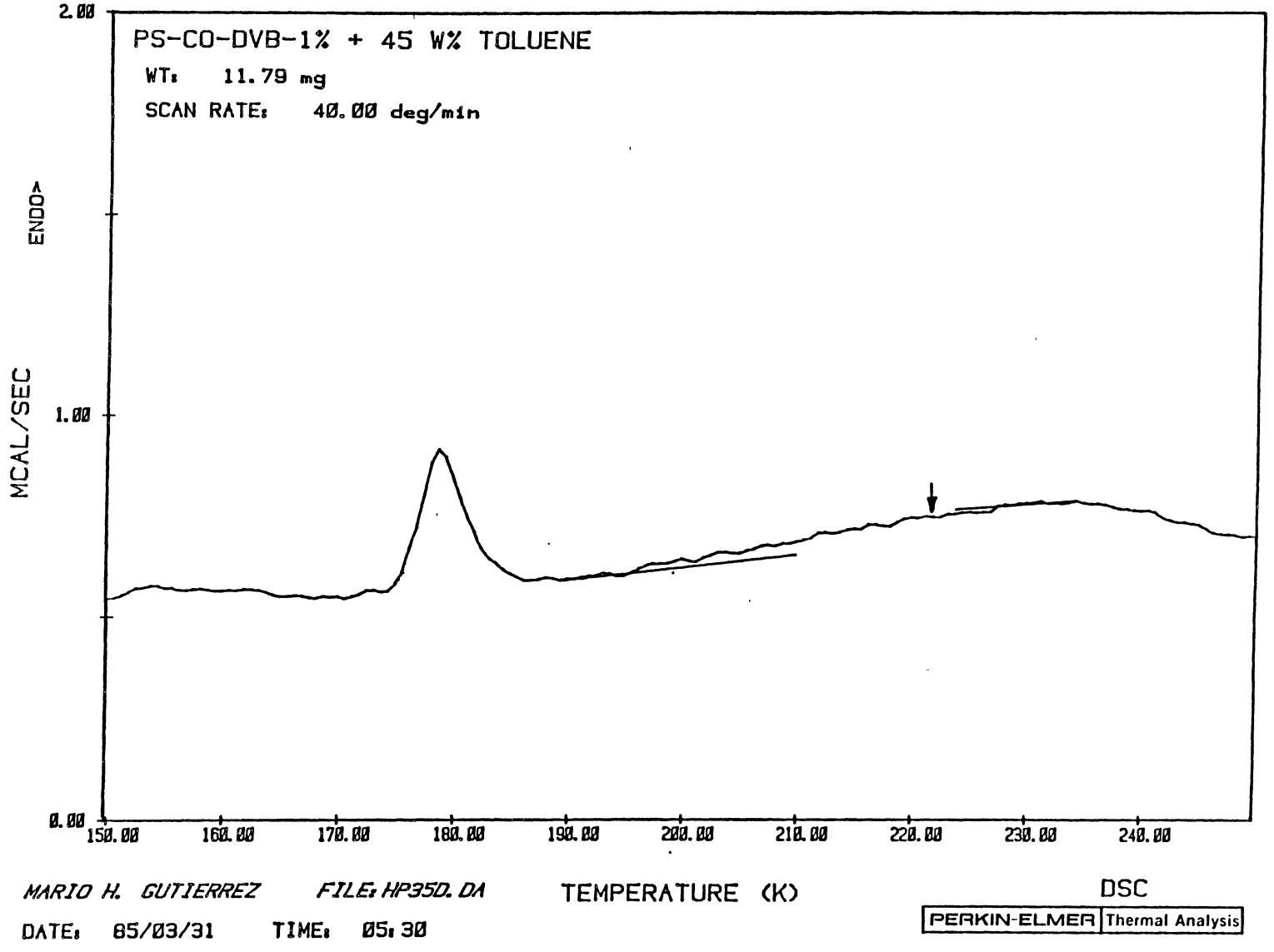

Figure 6. DSC thermograms of 1% DVB crosslinked polystyrene containing 45 weight percent of toluene.

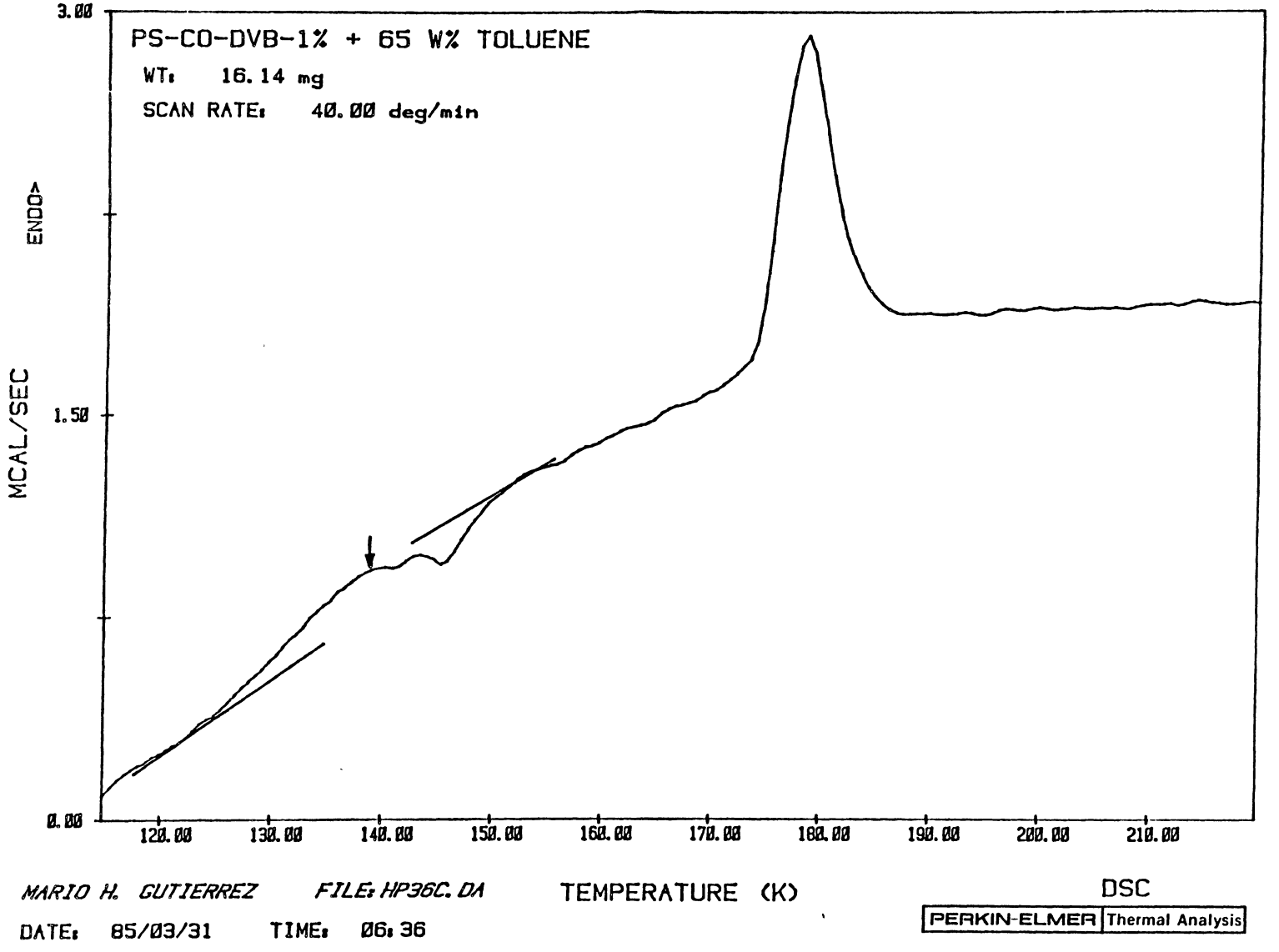

Figure 7. DSC thermogram of 1% DVB crosslinked polystyrene containing 65 weight percent of toluene.

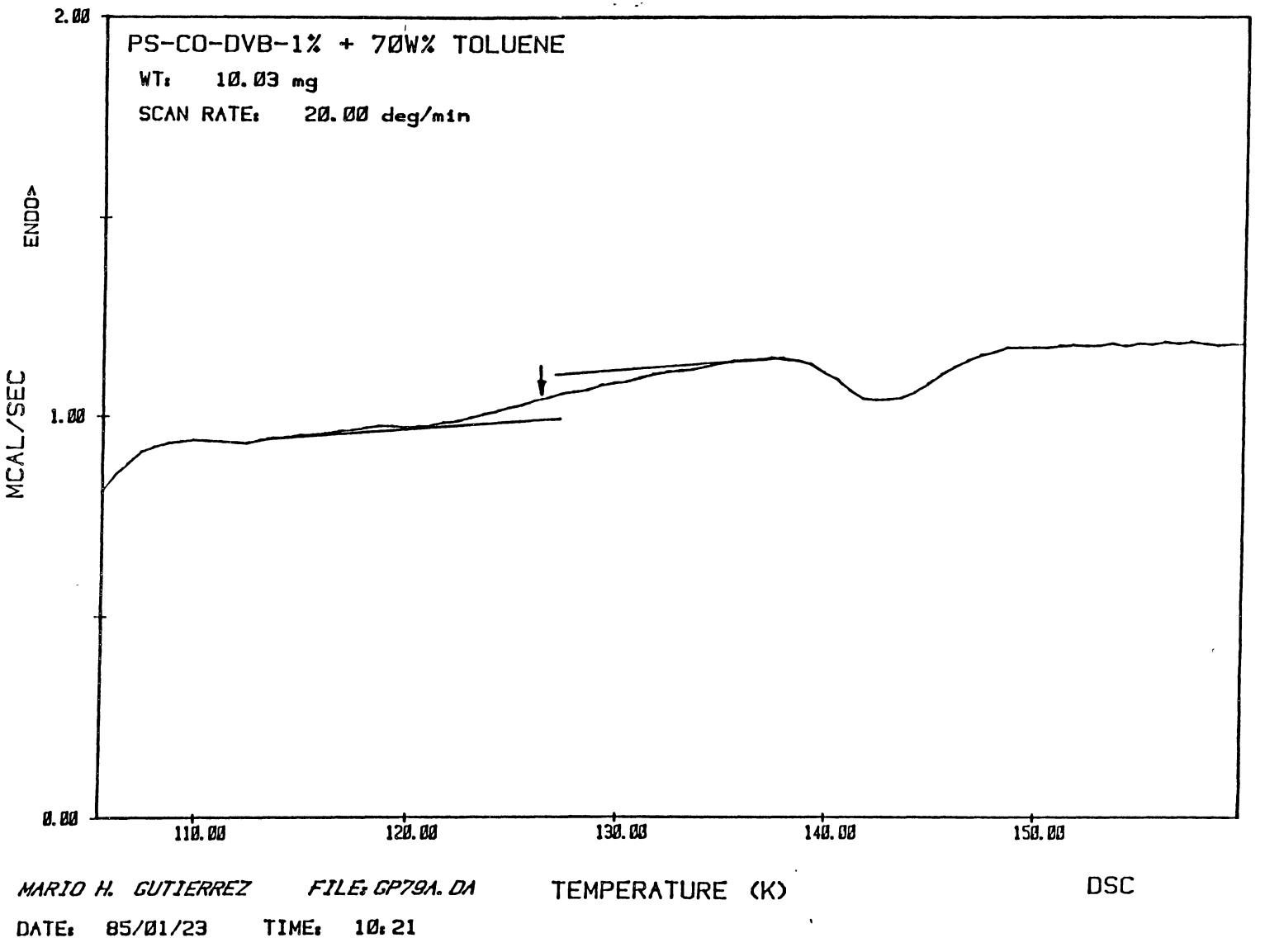

Figure 8. DSC thermogram of 1% DVB crosslinked polystyrene containing 70 weight percent of toluene.

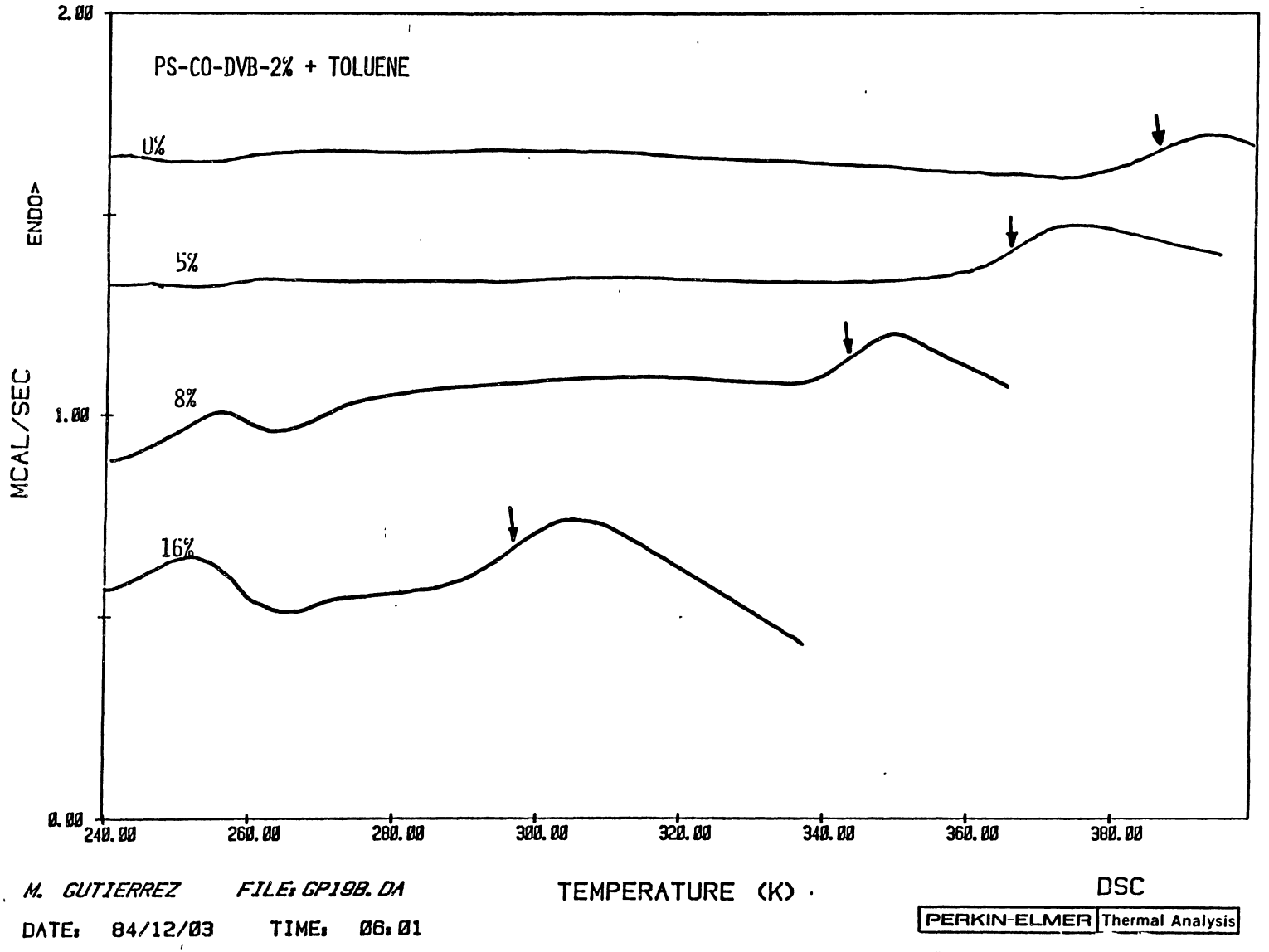

Figure 9. DSC thermograms of 2% DVB crosslinked polystyrene containing different weight percents of toluene

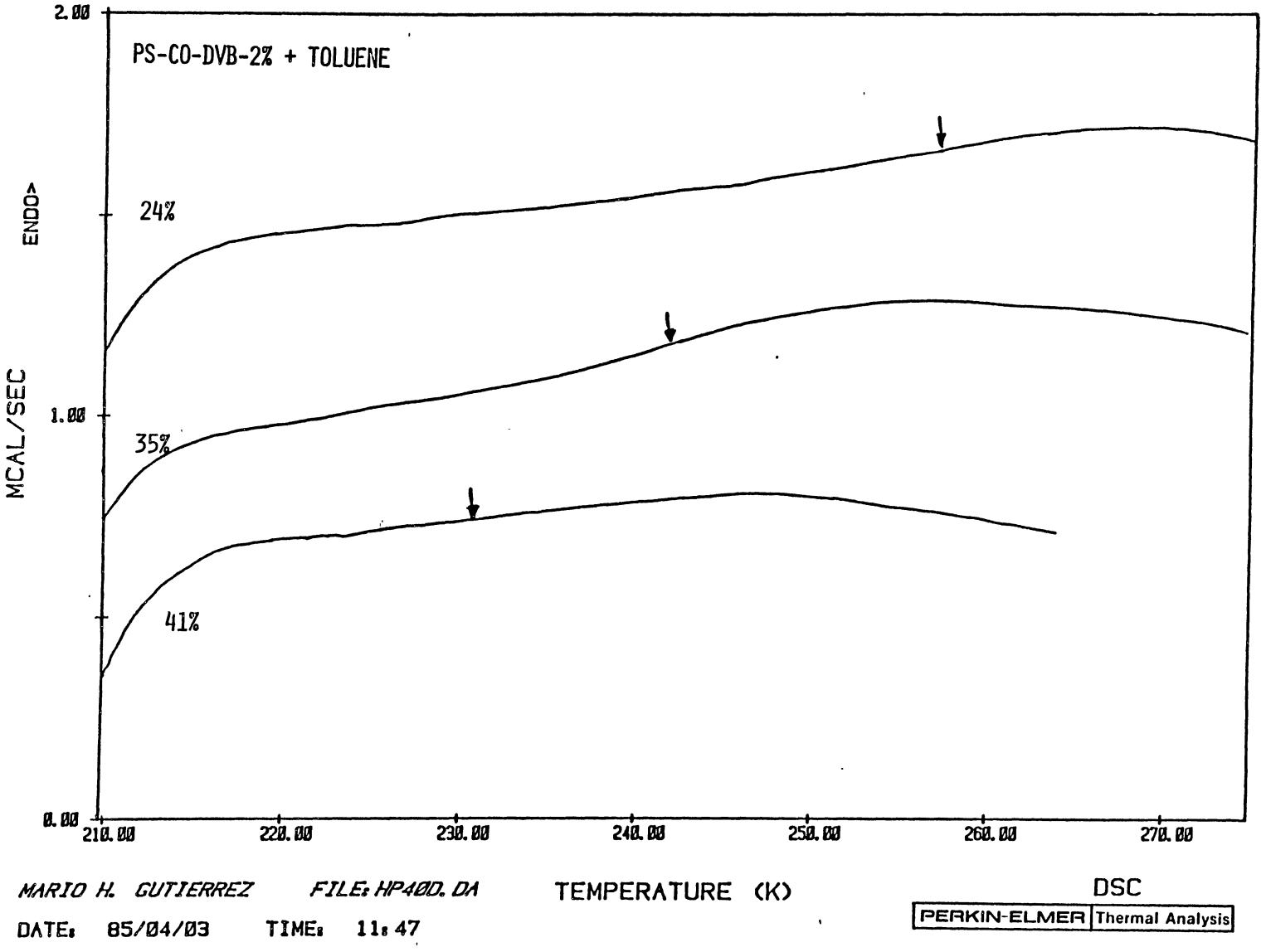

Figure 10. DSC thermograms of 2% DVB crosslinked polystyrene containing different weight percents of toluene.

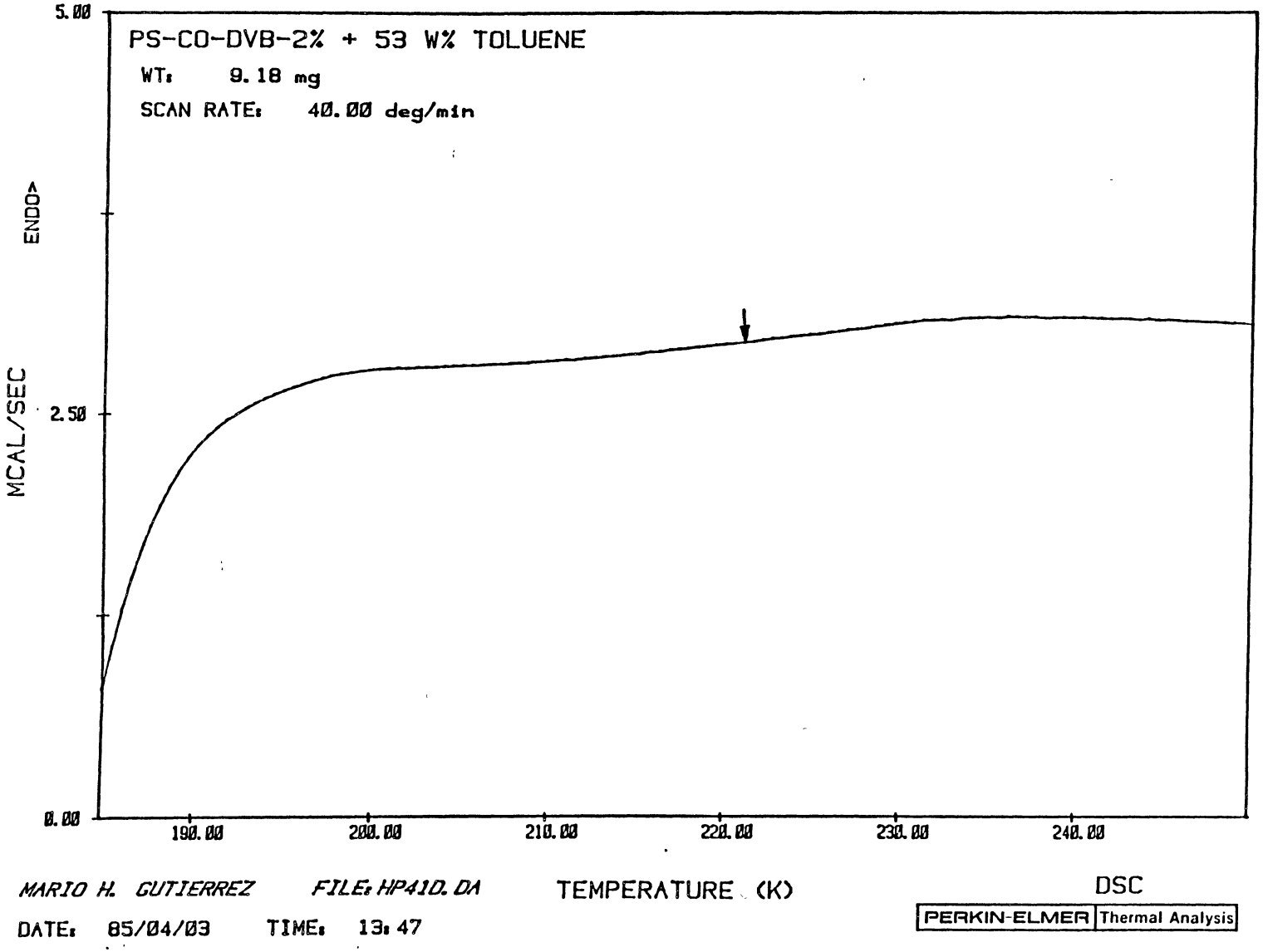

Figure 11. DSC thermograms of 2% DVB crosslinked polystyrene containing 53 weight percent of toluene.

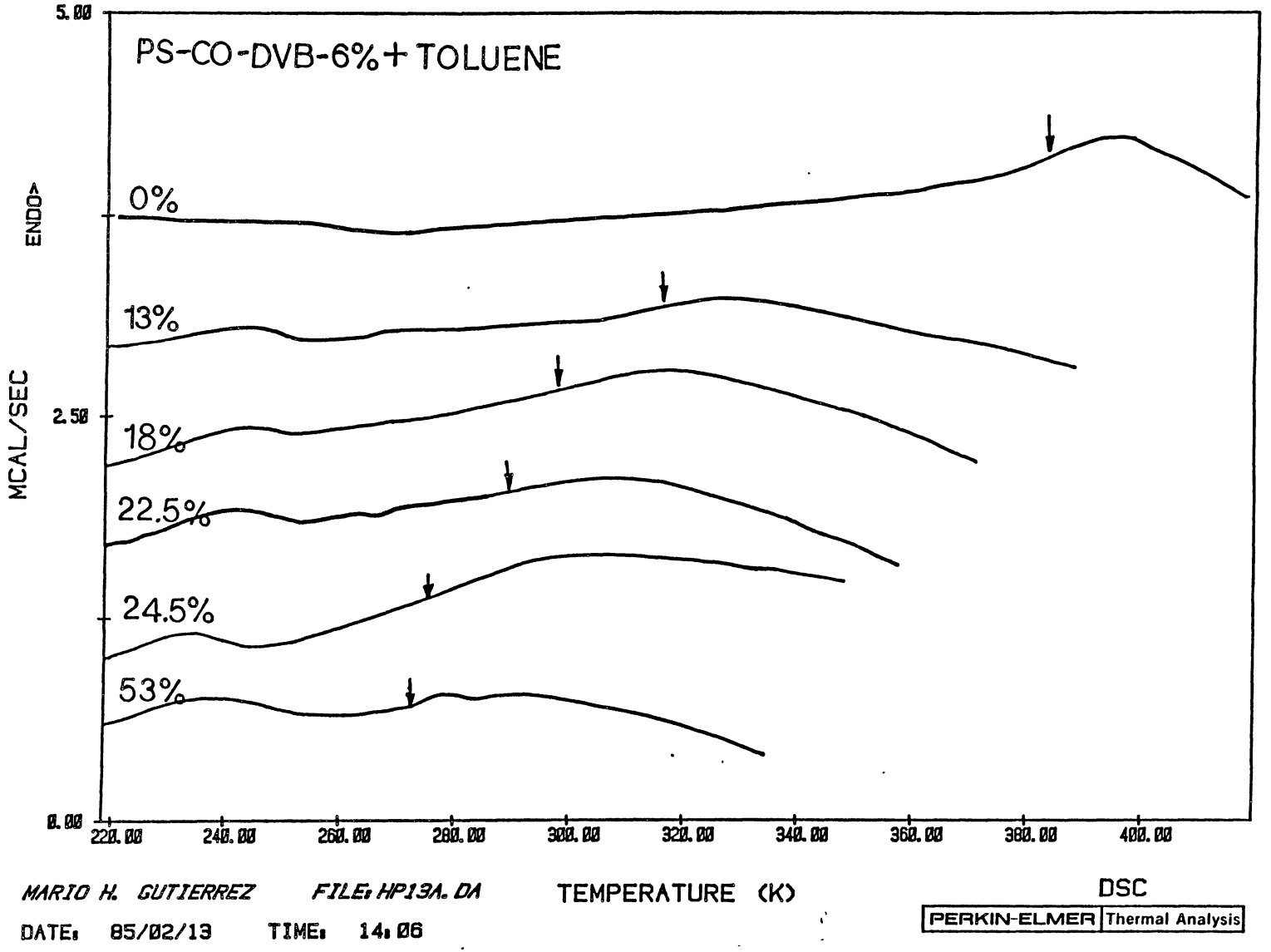

Figure 12. DSC thermograms of 6% DVB crosslinked polystyrene containing different weight percents of toluene.

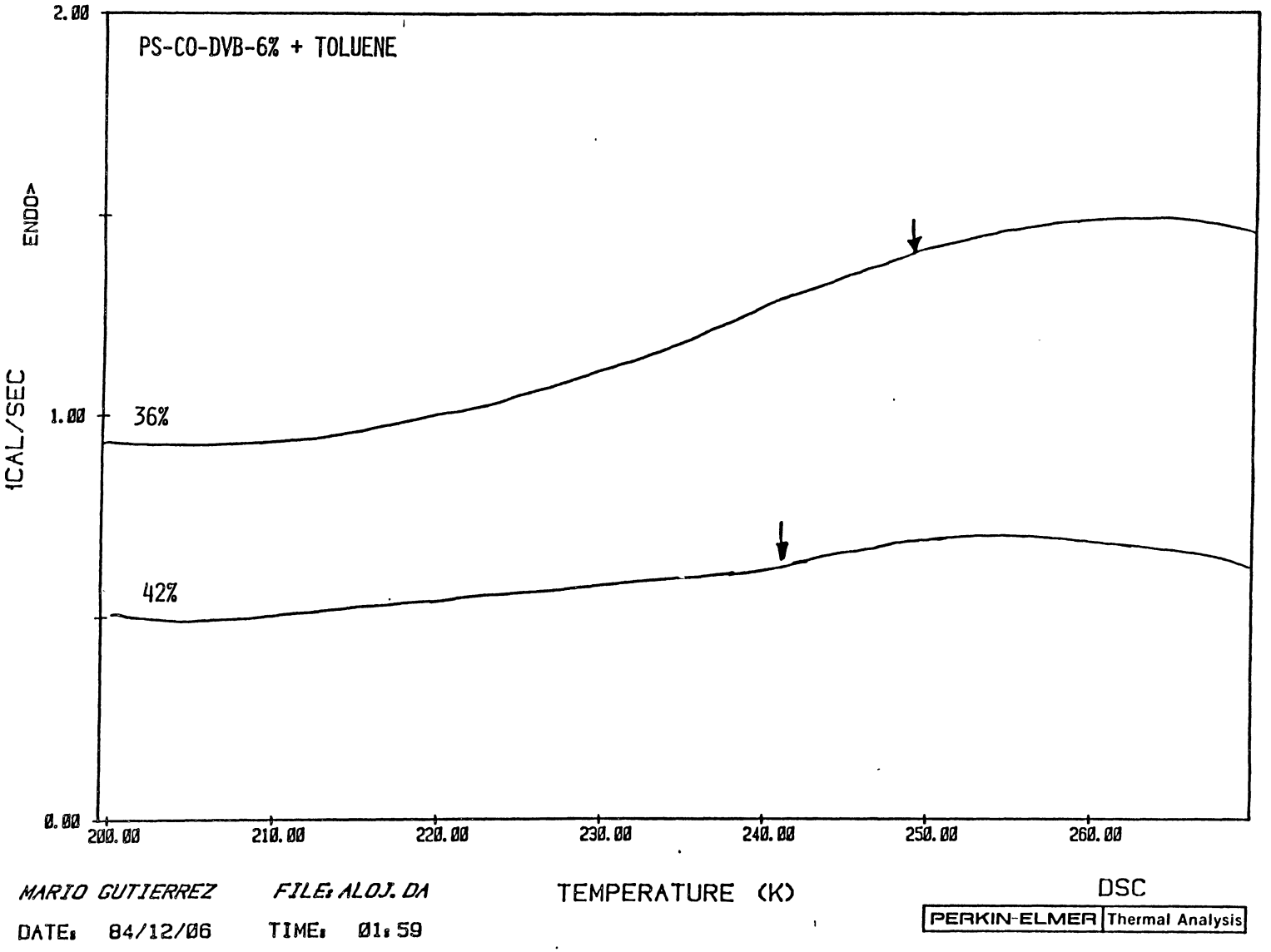

Figure 13. DSC thermograms of 6% DVB crosslinked polystyrene containing different weight percents of toluene.

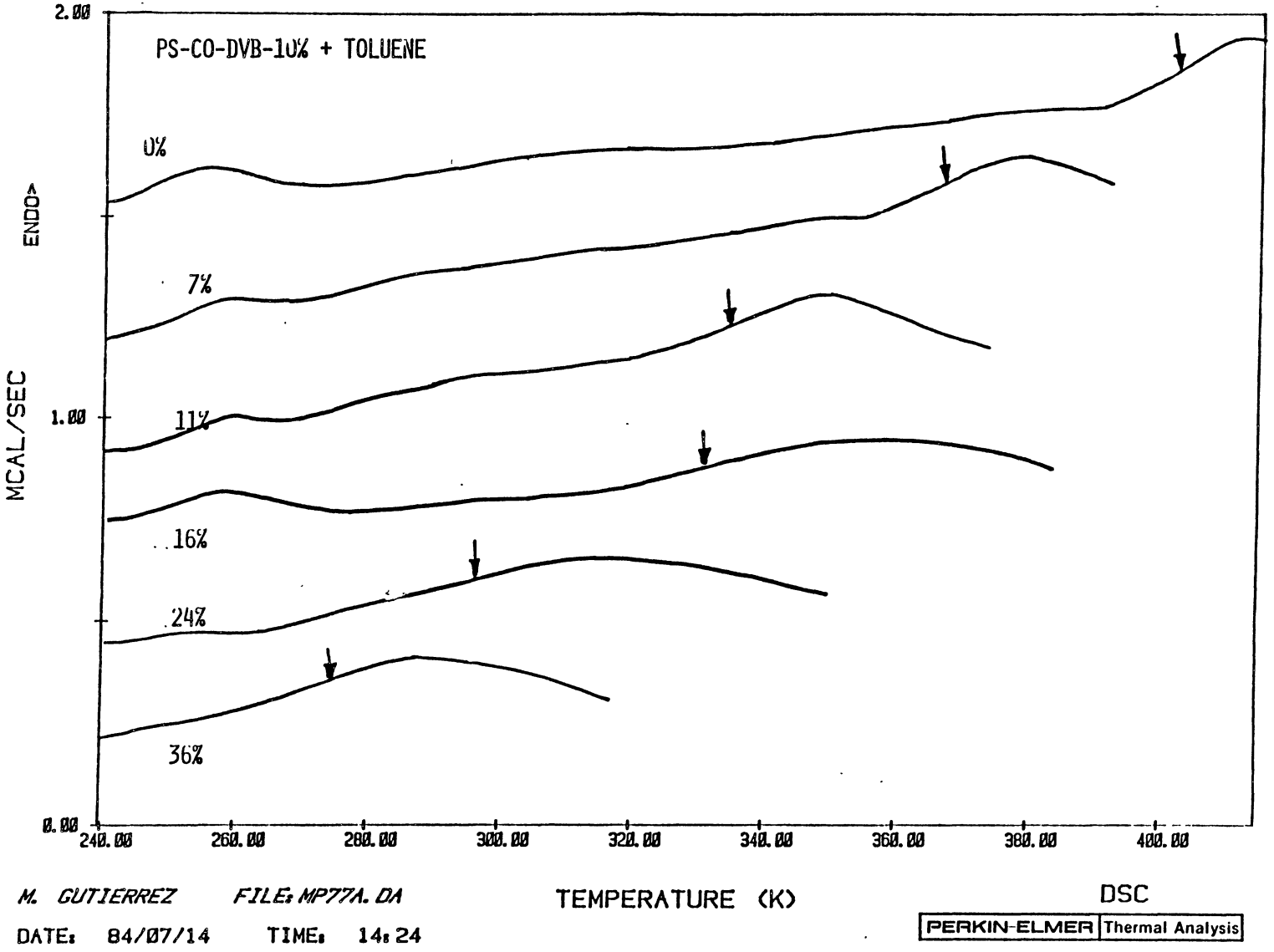

Figure 14. DSC thermograms of 10% DVB crosslinked polystyrene containing different weight percents of toluene.

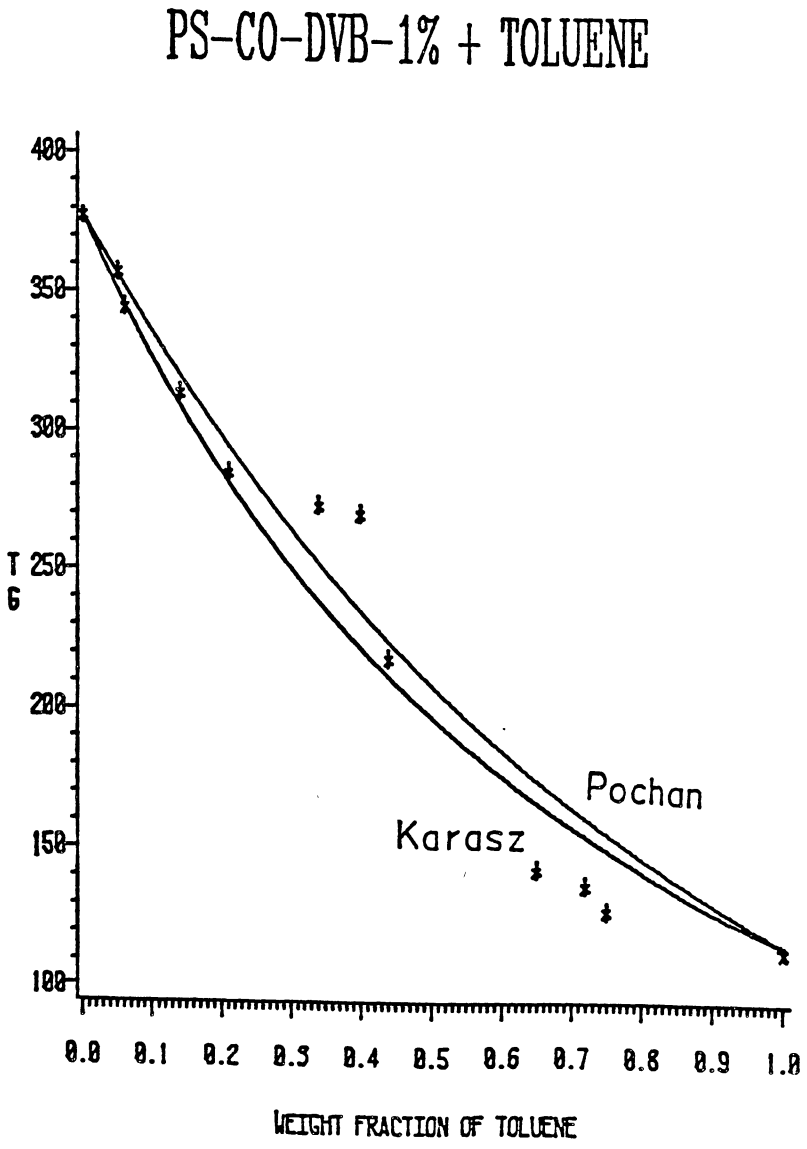

Figure 15. T_g of 1% DVB crosslinked polystyrene vs. weight fraction of toluene and comparison with Karasz and Pochan equations.

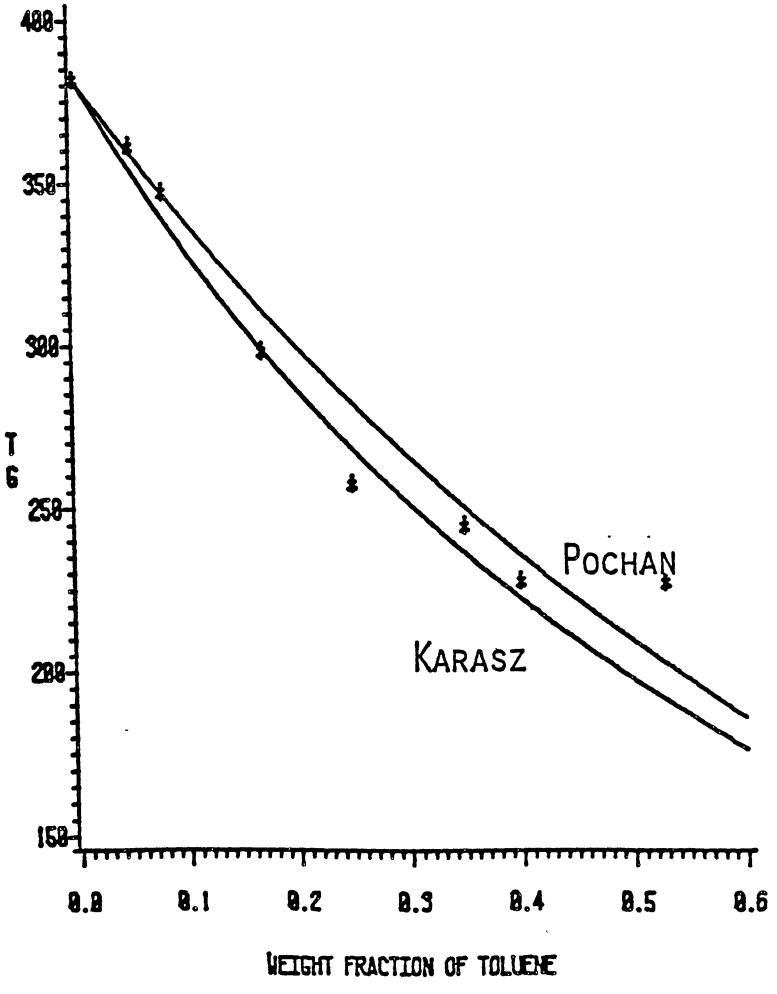

Figure 16. T_g of 2% DVB crosslinked polystyrene vs. weight fraction of toluene and comparison with Karasz and Pochan equations.

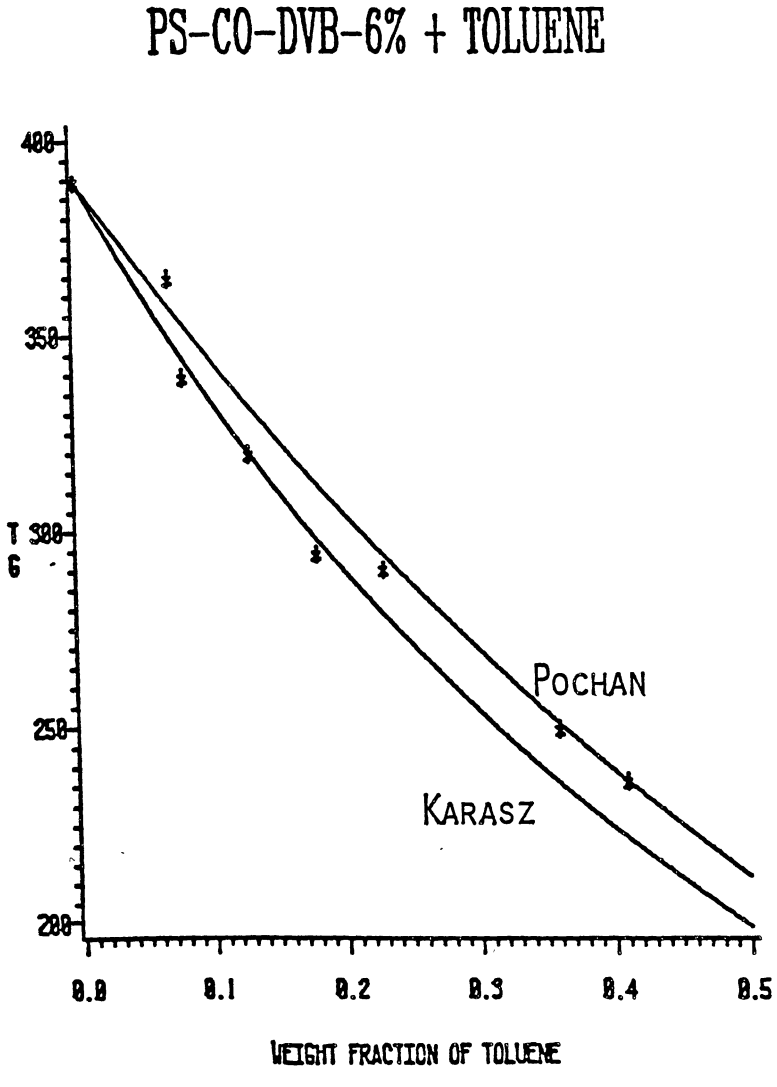

Figure 17. T_g of 6% DVB crosslinked polystyrene vs. weight fraction of toluene and comparison with Karasz and Pochan equations.

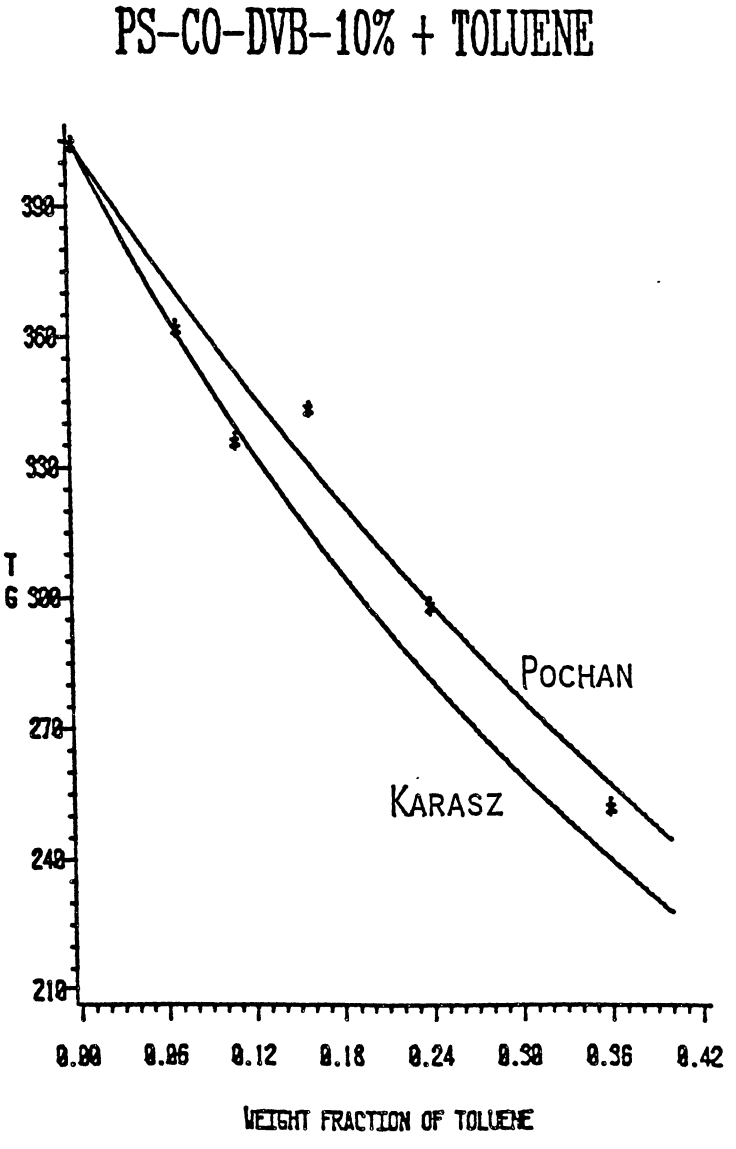

Figure 18. T_g of 10% DVB crosslinked polystyrene vs. weight fraction of toluene and comparison with Karasz and Pochan equations.

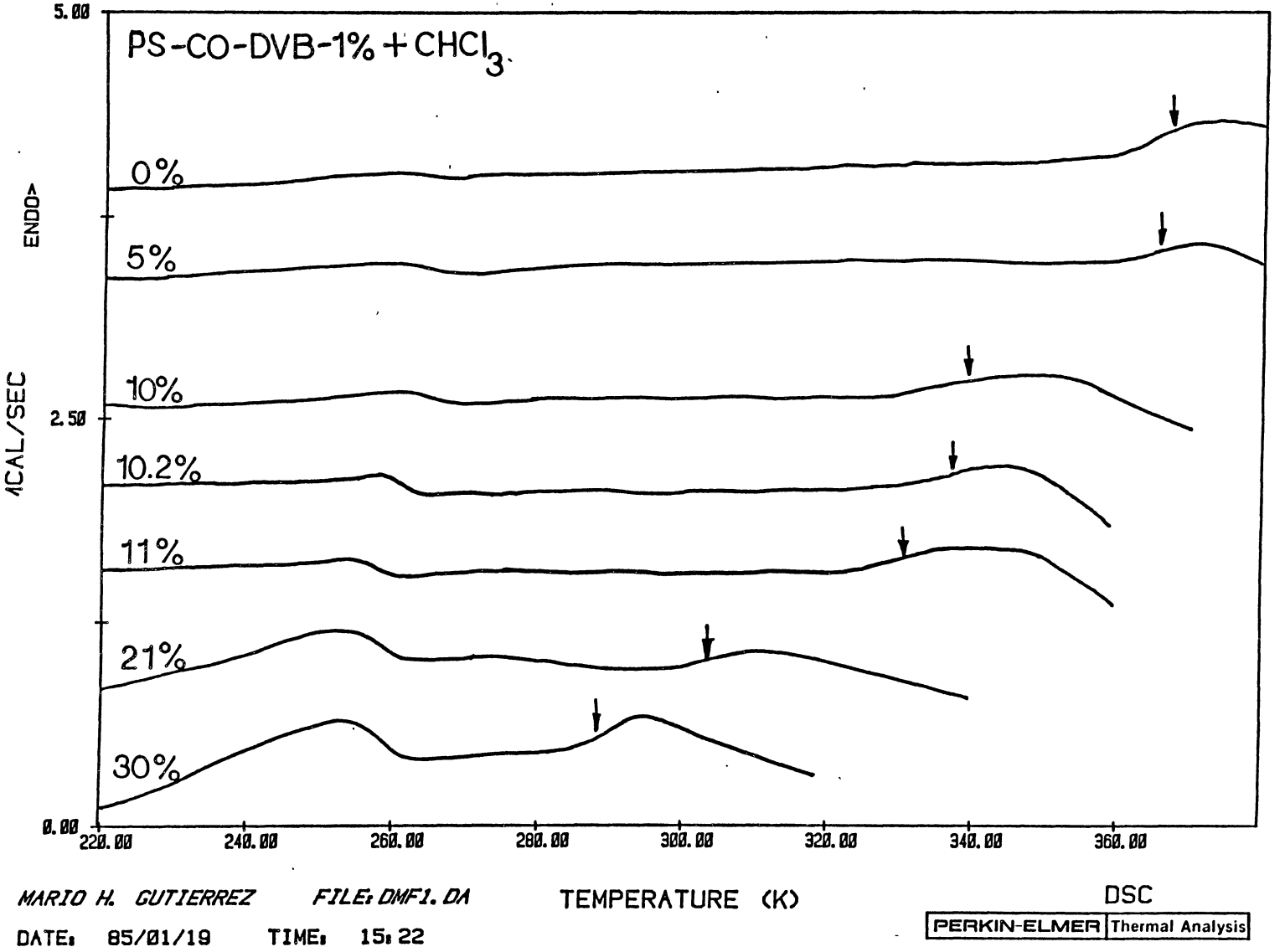

Figure 19. DSC thermograms of 1% DVB crosslinked polystyrene containing different weight percents of chloroform.

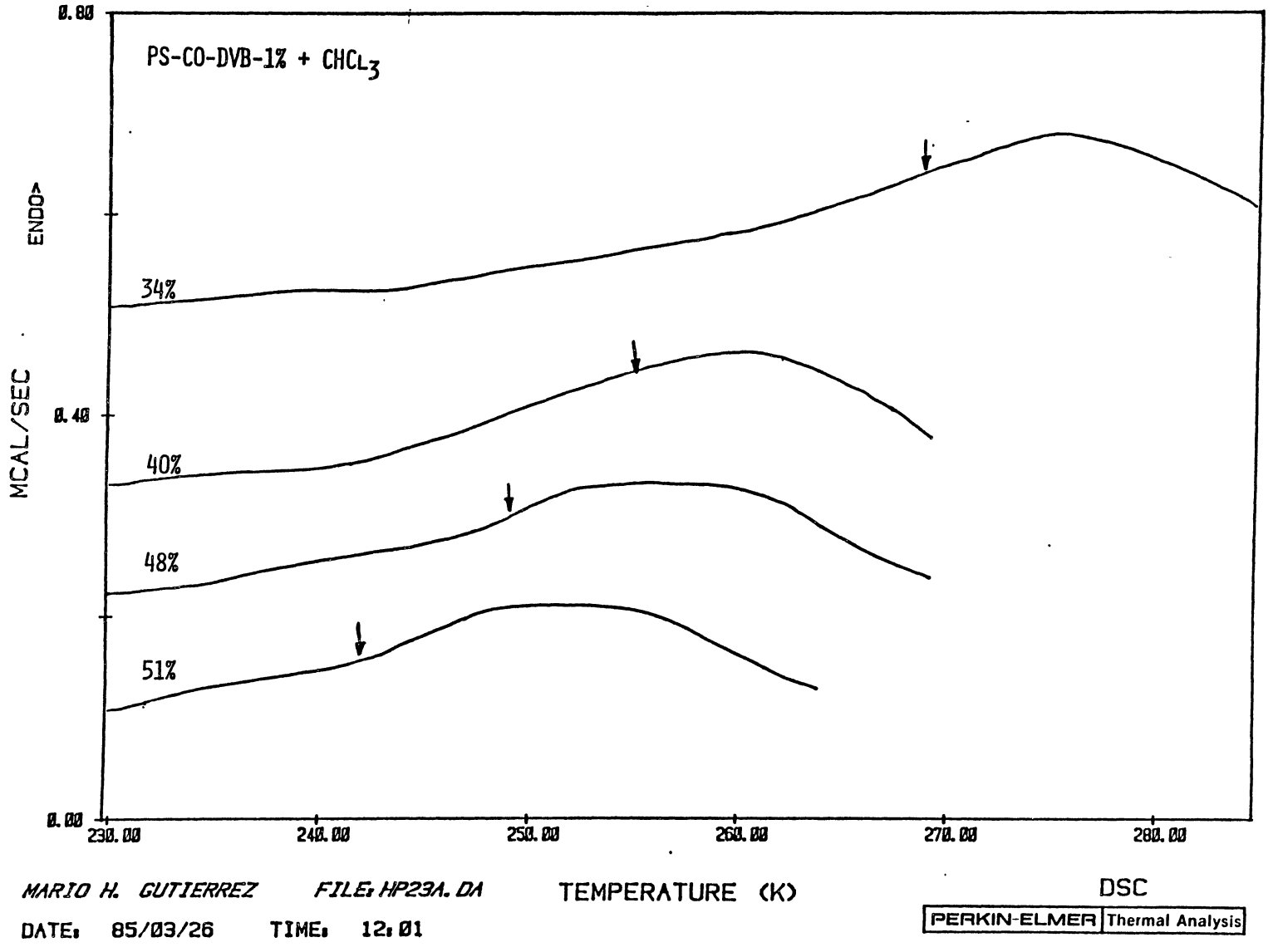

Figure 20. DSC thermograms of 1% DVB crosslinked polystyrene containing different weight percents of chloroform.

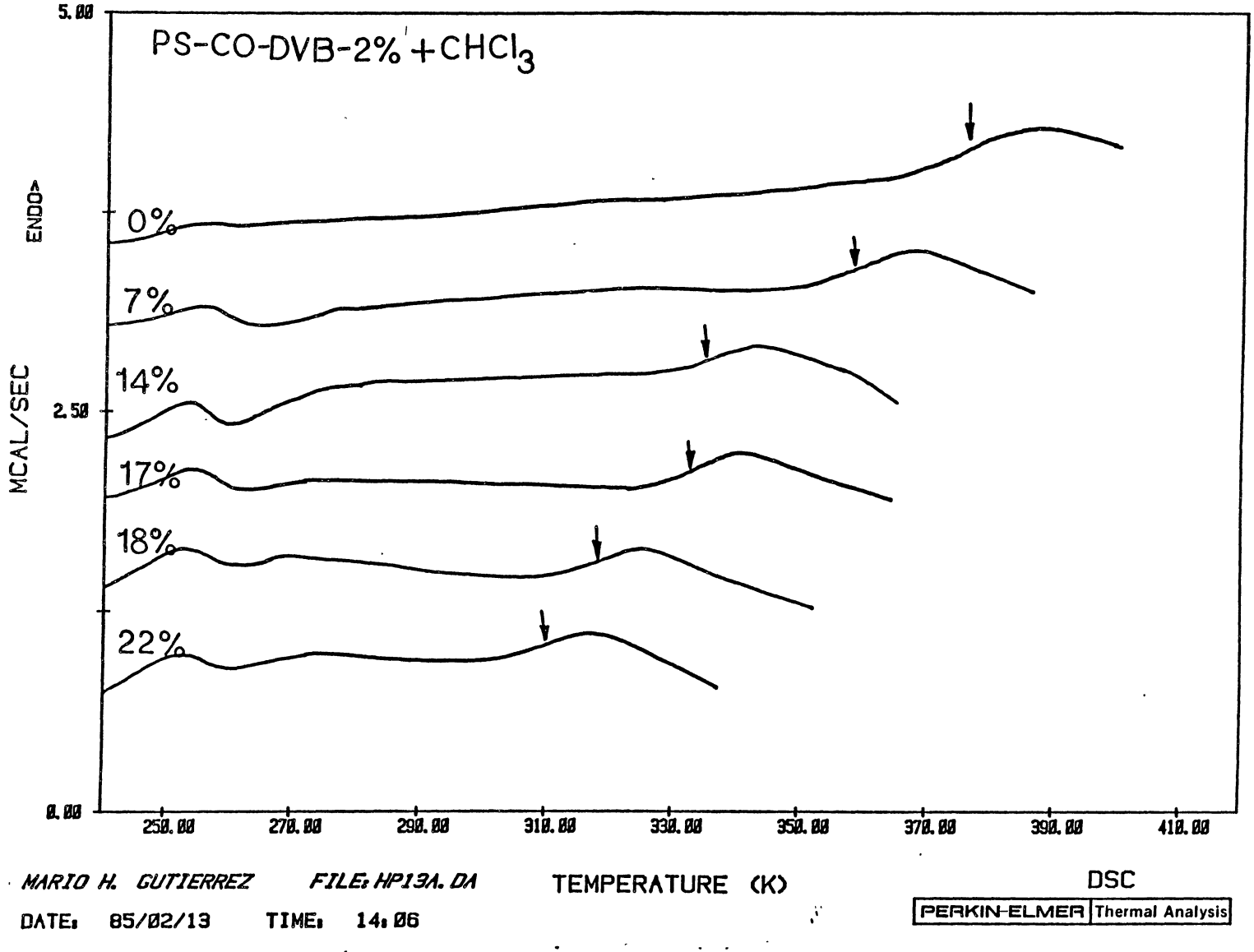

Figure 21. DSC thermograms of 2% DVB crosslinked polystyrene containing different weight percents of chloroform.

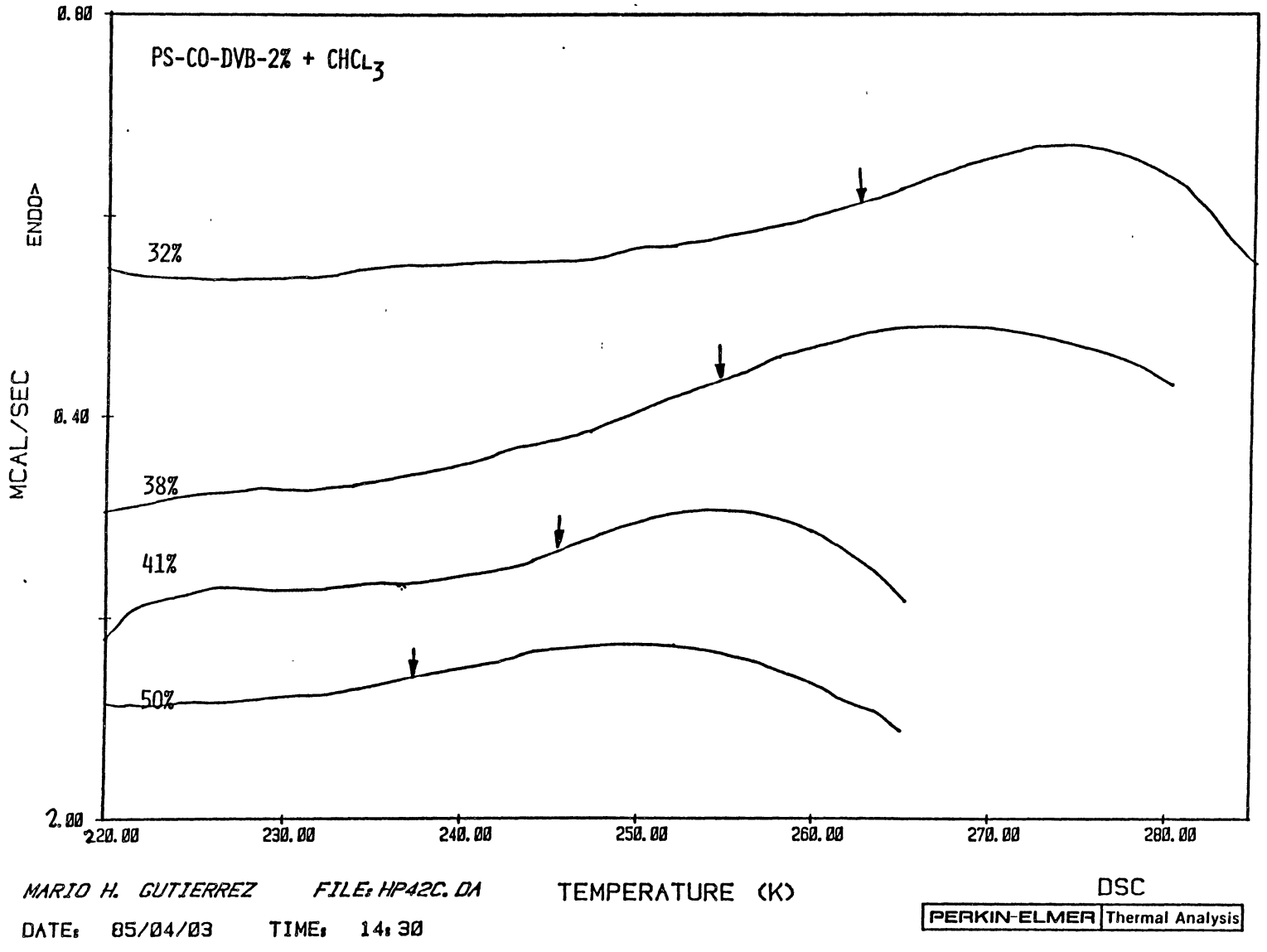

Figure 22. DSC thermograms of 2% DVB crosslinked polystyrene containing different weight percents of chloroform.

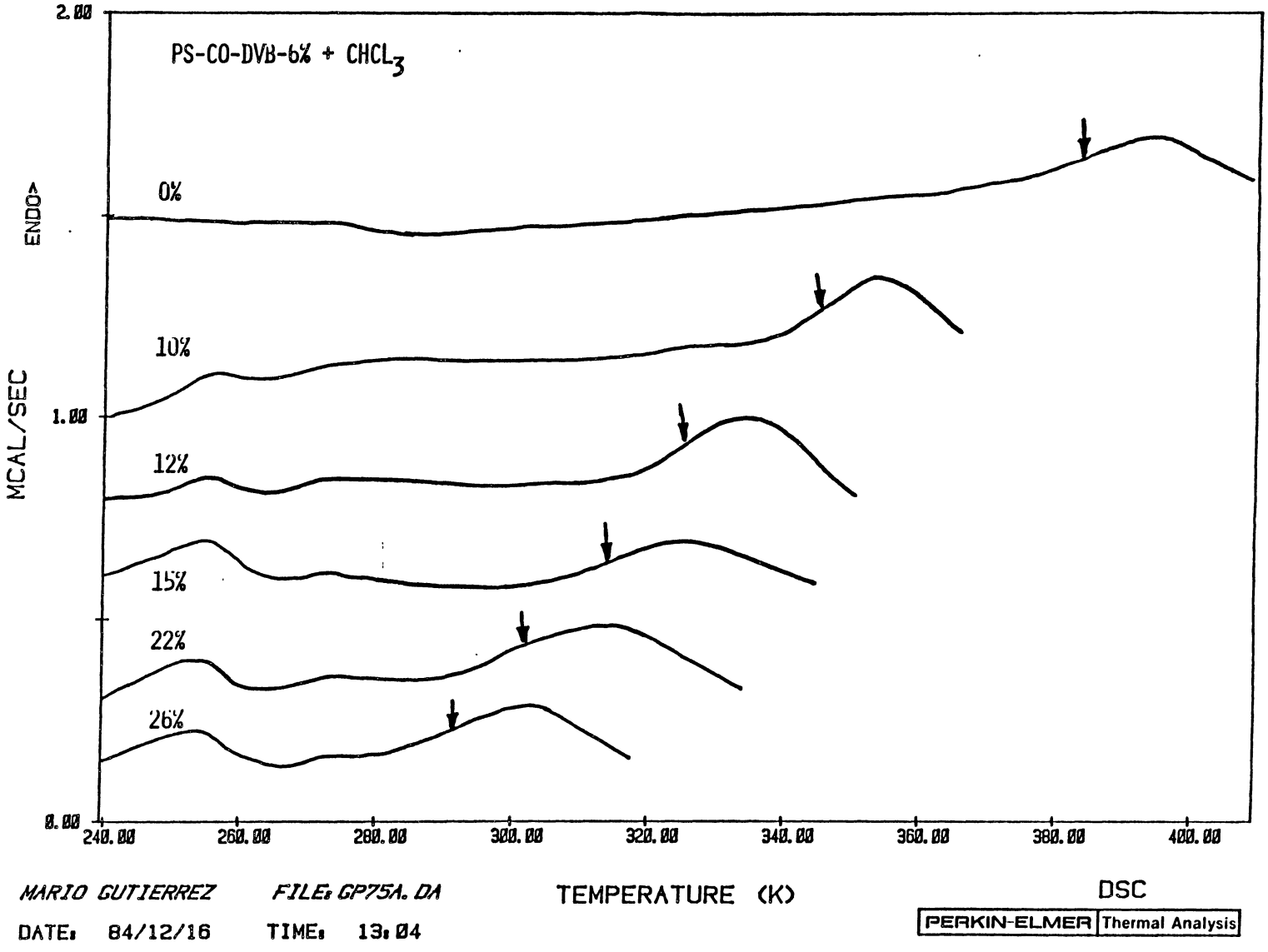

Figure 23. DSC thermograms of 6% DVB crosslinked polystyrene containing different weight percents of chloroform.

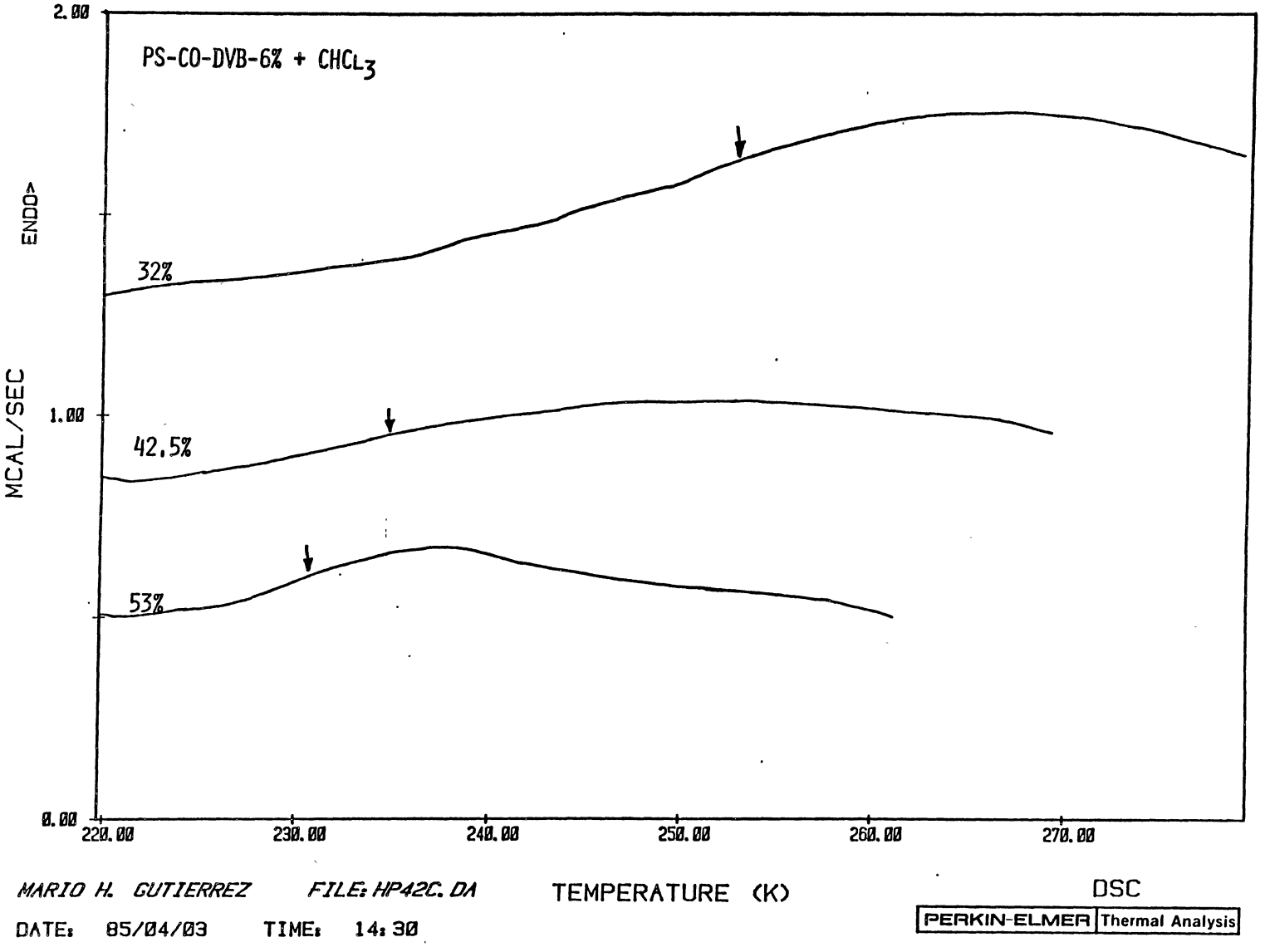

Figure 24. DSC thermograms of 6% DVB crosslinked polystyrene containing different weight percents of chloroform.

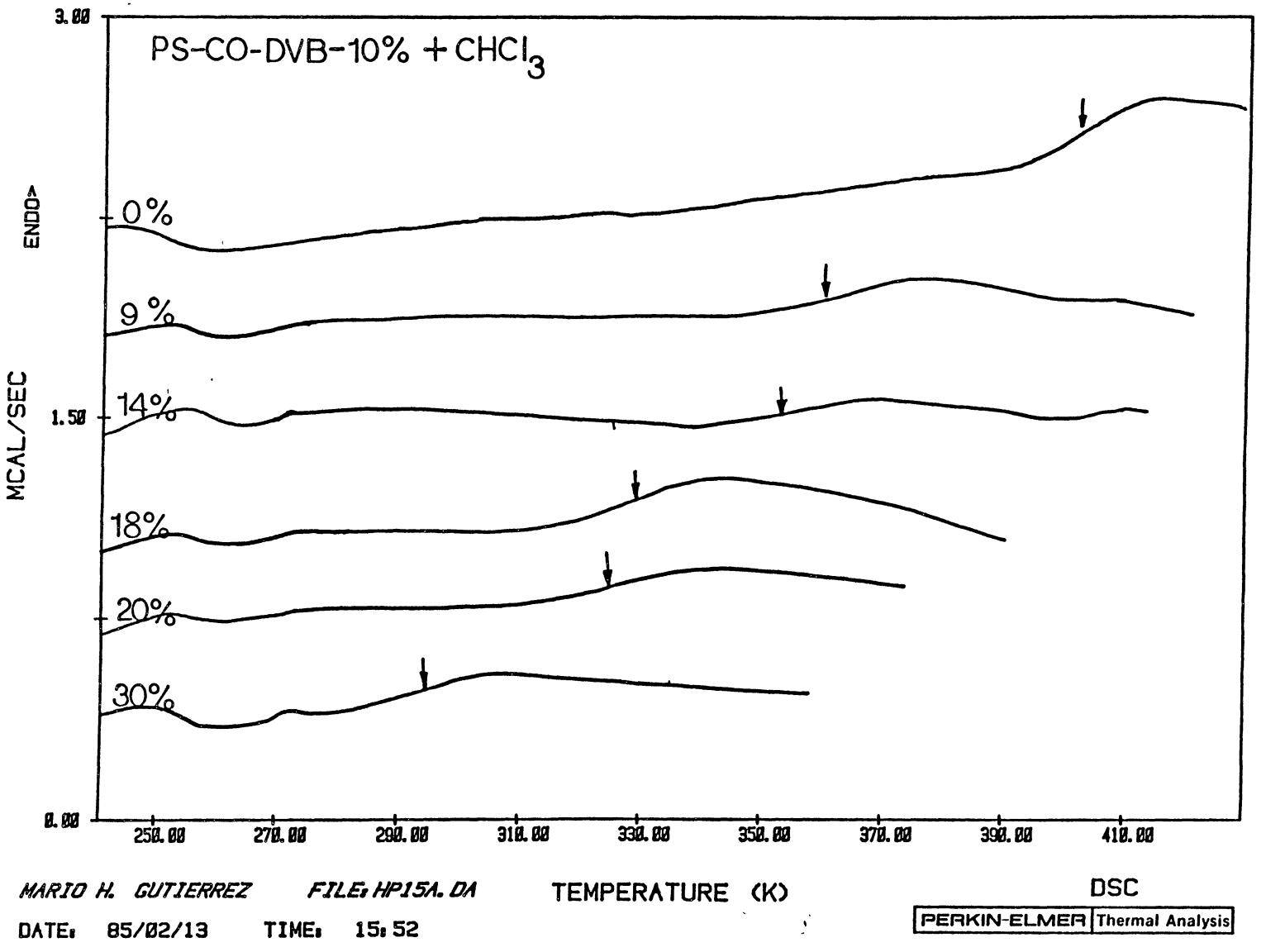

Figure 25. DSC thermograms of 10% DVB crosslinked polystyrene containing different weight percents of chloroform.

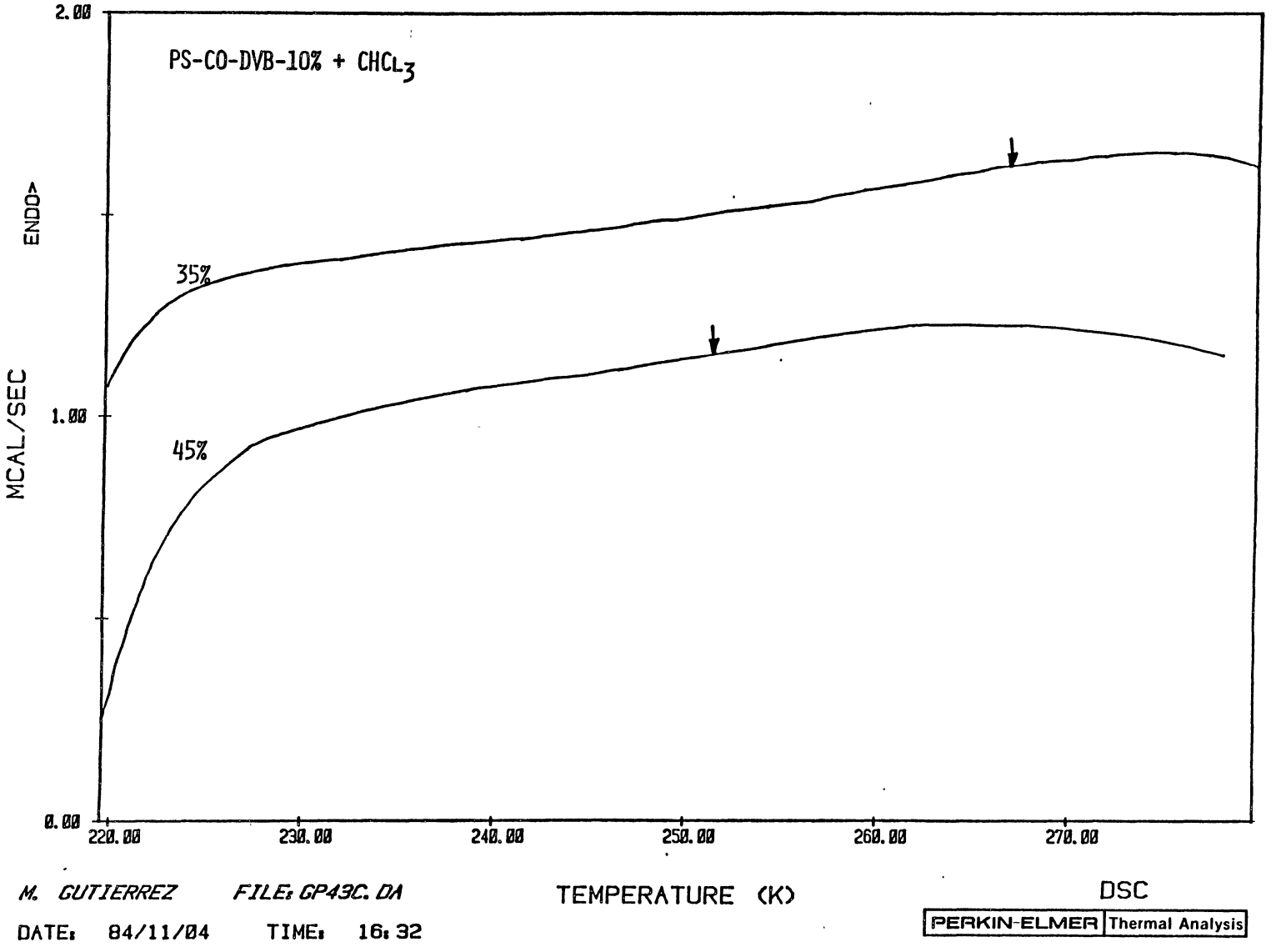

Figure 26. DSC thermograms of 10 % DVB crosslinked polystyrene containing different weight percents of chloroform

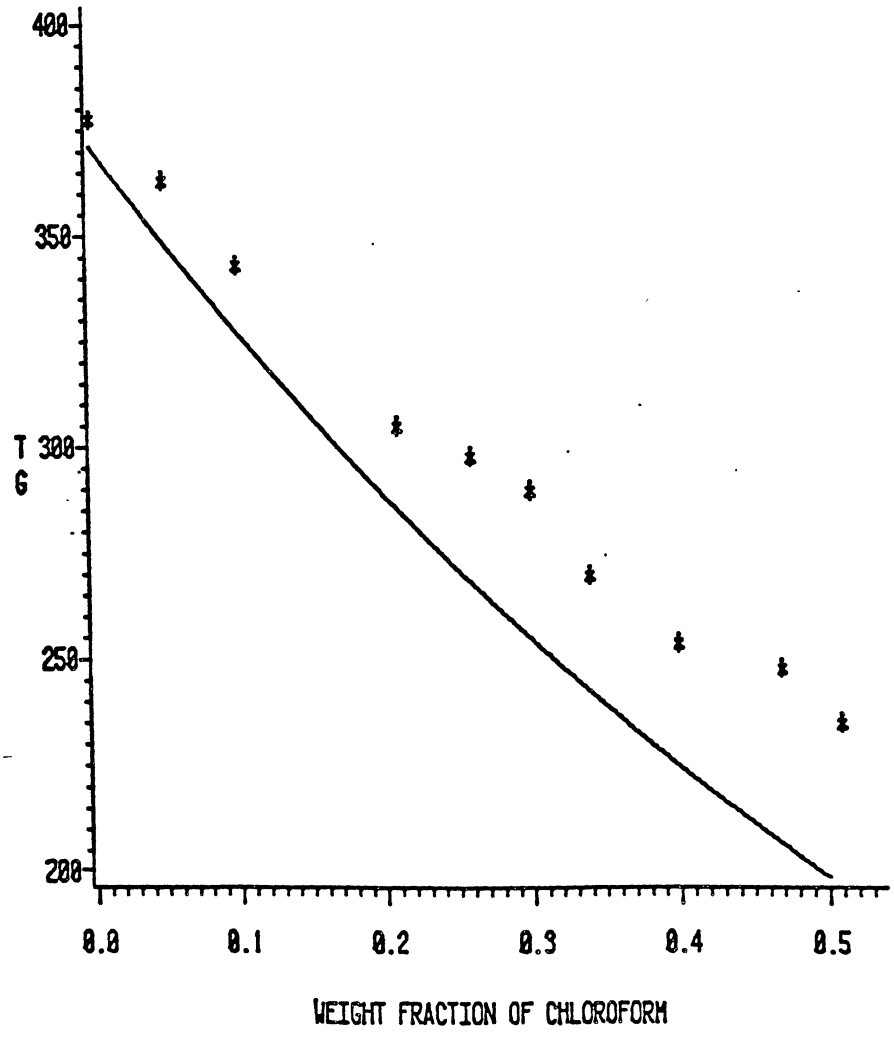

Figure 27. T_g of 1% DVB crosslinked polystyrene vs. weight fraction of chloroform.

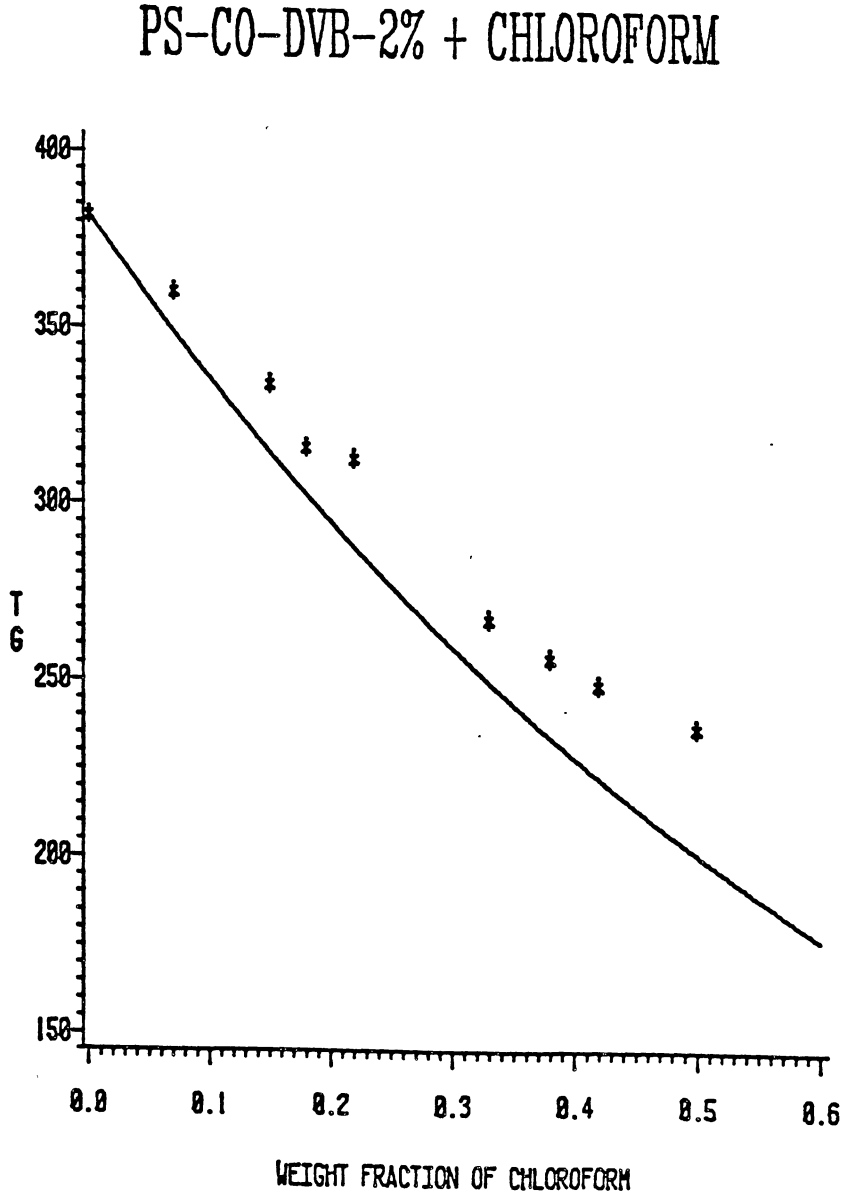

Figure 28. T_g of 2% DVB crosslinked polystyrene vs. weight fraction of chloroform.

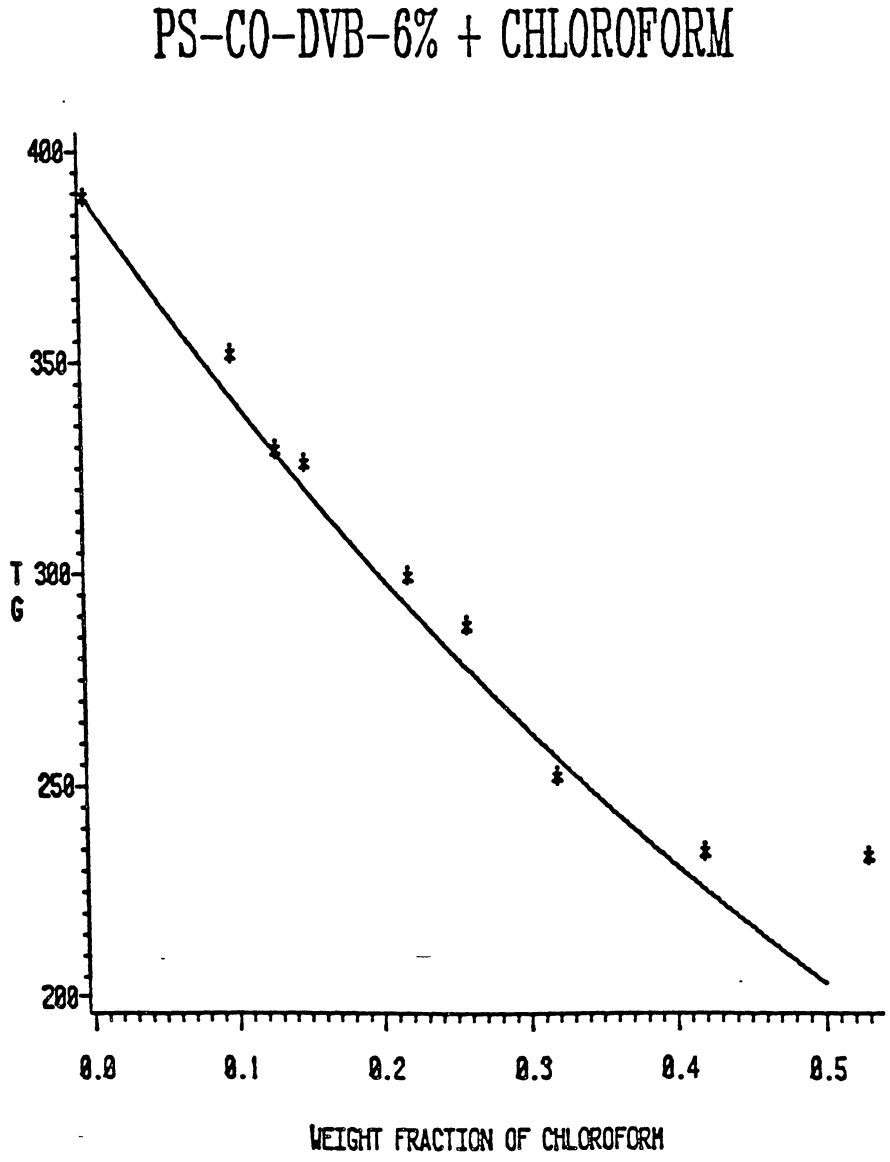

Figure 29. T_g of 6% DVB crosslinked polystyrene vs. weight fraction of chloroform.

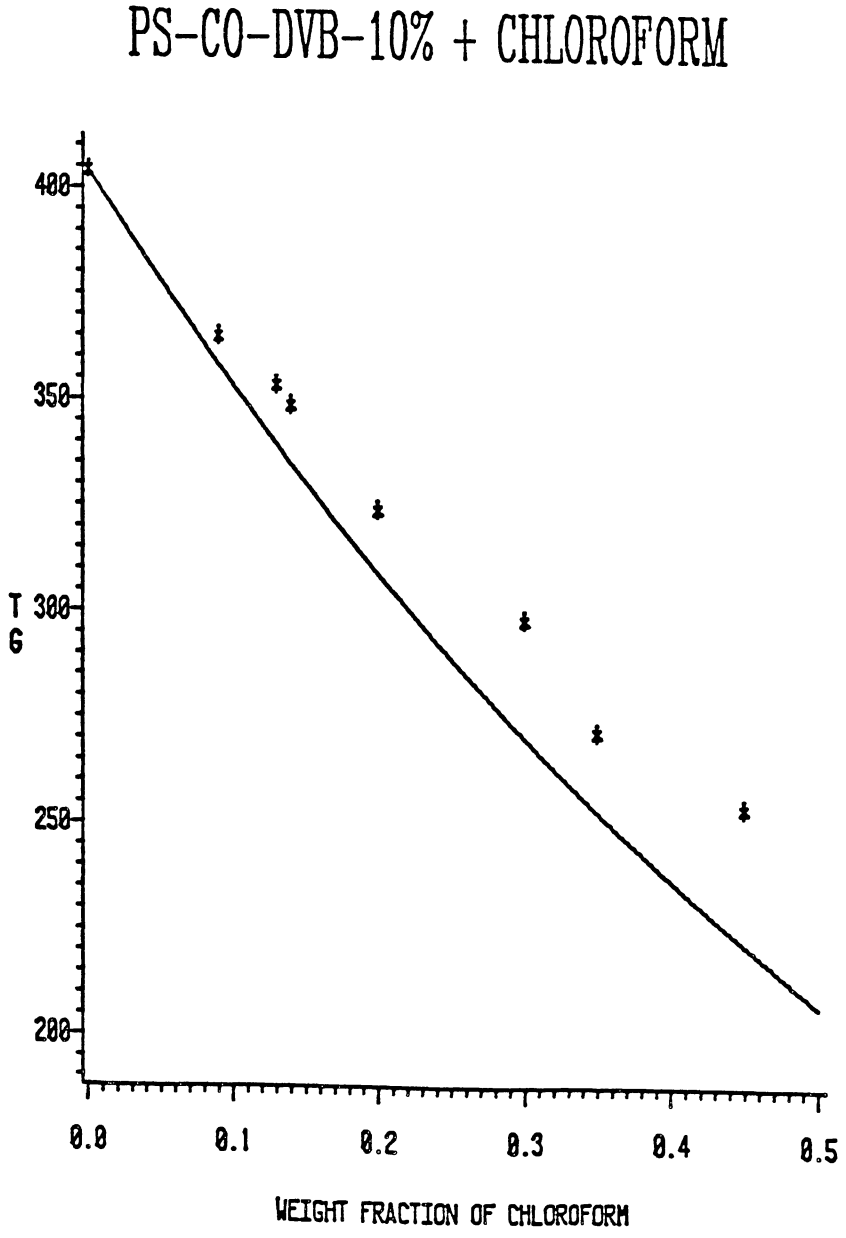

Figure 30. T_g of 10 % DVB crosslinked polystyrene vs. weight fraction of chloroform.

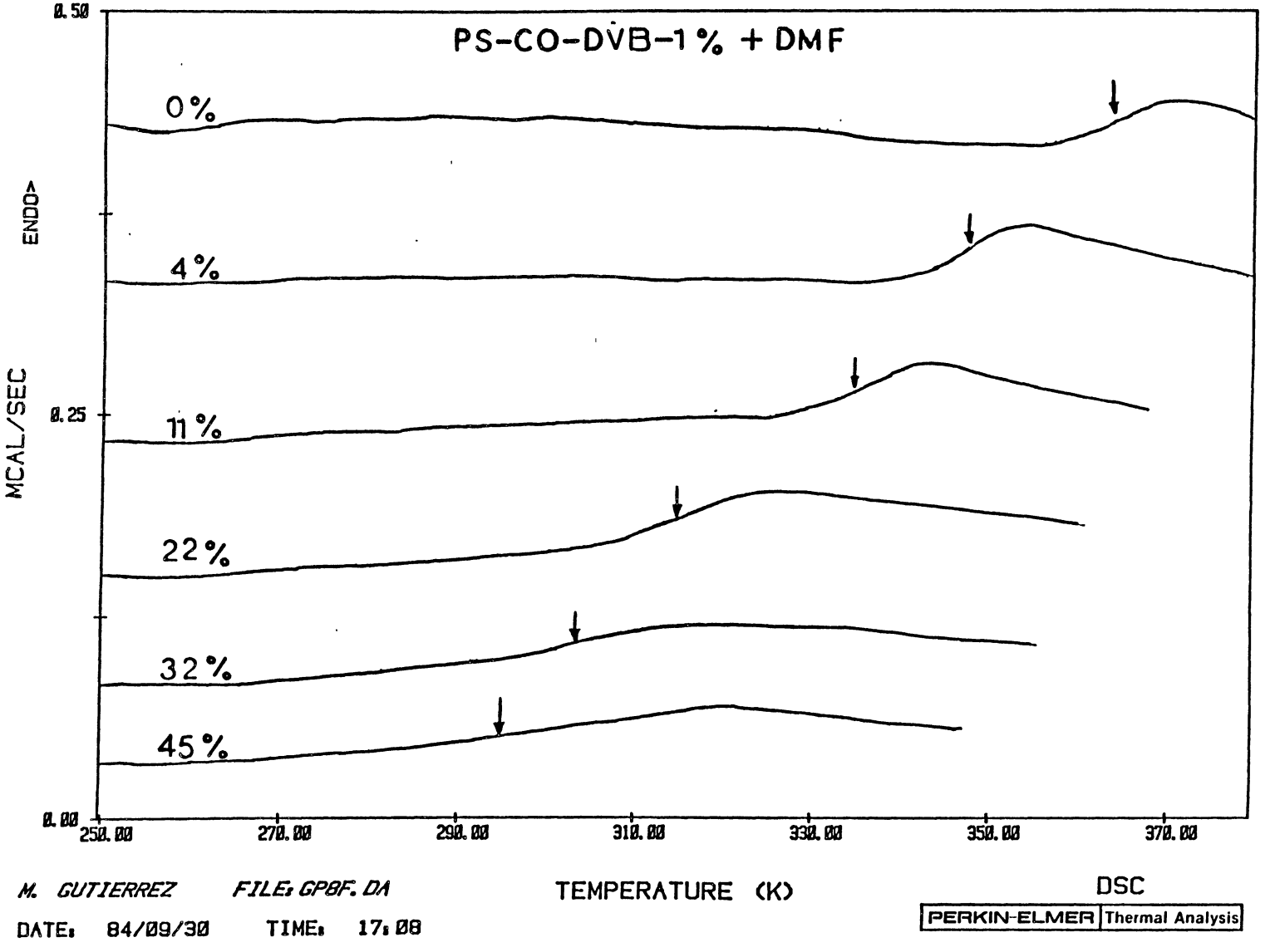

Figure 31. DSC thermograms of 1% DVB crosslinked polystyrene containing different weight percents of DMF.

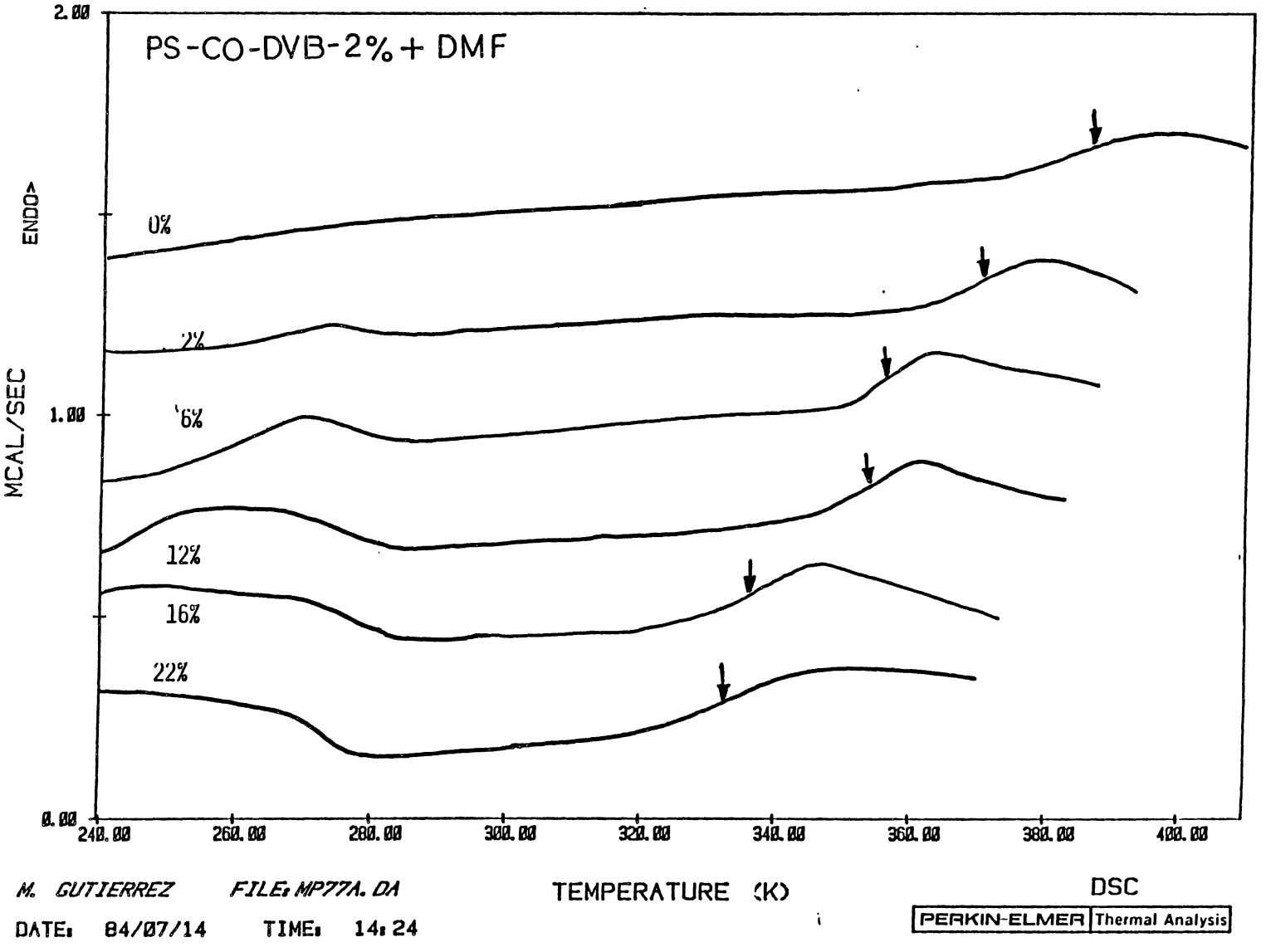

Figure 32. DSC thermograms of 2% DVB crosslinked polystyrene containing different weight percents of DMF.

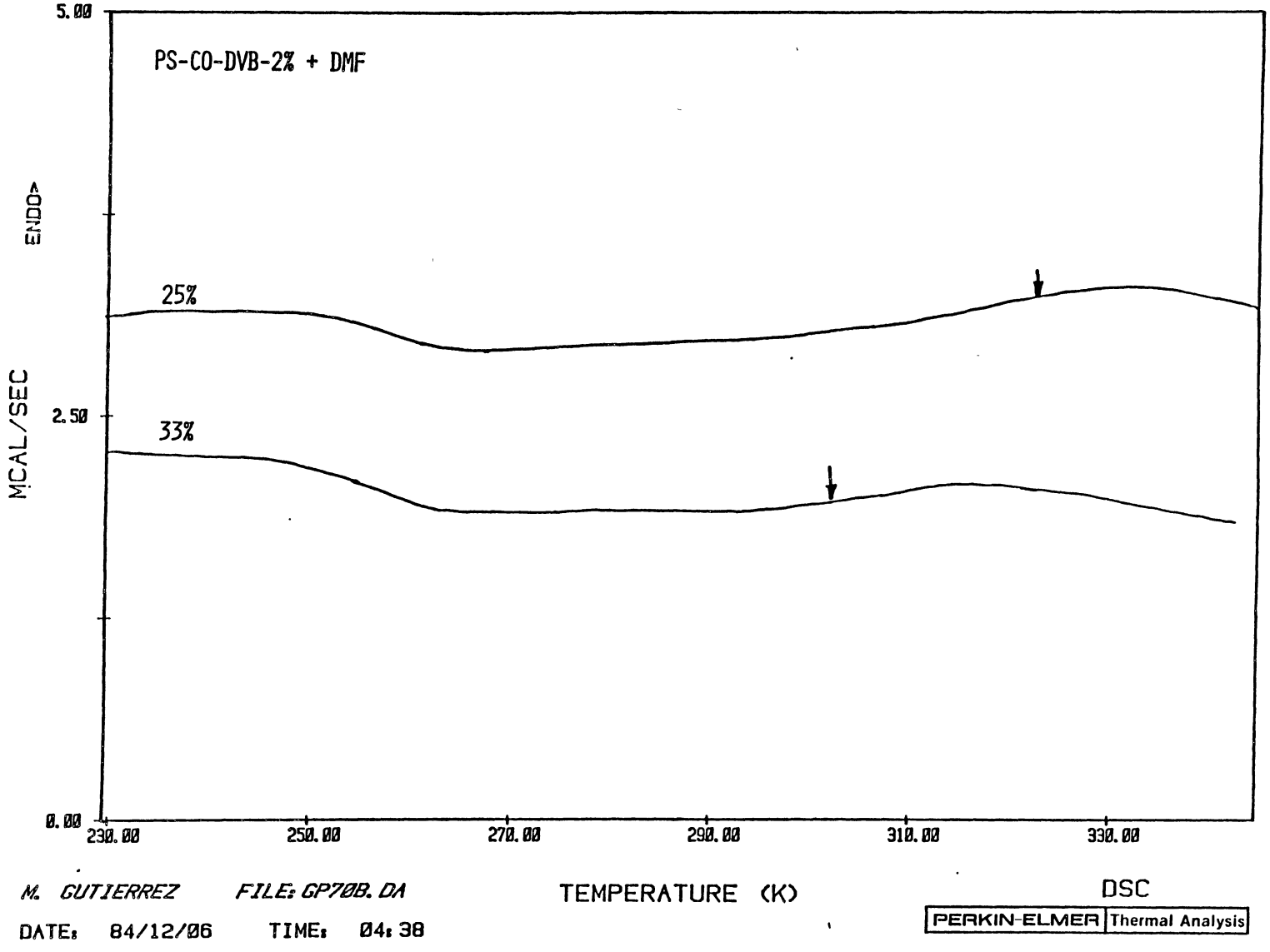

Figure 33. DSC thermograms of 2% DVB crosslinked polystyrene containing different weight percents of DMF.

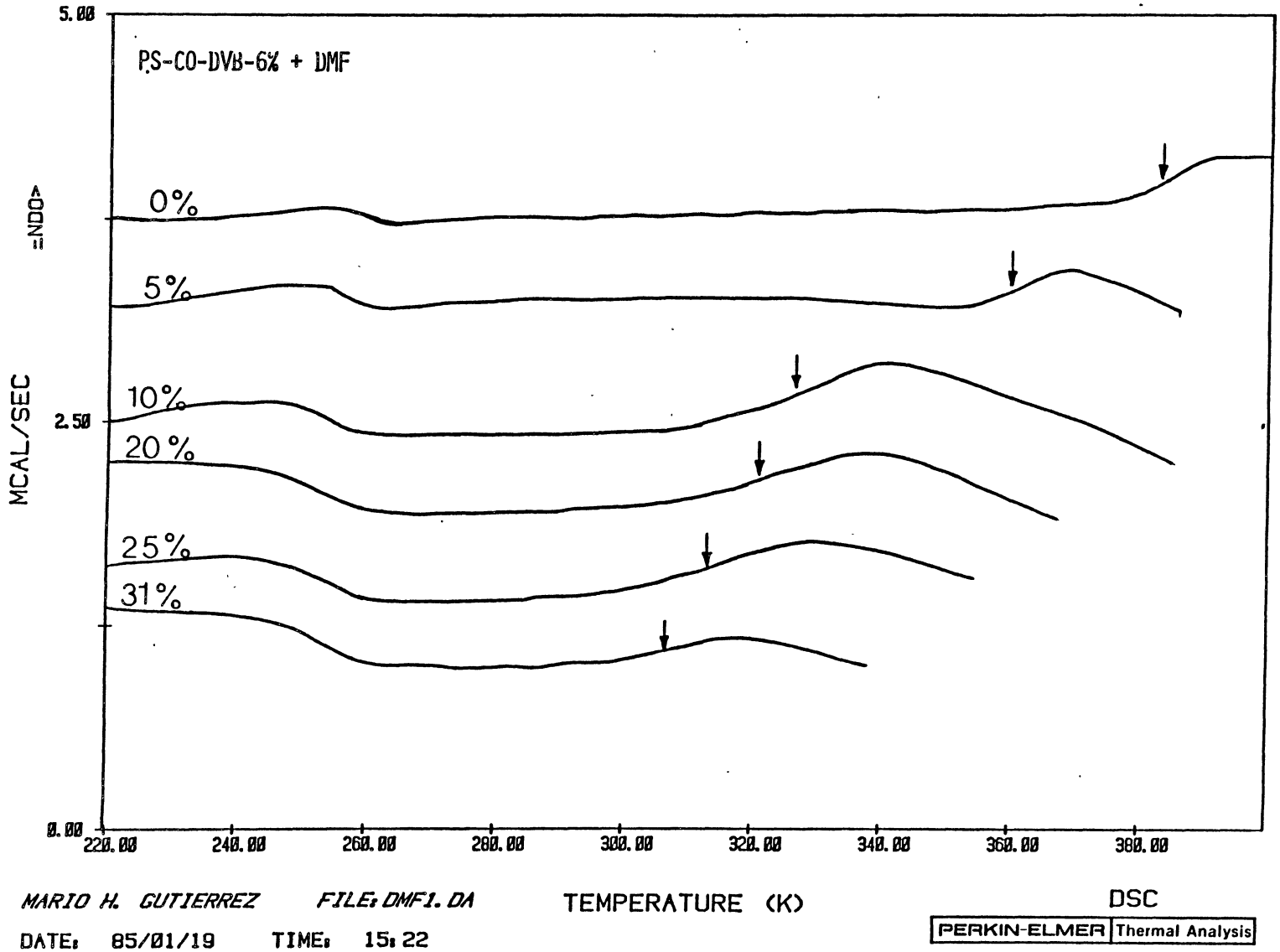

Figure 34. DSC thermograms of 6% DVB crosslinked polystyrene containing different weight percents of DMF.

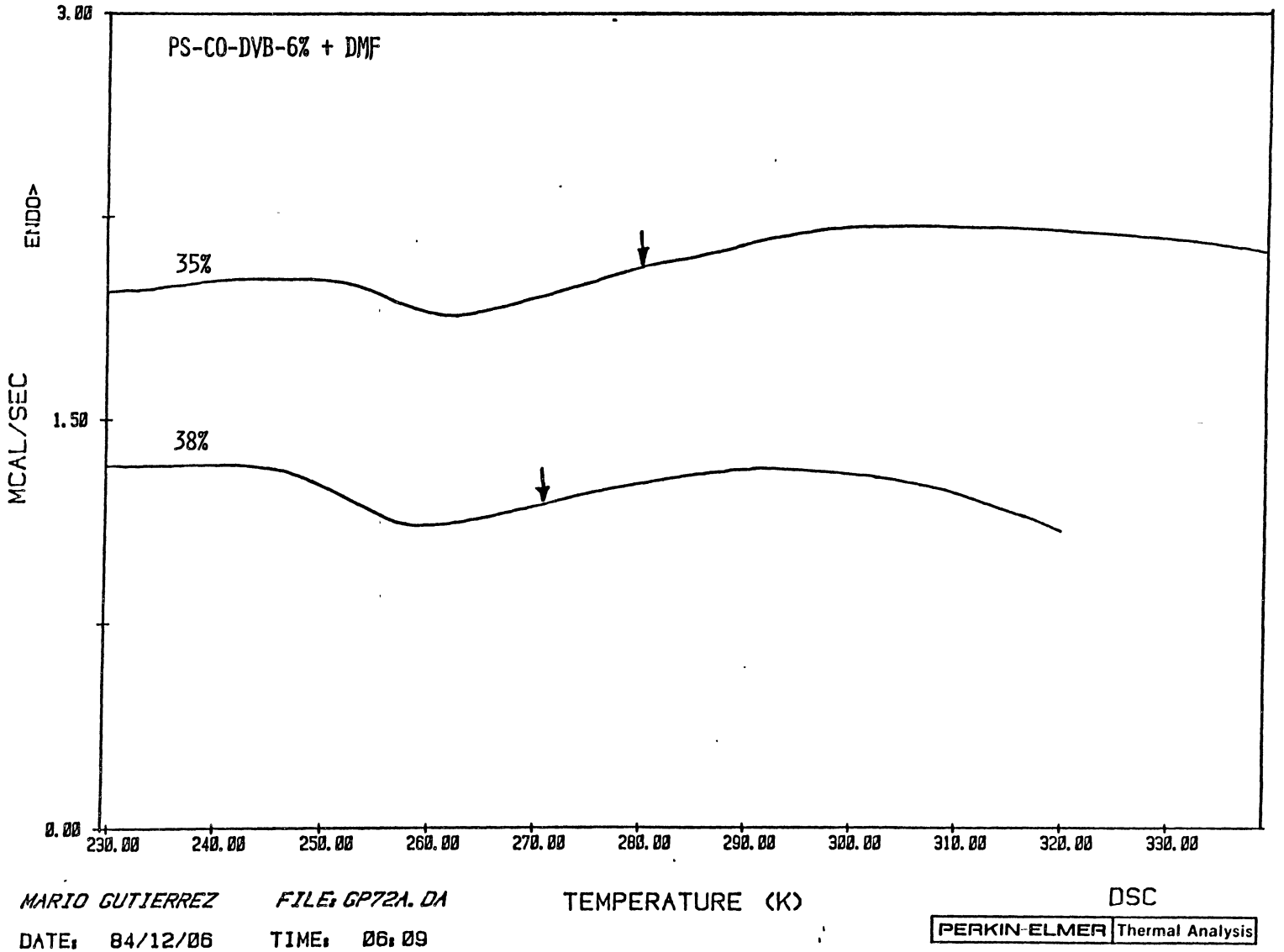

Figure 35. DSC thermograms of 6% DVB crosslinked polystyrene containing different weight percents of DMF.

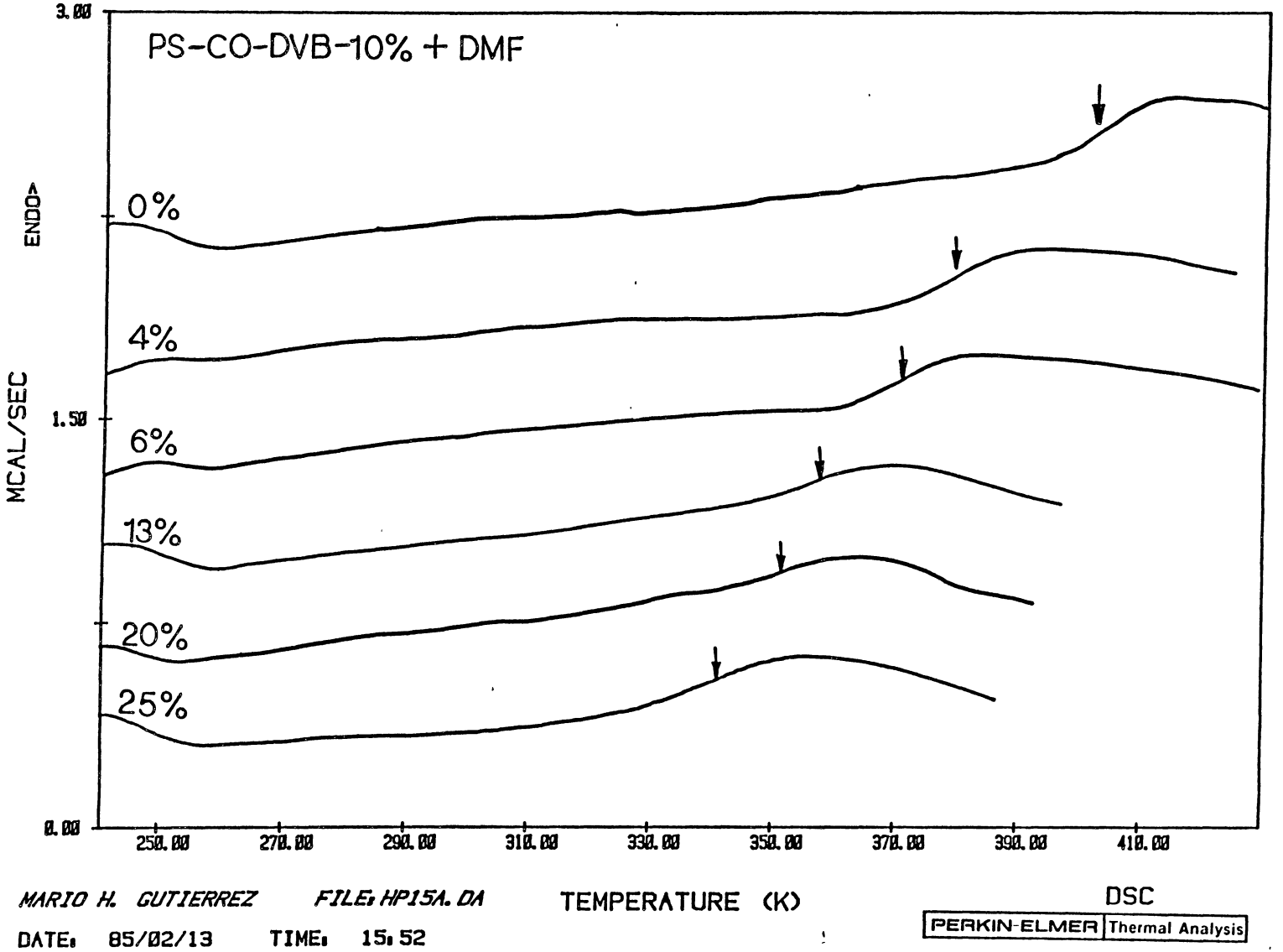

Figure 36. DSC thermograms of 10% DVB crosslinked polystyrene containing different weight percents of DMF.

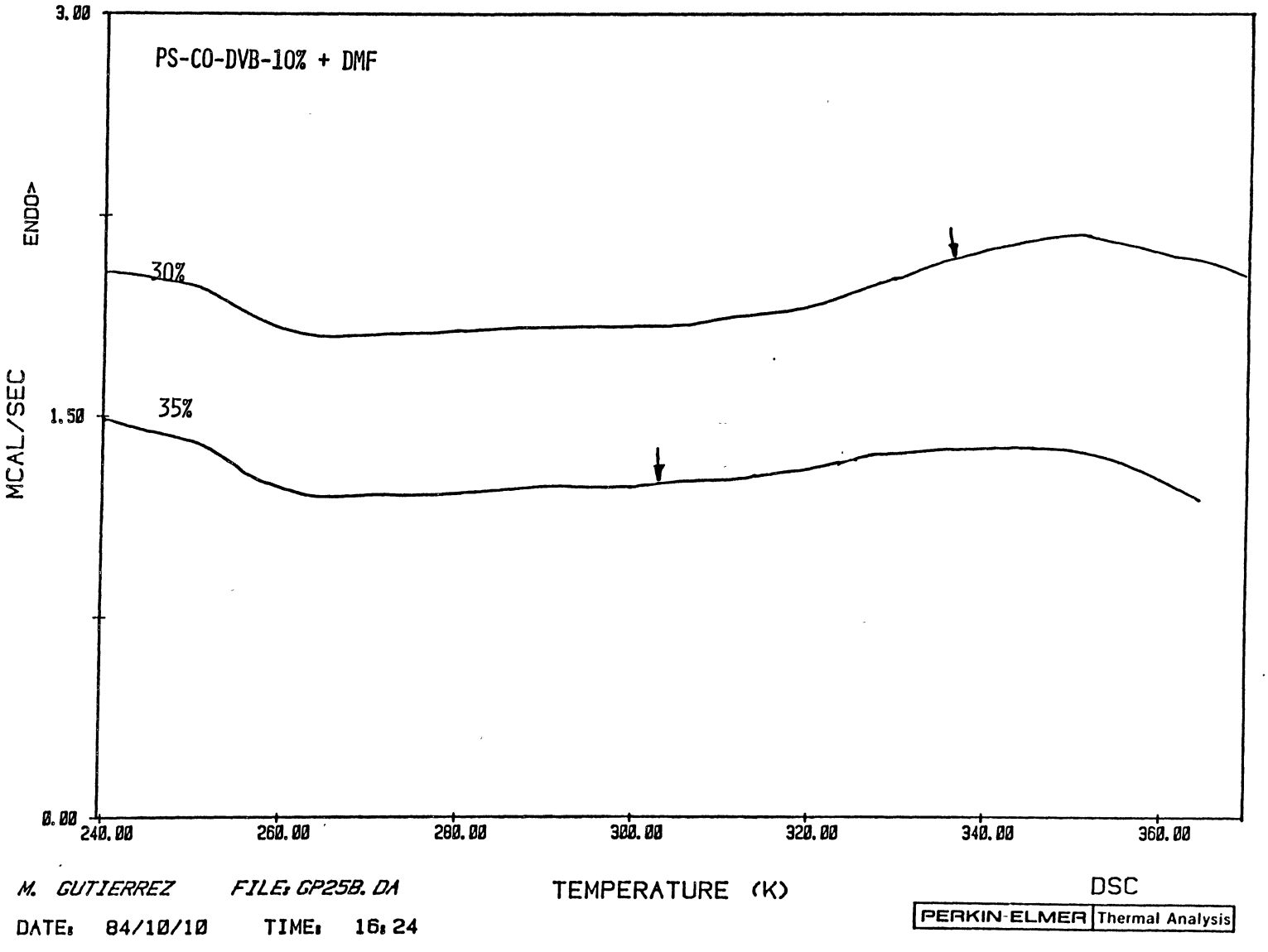

Figure 37. DSC thermograms of 10% DVB crosslinked polystyrene containing different weight percents of DMF.

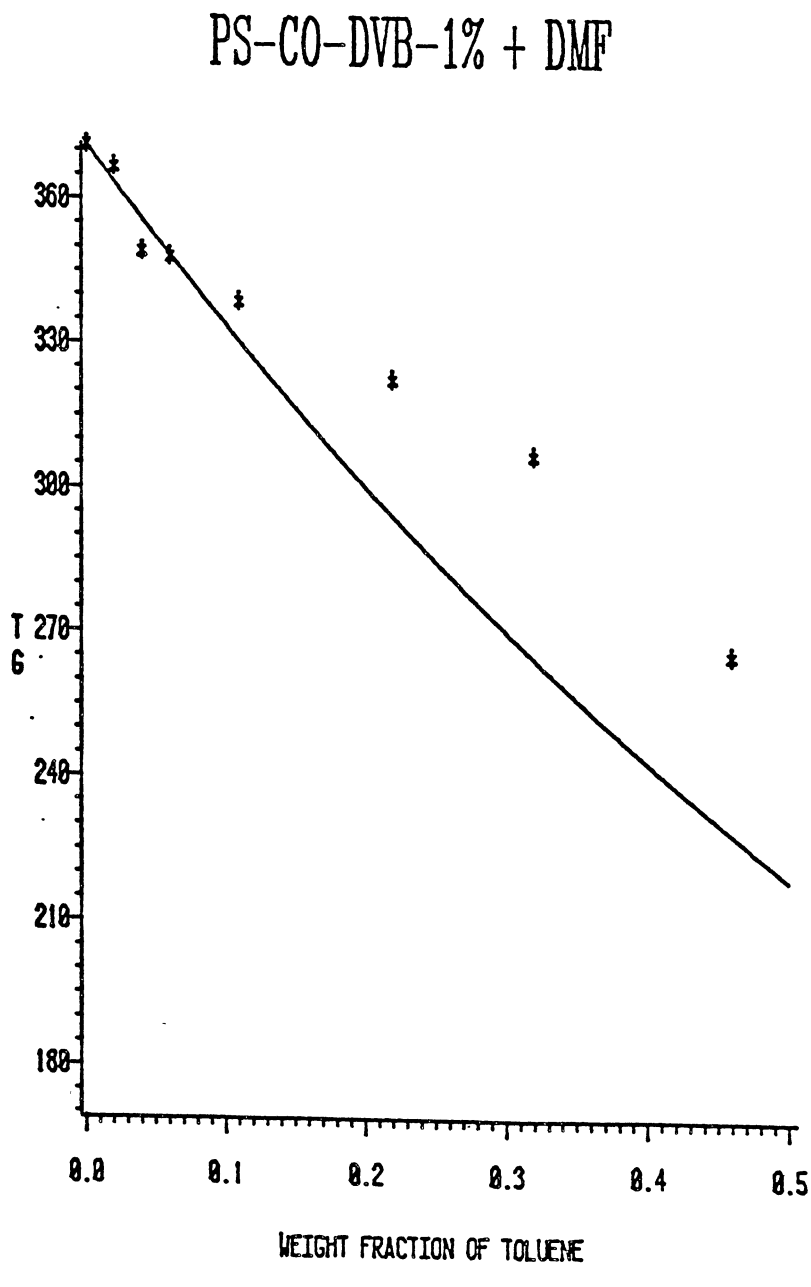

Figure 38. T_g of 1% DVB crosslinked polystyrene vs. weight fraction of DMF.

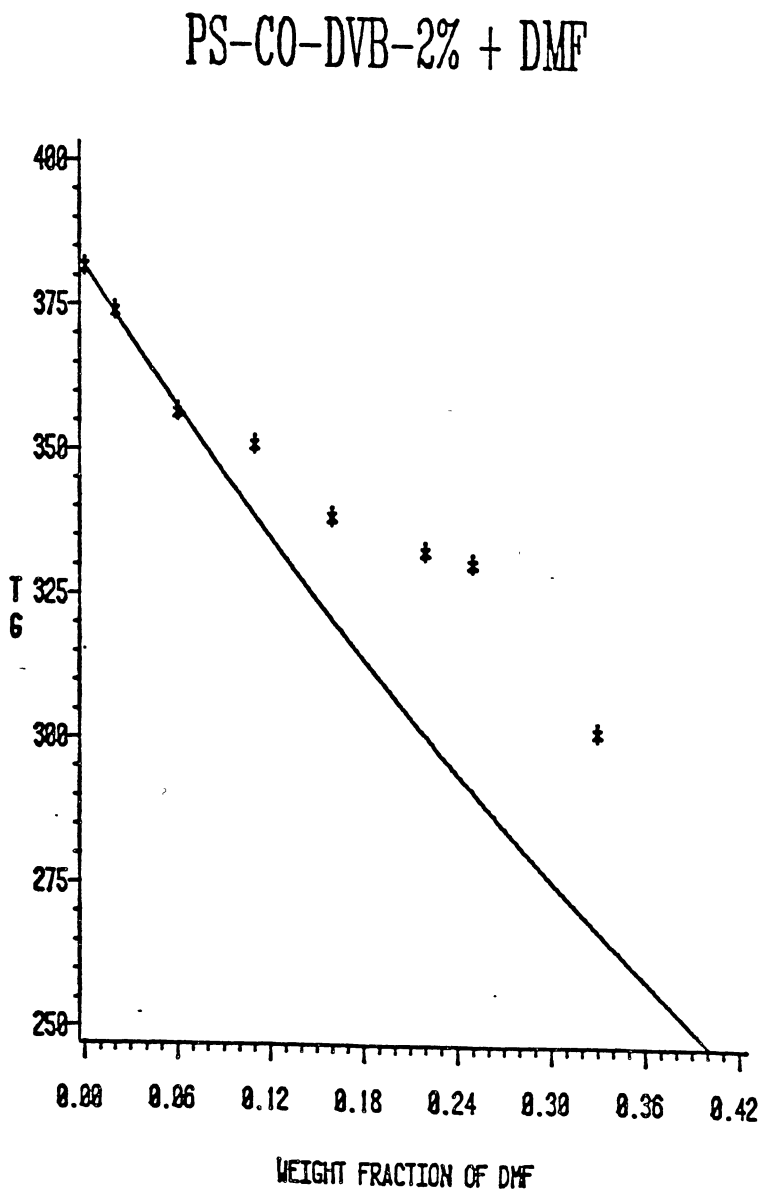

Figure 39. T_g of 2% DVB crosslinked polystyrene vs. weight fraction of DMF.

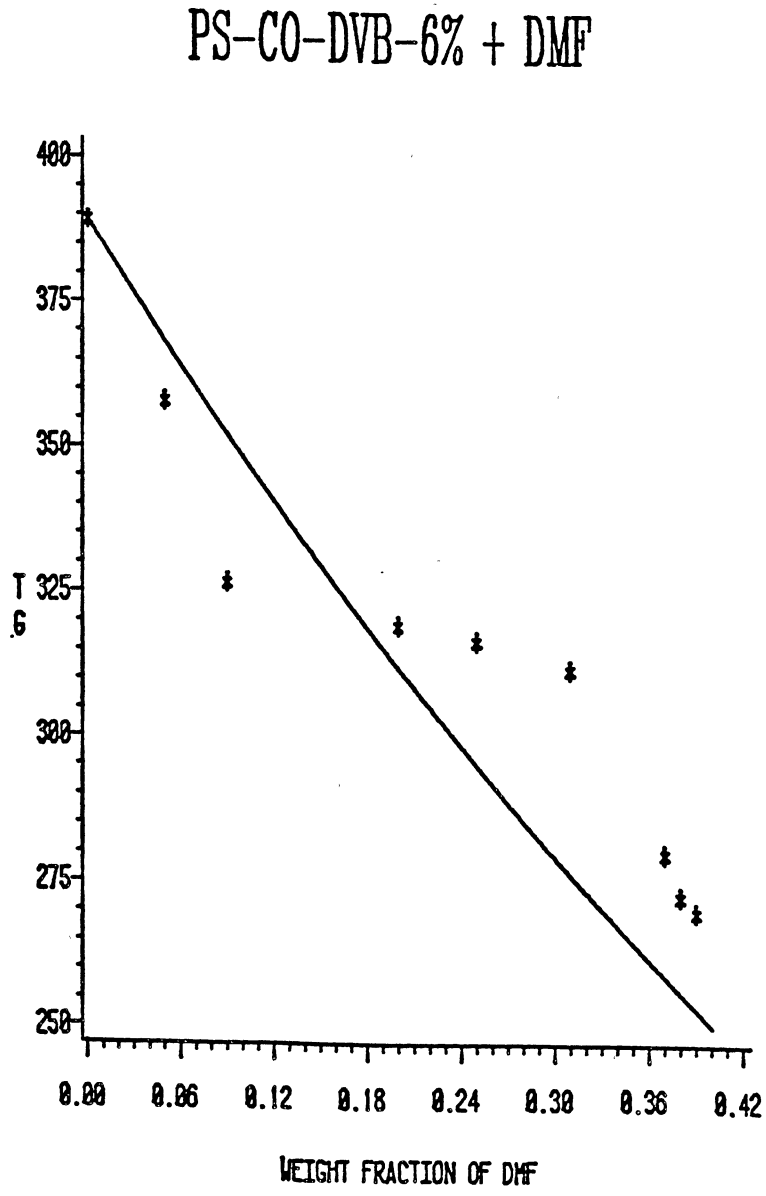

Figure 40. T_g of 6% DVB crosslinked polystyrene vs. weight fraction of DMF.

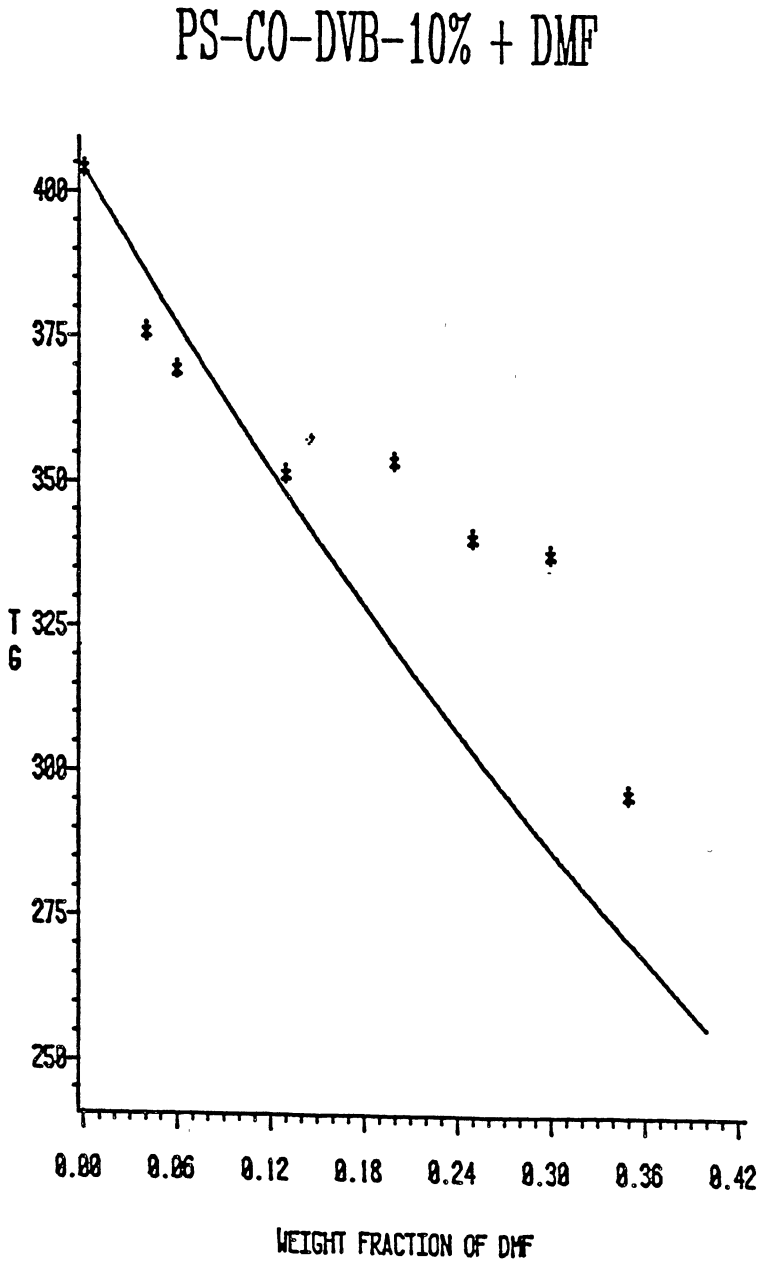

Figure 41. T_g of 10 % DVB crosslinked polystyrene vs. weight fraction of DMF.

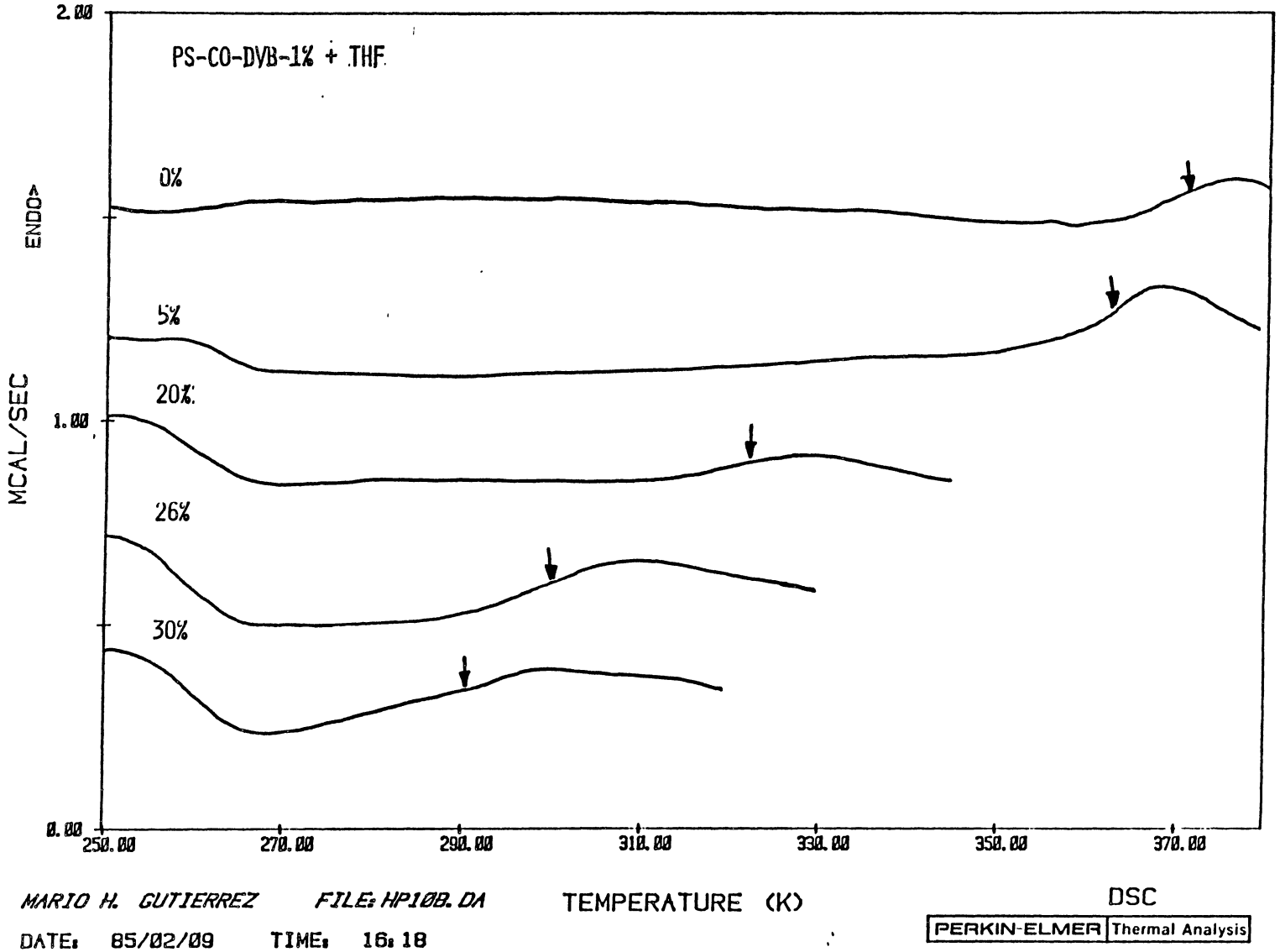

Figure 42. DSC thermograms of 1% DVB crosslinked polystryrene containing different weight percents of THF.

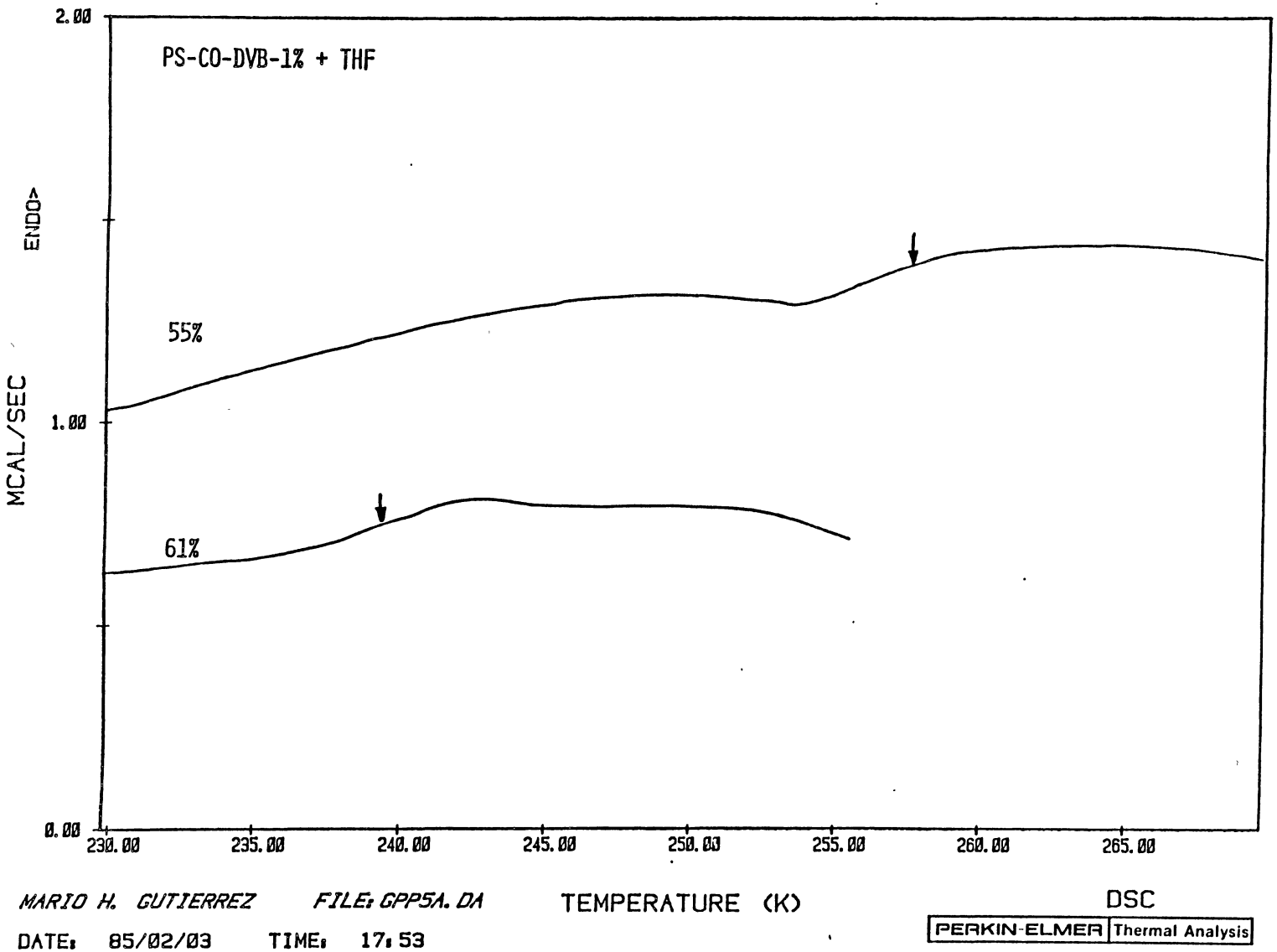

Figure 43. DSC thermograms of 1% DVB crosslinked polystyrene containing different weight percents of THF.

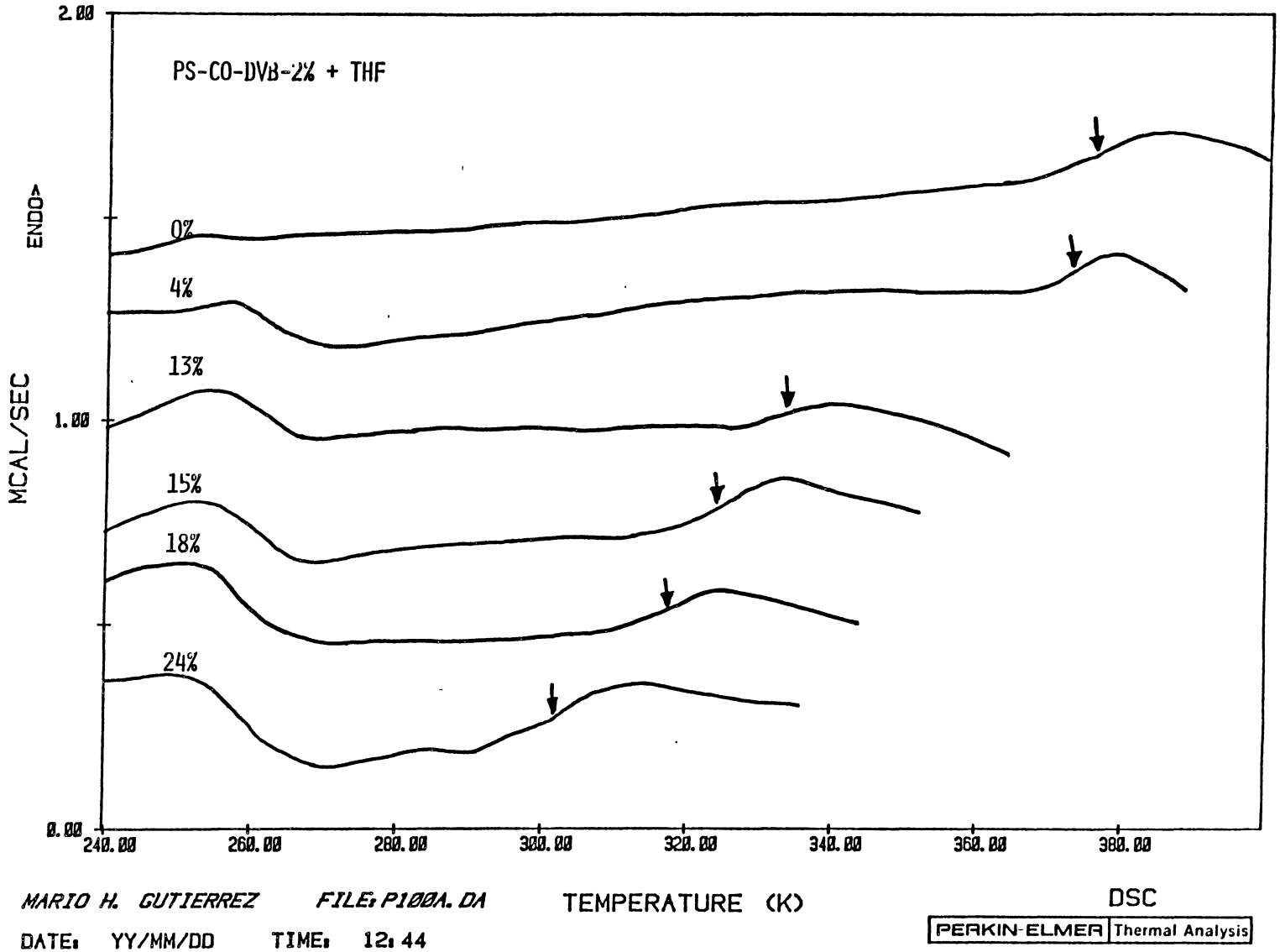

Figure 44. DSC thermograms of 2% DVB crosslinked polystyrene containing different weight percents of THF.

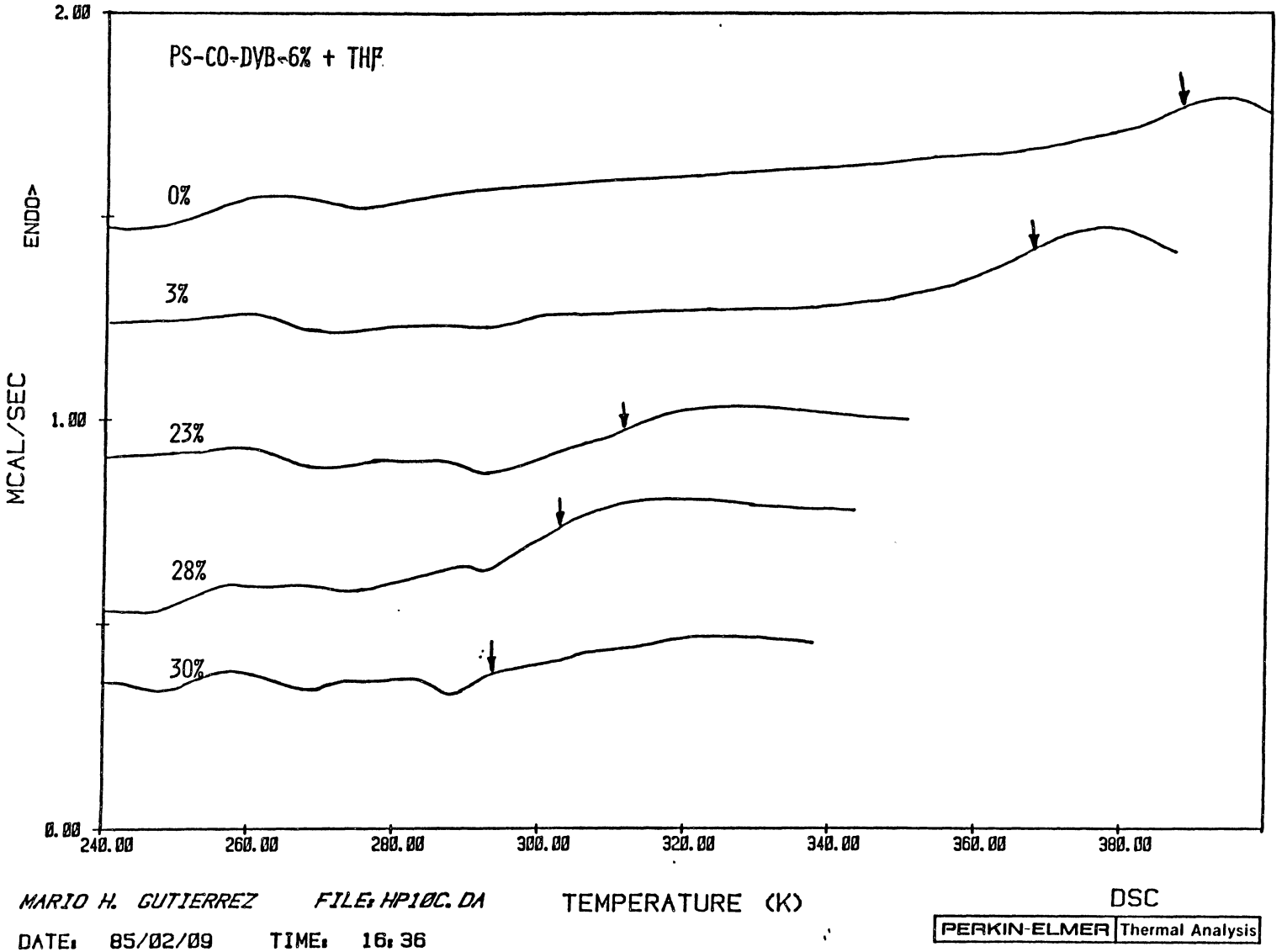

Figure 45. DSC thermograms of 6% DVB crosslinked polystyrene containing different weight percents of THF.

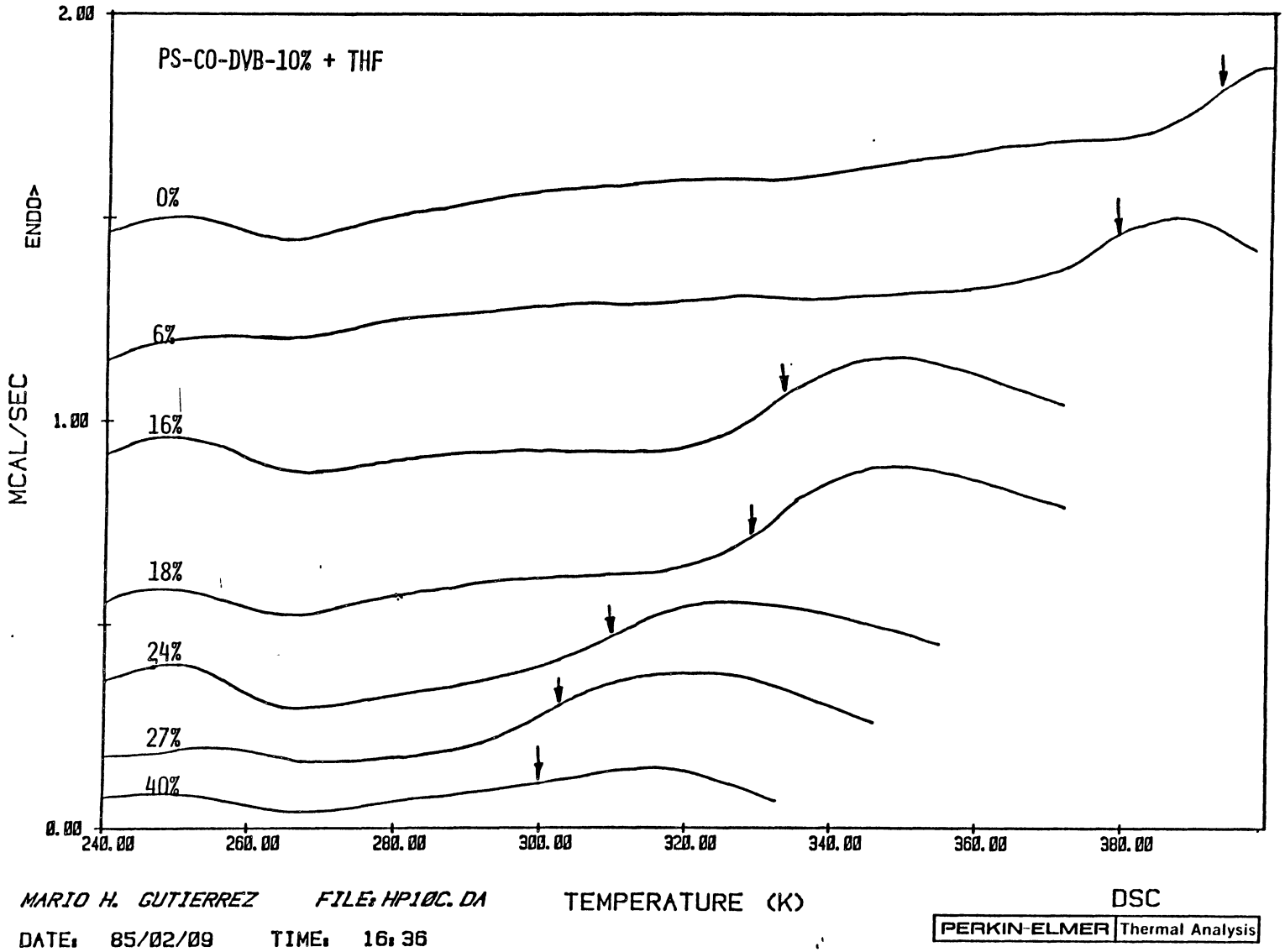

Figure 46. DSC thermograms of 10% DVB crosslinked polystyrene containing different weight percents of THF.

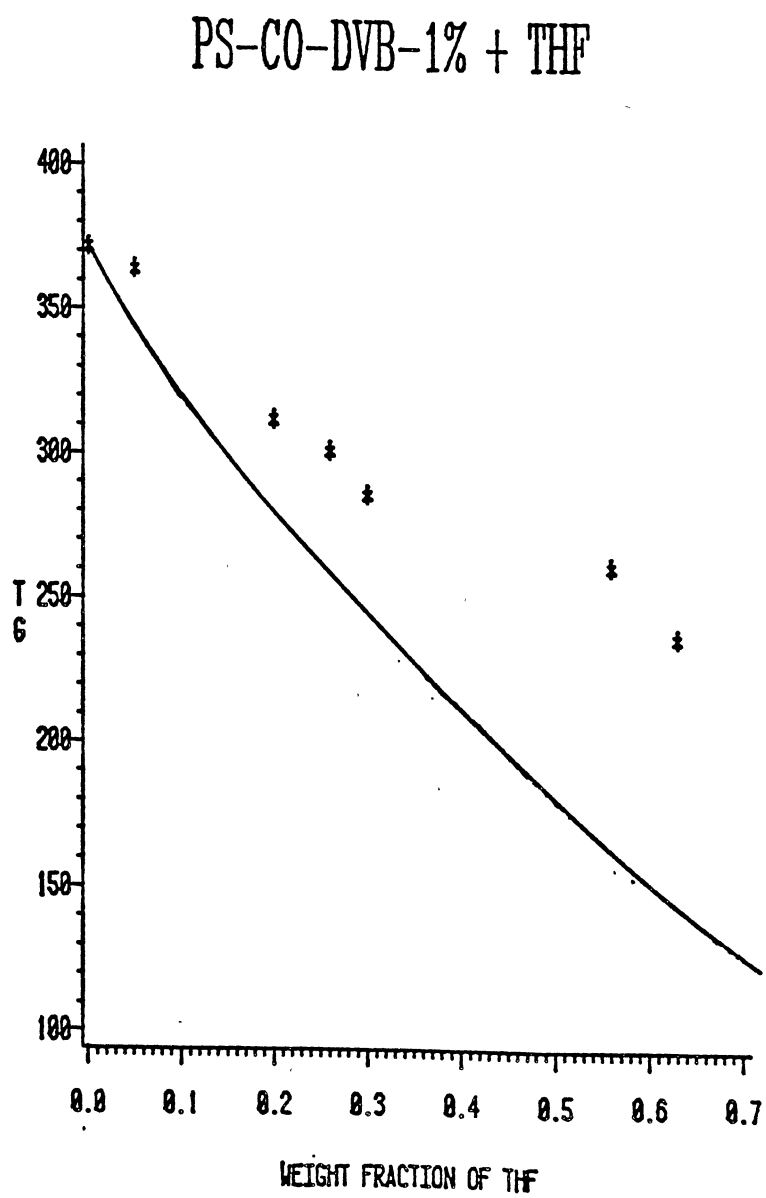

Figure 47. T_g of 1% DVB crosslinked polystyrene vs. weight fraction of THF.

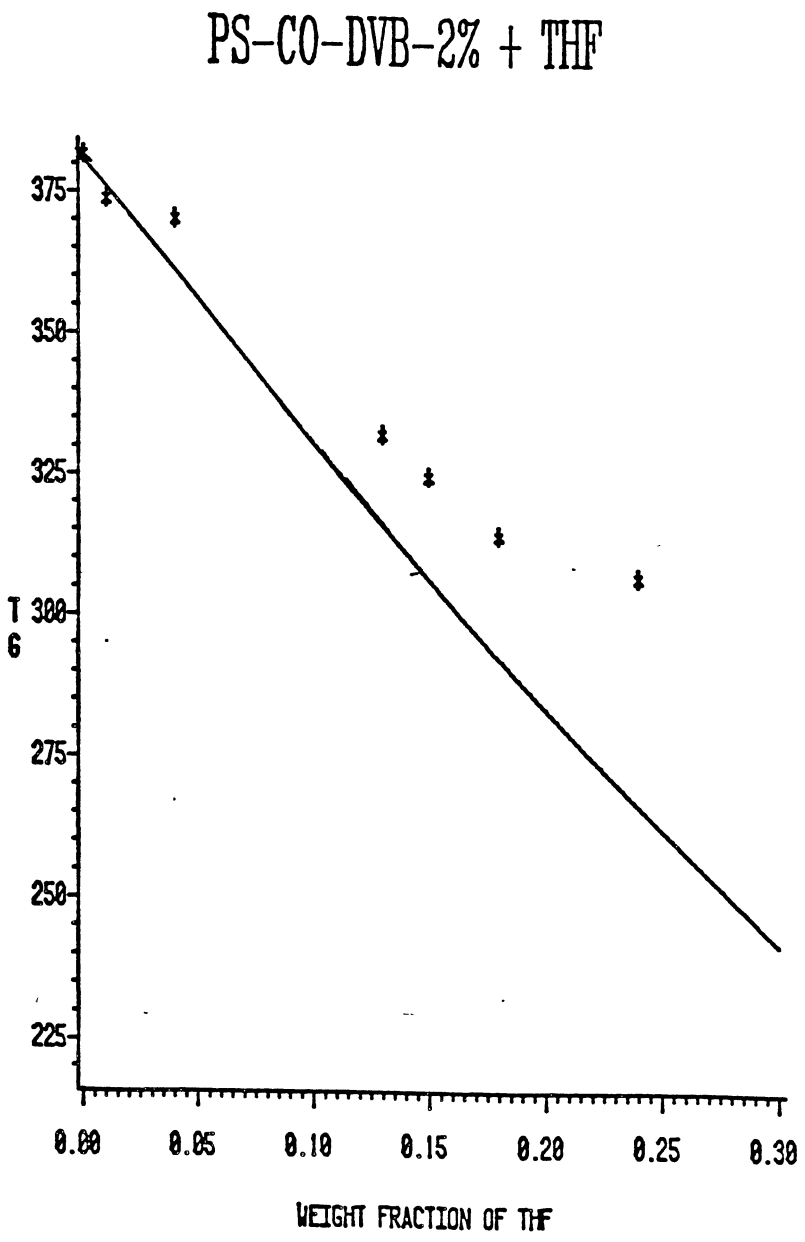

Figure 48. T_g of 2% DVB crosslinked polystyrene vs. weight fraction of THF.

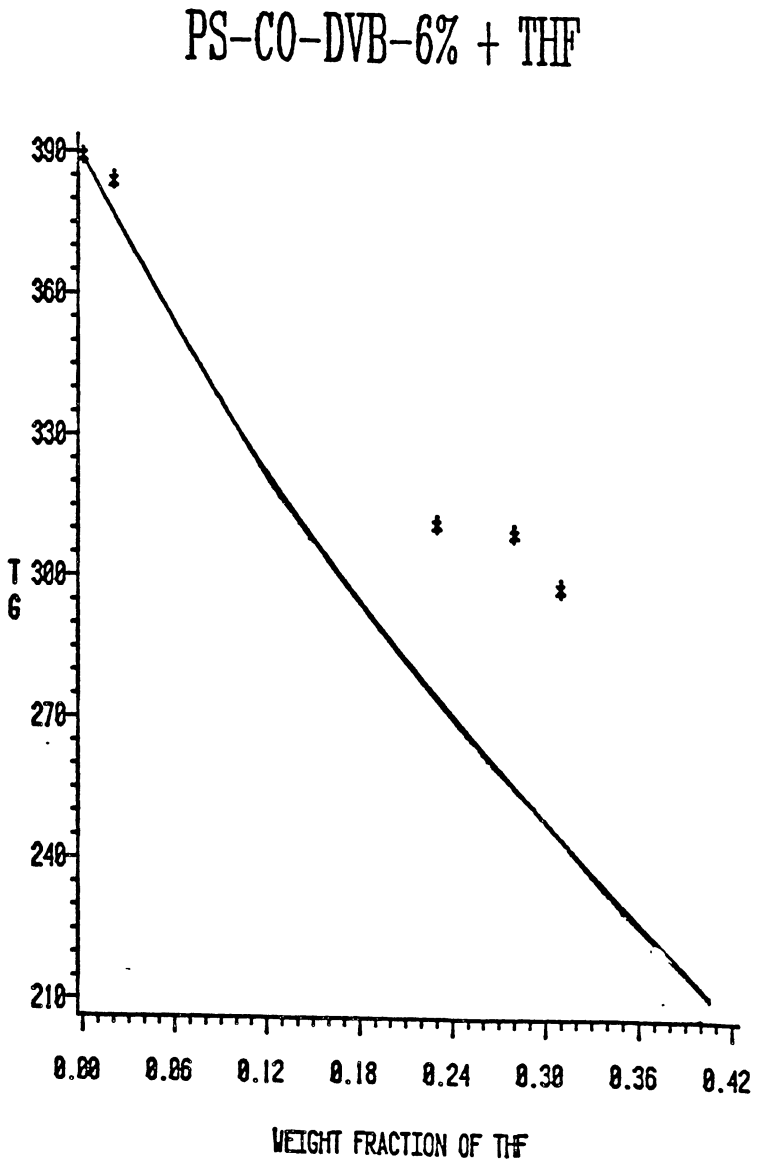

Figure 49. T_g of 6% DVB crosslinked polystyrene vs. weight fraction of THF.

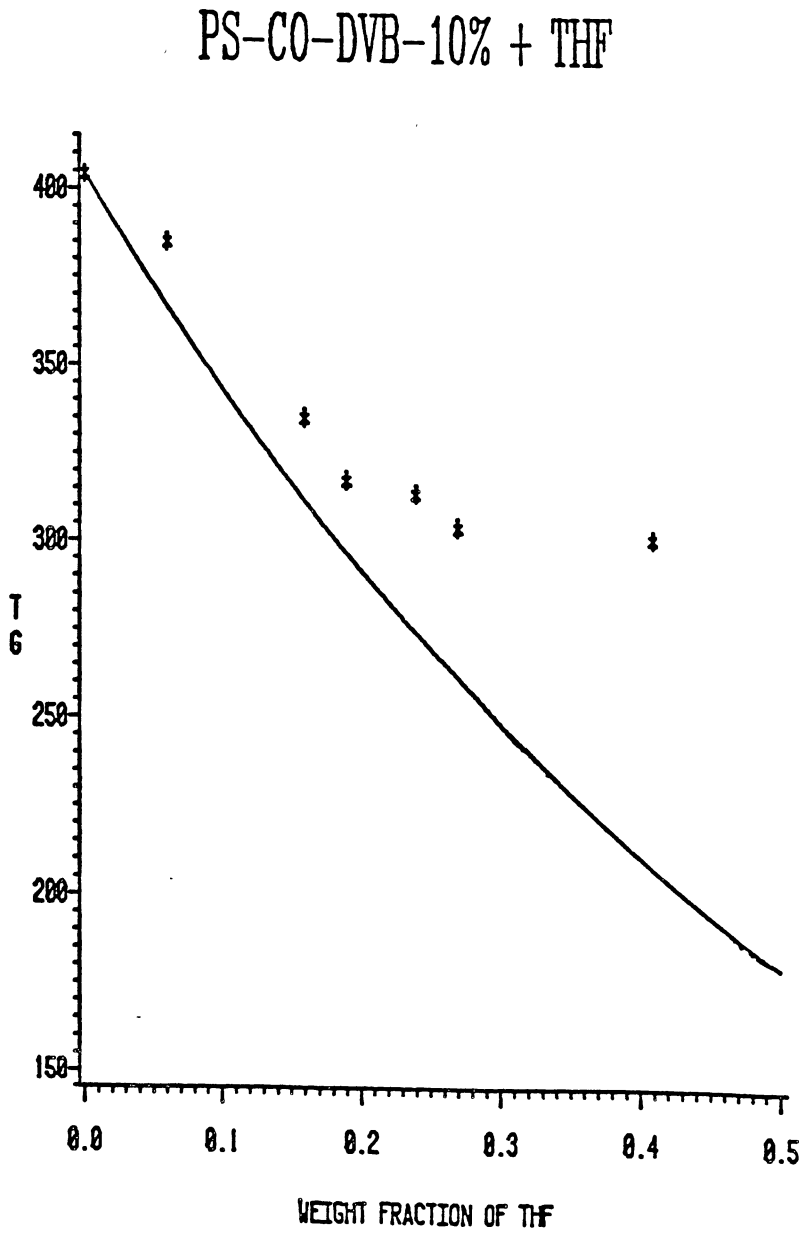

Figure 50. T_g of 10% DVB crosslinked polystyrene vs. weight fraction of THF.

BIBLIOGRAPHY

1. D. R. Paul and S. Newman, Ed., "Polymer Blends", Vol. 1, Academic Press, N.Y., 1978, Chapter 3 and 5.

2. M .C. Shen and A. Eisenberg, Prog. Solid State Chem., 3, 407 (1966).

3. E. Jenckel and R. Heusch, Kolloid-Z., 130, 89 (1953).

4. J. M. Pochan, C. L. Beatty, and D. F. Pochan, Polymer, 20, 879 (1979).

5. J. M. Gordon, G. B. Rouse, J. H. Gibbs and W. M. Risen, J. Chem. Phys. 66, 4971 (1977).

6. T. S. Chow, Macromolecules, 13, 362 (1980).

7. T. S. Ellis, F. E. Karasz, and G. Tenbrinke, J. App. Polym. Sci., 28, 23 (1983).

8. H. Staudinger, and W. Heuer, Ber., 67, 1164 (1934).

9. K. W. Pepper, J. Appl. Chem., 1, 124 (1951).

10. H. C. Hamman and D. H. Clemens, U.S. Patent 3,728,318 (1973).

11. R. L. Albright, U.S. Patent 4,185,077 (1980).

12. M. Tomoi and W. T. Ford, J. Am. Chem. Soc. 102, 7140 (1980); ibid, 103, 3721, 3728 (1981).

13. T. Balakrishnan and W. T. Ford, Tetrahedron Lett., 22, 4377 (1981).

14. T. Balakrishnan and W. T. Ford, J. Appl. Polym. Sci., 27, 133 (1982).

15. R. H. Boundy, R. F. Boyer, "Styrene, Its Polymers, Copolymers and Derivatives", p 725, Reinhold, N.Y. (1952).

16. P. J. Flory, "Principles of Polymer Chemistry", Cornell Univ. Press. Ithaca, New York, 1953.

17. A. J. Warner, ASTM Bull. No. 165, 53 (April 1950).

18. W. R. Richard and P. A. S. Smith, J. Chem. Phys., 18, 230 (1950).

19. Sh. L. Lep'chuck, and V. I. Sedlis., Zhur. Priklad. Khim., 30, 412 (1957).

20. G. Kanig., Kolloid Z., 190 (1), 1 (1963).

21. J. H. Gibbs, and E. A. Dimarzio., J. Chem. Phys., 28, 373 (1958).

22. G. A. Adam, and J. H. Gibbs., J. Chem. Phys., 43, 139 (1965).

23. B. Wunderlich, D. M. Bodily, and M. H. Kaplan., J. Appl. Phys. 35, 95 (1964).

24. R. Parthasarathy., K. J. Rao, and C. N. R. Rao., Chem. Soc. Rev., 361 (1983).

25. W. Kauzmann, Chem. Rev., 3, 219 (1948).

26. R. F. Boyer, Rubber Chemistry and Technology, 36, 1303 (1963).

27. J. Wong and C. A. Angell, "Glass: Structure by Spectroscopy", Marcel Dekker, New York, 1976.

28. A. Zdaniewski, G. E. Rindone, and D. E. Day., J. Mater. Sci., 14, 763 (1979).

29. C. A. Angell and L. M. Torell, J. Chem. Phys., 78, 937 (1983).

30. C. A. Angell in "Vibrational Spectroscopy of Molecular Liquids and Solids" ed. S. Bratos and R.M. Pick, Plenum, New York, 1980.

31. J. J. Dechter, D. E. Axelson, A. Dekmezian, M. Glotin, and L. Mandelkern., J. Polym. Sci.: Polym. Phys. Ed., 20, 641 (1979).

32. P. M. Smith, F. R. Boyer and P. L. Kumler., Macromolecules, 12, 61 (1979)

33. D. C. Champeney, Rep. Prog. Phys., 42, 1017 (1982).

34. J. Wong and F. W. Lytle, J. Non-Cryst. Solids., 37, 273 (1980).

35. M. J. Richardson and N. G. Savill, Brit. Polym. J., 11, 123 (1979).

36. E. S. Watson, M. J. O'Neill, J. Justin and N. Brenner, Anal. Chem., 36, 1233 (1964).

37. M. J. O'Neill, Analytical Chemistry., 38, 1331 (1966).

38. R. B. Beevers and E. F. T. White, Trans. Far. Soc., 56, 744 (1960).

39. T. G. Fox and P. J. Flory, J. Appl. Phys., 21, 581 (1950).

40. K. Ueberreiter and G. Kanig, J. Chem. Phys., 18, 399 (1950).

41. F. N. Kelley and F. Bueche, J. Polym. Sci., 50, 549 (1961).

42. E. Jenckel and R. Heusch, Kolloid Z., 130, 89 (1958).

43. W. Kauzman and H. Eyring , J. Am. Chem. Soc., 62, 3113 (1940).

44. T. G. Fox and S. Loshaek, J. Polym. Sci., 15, 371 (1955).

45. L. A. Wood, J. Polym. Sci., 28, 319 (1958).

46. M. Gordon and J. S. Taylor, J. Appl. Chem., 2, 493 (1952).

47. T. G. Fox, Bull. Amer. Phys. Soc., 1, 123 (1956).

48. G. T. Brinke, F. E. Karasz, and T. S. Ellis, Macromolecules, 16, 244 (1983).

49. G. T. Furukawa, T. B. Douglas, R. E. McCoskey, and D. C. Ginnings, Journal of Research of the National Bureau of Standards, 57, 67 (1956). Research Paper 2694.

50. J. H. Flynn, Thermochim. Acta., 8, 69 (1974)

51. P. D. Garn and O. Menis, J. Macromol. Sci.-Phys., B13(4), 611 (1977).

52. R. O. Davis and G. O. Jones, Advan. Phys., 2, 370 (1953); Proc. Roy. Soc., Ser. A, 217, 26 (1953).

53. S. M. Wolpert, A. Weitz, and B. Wunderlich, J. Polym. Sci. A-2, 9, 1887 (1971).

54. C. T. Moynihan, J. Eastel, J. Wilder; J. Phys. Chem., 78, 2673 (1974).

55. J. H. Glans and D. T. Turner, Polymer, 22, 1540 (1981).

56. A. Lambert, Polymer, 10, 319 (1969).

57. P. Moy, Ph. D. Thesis, University of Massachusetts, (1981).

58. R. J. Roe and A. E. Tonelli, Macromolecules., 12, 114 (1978).

59. R. J. Roe and A. E. Tonelli, Macromolecules., 12, 878 (1979).

60. M. Goldstein, J. Chem. Phys., 64, 4767 (1976).

61. R. Simha and R. F. Boyer, J. Chem. Phys., 37, 1003 (1962).

62. B. Wunderlich, J. Phys. Chem., 64, 1052 (1960).

63. M. Seno and T. Yamabe, Bull. Chem. Soc. Japan, 37, 754 (1964).

64. P. R. Couchman and F. E. Karasz, Macromolecules, 11, 117 (1978).

65. A. V. Lesikar, J. Phys. Chem., 80, 1005 (1976).

66. C. A. Angell, J. M. Sare, and E. J. Sare, J. Phys. Chem., 82, 2622 (1978).

67. O. Haida, H. Suga and S. Seiki, Thermochim. Acta. 3, 177 (1972).

68. R. R. Driesbach, "Physical Properties of Chemical Substances", Midland, Mich., Dow Chemical Co. 1953 Vol. 1, Serial No. 1.2.

VITA 2

Mario Humberto Gutierrez

Candidate for the Degree of

Doctor of Philosophy

Thesis: STRUCTURE AND ELECTRICAL PROPERTIES OF THIOPHENE POLYMERS, AND THE EFFECT OF DILUENTS ON THE GLASS TRANSITION TEMPERATURE OF STYRENE/DIVINYL-BENZENE POLYMER NETWORKS

Major Field: Chemistry

Biographical:

Personal Data: The author was born in San Nicolas de los Garza, Nuevo Leon, Mexico, on July 13, 1950, the son of Manuel Gutierrez (+) and Petrita Gutierrez; married to Nelly L. Rivera on December 11, 1977; has two daughters, Nellyta and Cecy.

Education: The author was graduate from Instituto Regiomontano High School, Monterrey, Nuevo Leon, Mexico, in 1968; received the Bachelor of Science degree in Chemistry from Universidad de Nuevo Leon, Mexico, in 1972; received the Master of Science degree in Chemistry from Centro de Estudios Avanzados del Instituto Politecnico Nacional, Mexico D.F., in 1977; completed the requirements for the Doctor of Philosophy degree in Chemistry at Oklahoma State University, Stillwater, Oklahoma in July, 1985.

Professional Experience: Teaching Assistant in Chemistry Department at the Universidad de Nuevo Leon, Monterrey, Mexico, from August 1971-August 1972; Lecturer in Chemistry, Chemistry Department at the Universidad de Nuevo Leon, Monterrey, Mexico, from February 1972-August 1972; Lecturer in Chemistry in the Department of Chemistry at Universidad de Monterrey, Mexico, from September 1972-December 1978; Lecturer in Chemistry in the Department of Chemistry at Universidad Regiomontana, Monterrey, Mexico, from January 1979-December 1980; Graduate Teaching Assistant in the Department of Chemistry at Oklahoma State University, Stillwater, Oklahoma, from August 1984-May 1985. The author is a memeber of the American Chemical Society and the Mexican Chemical Society.